SOIL EROSION, SEDIMENT YIELD AND MITIGATION MEASURES UNDER CLIMATE CHANGE: CASE STUDY OF BERESSA WATERSHED, UPPER BLUE NILE BASIN, ETHIOPIA

GETACHER KASSA MITIKU

MASTER OF SCIENCE IN

SOIL AND WATER ENGINEERING

JOMO KENYATTA UNIVERSITY

OF

AGRICULTURE AND TECHNOLOGY

2026

Soil Erosion, Sediment Yield, and Mitigation Measures under Climate Change: Case Study of Beressa Watershed, Upper Blue Nile Basin, Ethiopia

Getacher Kassa Mitiku

A Thesis Submitted in Partial Fulfillment of the Requirements for the Degree of Master of Science in Soil and Water Engineering of the Jomo Kenyatta University of Agriculture and Technology

2026

DECLARATION

This thesis is my original work and has not been presented for a degree in any other University.

Signature: ……………………………… Date: ………………………..

Getacher Kassa Mitiku

This thesis has been submitted for examination with our approval as the University Supervisors:

Signature: ………………………………………. Date: ……………………………..

Prof. John Mwangi Gathenya, PhD

JKUAT, Kenya

Signature……………………………................ Date: ……………………………..

Prof. Bancy Mbura Mati, PhD

JKUAT, Kenya

Signature……………………………................ Date: ……………………………..

Dr. Hailu Kendie Addis, PhD

Amhara Agricultural Research Institute, Ethiopia

DEDICATION

This thesis is dedicated to my beloved father, whom I lost on May 27, 2025. Although I was far from him, his love, prayers, and unwavering support were always with me. He sacrificed everything for his children and inspired me through his wisdom and strength. I miss him deeply and will carry his memory with me on every step of my journey. May his soul rest in eternal peace. Thank you, Dad. I will never forget you.

ACKNOWLEDGEMENT

First and foremost, I want to thank God Almighty for granting me good health, strength, and perseverance throughout my thesis journey. I am also deeply grateful to the Virgin Mary for her spiritual intercession. My sincere thanks go to Jomo Kenyatta University of Agriculture and Technology (JKUAT), especially the SWEED Department, for providing continuous support. I want to acknowledge the German Academic Exchange Service (DAAD) for providing financial support that made this study possible. I am also thankful to the Amhara Agricultural Research Institute, particularly the Debre Birhan Agricultural Research Center, for granting me study leave and supporting my academic development. I am immensely grateful to my supervisor, Prof. John Gathenya, for his invaluable guidance, ongoing encouragement, and support throughout every stage of this thesis. Prof. Bancy Mati for her motivational advice, guidance, and for sharing her academic journey, which greatly inspired me. Dr. Hailu Kendie for his close follow-up during data collection, organizing expert support for model training, and guiding the scientific writing process. I sincerely thank Mr. Tilahun Getachew and Mr. Ayele Desalegn for their invaluable assistance during the setup of the SWAT model and the calibration and validation stages of SWAT-CUP for my research. I would also like to sincerely thank Dr. Joseph Sang, the Dean, and Dr. Hosea Mwangi, the Chairman, for their support and understanding during challenging times. I appreciate Prof. Patrick Home for his valuable advice during progress presentations and Prof. James Meso for his support in developing the conceptual framework. Lastly, I would like to express my heartfelt gratitude to my entire family for their unconditional love, encouragement, and unwavering support throughout my academic journey.

TABLE OF CONTENTS

LIST OF TABLES

LIST OF FIGURES

LIST OF APPENDICES

ACRONYMS AND ABBREVIATIONS

BMPs	Best Management Practices
BCC-CSM2-MR	Beijing Climate Center Climate System Model version 2 – Medium Resolution
CA	Conservation Agriculture
CF	Contour Farming
CMIP5	Coupled Model Intercomparison Project Phase 5
CMIP6	Coupled Model Intercomparison Project Phase 6
GDP	Gross Domestic Product
GUI	Graphical User Interface
Mg/ha/year	Megagram per hectare per year, equivalent to metric ton per hectare per year
MRI-ESM2-0	Meteorological Research Institute Earth System Model version 2.0
NSE	Nash-Sutcliffe Efficiency
PBIAS	Percent Bias
R^2	Coefficient of Determination
RSR	Ratio of the Root Mean Square Error to the Standard Deviation of Measured Data
SDR	Sediment Delivery Ratio
SSP2-4.5	Shared Socioeconomic Pathway 245 (Intermediate Scenario)
SSP5-8.5	Shared Socioeconomic Pathway 585 (High Emissions Scenario)
SUFI-2	Sequential Uncertainty Fitting Version 2
SWAT	Soil and Water Assessment Tool

ABSTRACT

Soil erosion is a major environmental challenge in Ethiopia, particularly in the Upper Blue Nile Basin, where it contributes to severe land degradation and sediment-related problems. Climate change worsens these problems. However, the links among soil erosion, climate projections from the Coupled Model Intercomparison Project Phase 6 (CMIP6), and mitigation efforts remain poorly understood. This study aimed to assess climate change impacts on soil erosion and sediment yield and to evaluate the effectiveness of best management practices (BMPs) for future climate in the Beressa watershed using the Soil and Water Assessment Tool (SWAT). This study is among the first in the Upper Blue Nile Basin to integrate CMIP6 climate projections with SWAT for evaluating future BMP performance. Both observed and bias-corrected future climate data were used. The MRI-ESM2-0 and BCC-CSM2-MR model were selected based on their superior performance in reproducing observed temperature and precipitation patterns in the study region, respectively. Simulations covered the baseline period (1995–2023), near-term period (2030–2059), and far-term period (2060–2089), under SSP2-4.5 and SSP5-8.5 scenarios. The SWAT model demonstrated satisfactory performance in simulating observed streamflow and sediment yield during calibration and validation. Climate projections indicated increasing temperature and precipitation, leading to higher soil erosion and sediment yield, with shifts in erosion hotspot areas. Sediment yield is projected to increase under both SSP2-4.5 (32% near-term, 27.9% far-term) and SSP5-8.5 (19.2% near-term, 45.4% far-term) compared to the baseline. BMP evaluation showed sediment-yield reductions by terracing (48.36–50.64%), conservation agriculture (29.70–32.76%), contour farming (19.65–20.40%), and combined use (58.20–59.86%). Variations among sub-watersheds highlighted the influence of local watershed characteristics on erosion response to climate change and on the effectiveness of BMPs. These findings enhance understanding of climate-driven erosion processes and support the development of adaptive conservation strategies.

CHAPTER ONE

INTRODUCTION

1.1 Background Information

Climate change is one of the most pressing global challenges, significantly accelerating soil erosion and sedimentation, and has detrimental effects on ecosystem services and human welfare (Eekhout & Vente, 2022). Millions of people worldwide, particularly in Africa, Asia, and Latin America, are at risk of severe food and water insecurity due to climate-related hazards (IPCC, 2023). Soil erosion rates are significantly impacted by temperature variations and precipitation patterns (Nearing, Pruski, & Neal, 2004; Trenberth, 2011). Although precipitation is the direct driver for soil detachment and transport, increasing temperature can also make soil more prone to erosion by changing vegetation cover and soil moisture. Soil erosion involves the detachment and transportation of soil particles by water, wind, or machinery, leading to sedimentation in bodies of water such as rivers and reservoirs (Pimentel & Kounang, 1998). This process degrades soil quality, lowers agricultural productivity, and affects hydrological systems. In Ethiopia, water erosion is the most severe cause of land degradation, with a higher rate occurring in the Ethiopian highlands and upper Blue Nile Basin (Tamene et al., 2022; Gashaw et al., 2018).

Climate change is expected to increase soil erosion processes through increases in intensity and variation of precipitation integrated with temperature regime changes. Various studies have assessed future soil erosion under climate change and reported increasing erosion and sediment trends. For example, studies in the Kagera basin (Li et al., 2021), West Africa (Adeyeri et al., 2024), Agewmariam watershed (Girmay et al. 2021), Andit Tid (Woldemariam, Ddumba, & Addis, 2024), and Abay basin (Adem et al. 2016) projected increased erosion risks under future climate scenarios. However, the majority of previous studies used CMIP5 climate projections, which have now been replaced by the more advanced CMIP6 framework, which offers updated socioeconomic pathways and better representation of climatic processes.

Soil erosion is still a problem in Ethiopia despite continuous efforts to measure erosion rates and map their spatial distribution (Hurni et al., 2015). One example is the Grand Ethiopian Renaissance Dam (GERD), which is threatened by sedimentation from upstream catchments and currently receives an estimated 300 million tons of sediment annually (Hurni et al., 2015). The construction of the dam commenced in 2011, reservoir filling began in 2020 (Figure 1.1), and hydropower generation started in 2022.

Figure 1.1: Satellite Image Showing the Grand Ethiopian Renaissance Dam (GERD) Reservoir during the Initial Filling Stage in 2020. Source: NASA Earth Observatory

Practical erosion modeling tools and well-informed land management plans that take into consideration the nation's varied landscapes and climate variability are necessary to address this problem. Managing sediment sources within upstream watersheds is essential to prolong the operational lifespan of the GERD and maintain its efficiency. The Beressa watershed was selected for this study because its agroecological, topographic, and land use characteristics are representative of much of the Ethiopian highlands. Site-specific assessments are necessary because watershed characteristics such as land use type, slope, size, and existing management practices influence erosion vulnerability under changing climatic conditions (Addis et al., 2016).

Although many studies assessed the impacts of climate change on soil erosion in Ethiopia, the application of CMIP6 projections for evaluating future erosion and sediment dynamics is limited. In addition, the evaluation of best management practices under future climate scenarios is limited. This gap in knowledge constrains the development of climate-resilient planning strategies capable of addressing future erosion risks. Erosion models provide cost-effective alternatives to field-based measurements for estimating sediment and erosion risks and supporting management decisions. Among these, the Soil and Water Assessment Tool (SWAT) has demonstrated significant effectiveness in modeling erosion dynamics and evaluating BMP effectiveness under varying climatic conditions (Pandey et al., 2021). Therefore, integrating the SWAT model and CMIP6 climate projections improves understanding of climate-driven erosion processes and supports climate-resilient watershed planning through the identification of effective soil conservation measures under changing climate conditions.

1.2 Statement of the Problem

Climate change is projected to worsen soil erosion through changes in rainfall patterns and intensity, which affect soil moisture and runoff generation. In Ethiopia, especially in the Upper Blue Nile basin, soil erosion remains a significant environmental and agricultural issue (Haregeweyn et al., 2017). It reduces crop production and leads to sedimentation in water bodies. Studies in Ethiopia have reported significant increases in soil loss and sedimentation under future climate conditions (Girmay et al., 2021;

Woldemariam, Ddumba, & Addis, 2024; Tullu & Tumsa, 2024). Climate projections for Ethiopia further indicate increases in temperature and changes in rainfall variability (Alaminie et al., 2021; Enyew et al., 2024), which may increase erosion and sediment transport in the future. For example, the Grand Ethiopian Renaissance Dam is already facing sedimentation issues caused by poorly managed upper catchments and unsustainable farming practices (Hurni et al., 2015), highlighting the need for effective watershed management and sediment control measures.

The majority of previous studies in Ethiopia have projected future soil erosion using CMIP5 climate models and generally reported increasing trends under changing climatic conditions. However, the use of the more advanced CMIP6 projections remains limited in the upper Blue Nile Basin. Although the impact of climate change on soil erosion has been studied in several watersheds, such as Andit-Tid, Megech, and Nashe (Admas, Melesse, & Tegegne, 2024; Woldemariam, Ddumba, & Addis, 2024), the potential impacts of future climate change on erosion and sediment dynamics in the Beressa watershed remain unknown. In addition, traditional farming practices, increased land-use pressures, and steep slopes in the Beressa watershed make the watershed more vulnerable to climate-driven changes in runoff and sediment yield. Lastly, no previous studies have evaluated the effectiveness of best management practices (BMPs) for reducing sediment yield under projected climate conditions. These gaps constrain the development of climate-resilient watershed management strategies and evidence-based conservation planning. Therefore, this study aimed to integrate CMIP6 climate projections into SWAT modelling to assess erosion and sediment dynamics and to evaluate the effectiveness of selected BMPs under changing climatic conditions in the Beressa watershed.

1.3 Objectives

1.3.1 General Objective

The general objective of the study was to evaluate the impacts of climate change on soil erosion and sediment yield in the Beressa watershed, and to identify effective mitigation strategies for sustainable watershed management.

1.3.2 Specific Objectives

The specific objectives of the study were to:

1. Quantify the effects of climate change on soil erosion and sediment yield in the Beressa watershed using the Soil and Water Assessment Tool (SWAT).
2. Analyze the spatial and temporal dynamics of erosion and sediment hotspots in the Beressa watershed under future climate scenarios.
3. Assess the effectiveness of selected best management practices (BMPs) in reducing sediment yield under projected climate conditions in the Beressa watershed.

1.4 Research Question

1. To what extent does climate change affect soil erosion and sediment yield in Beressa Watershed under projected climate scenarios?
2. How do the spatial and temporal patterns of soil erosion and sediment yield hotspots change across the Beressa Watershed under future climate scenarios?
3. To what extent can selected best management practices (BMPs) reduce sediment yield in the Beressa Watershed under projected future climate conditions, and which practices are most effective?

1.5 Justification of the Study

This study provides scientific evidence to support sustainable watershed management and soil conservation planning in the Beressa Watershed. By integrating advanced climate projections (CMIP6) and the Soil and Water Assessment Tool, the study generates quantitative information on future erosion and sediment dynamics for a better understanding of areas that may require priority intervention. Climate projections from CMIP6 offer the most up-to-date, scenario-based representation of future climate and capture climate uncertainty across emission pathways. The identification of erosion and sediment hotspot areas can help decision-makers allocate resources efficiently and design targeted land management interventions. In addition, the evaluation of best management practices under projected climate conditions provides practical guidance for choosing effective soil and water conservation measures. The Beressa watershed was selected because it has sufficient data for SWAT model simulation and is representative of the Ethiopian Highlands in terms of topography, land use, and erosion processes. In addition, sediment generated from upstream watersheds contributes to reservoir sedimentation, which can reduce storage capacity and affect the operation of downstream hydraulic infrastructure, including the Grand Ethiopian Renaissance Dam (GERD) (Hurni et al., 2015). The findings of this study will support government agencies, watershed managers, and local communities in making informed decisions for soil and water conservation. Furthermore, the methodological framework and findings may serve as a reference for similar watersheds in Ethiopia and other regions facing comparable environmental challenges.

1.6 Scope and Limitations of the Study

1.6.1 Scope of the Study

The study assessed climate change impacts on soil erosion and sediment yield in the Beressa watershed and evaluated selected best management practices for reducing future erosion risks. The analysis was conducted by integrating the SWAT model and CMIP6 climate projections under SSP2-4.5 and SSP5-8.5 scenarios. SSP2-4.5 was selected because it represents an intermediate greenhouse gas emission pathway under moderate climate mitigation, while SSP5-8.5 represents a high-emission pathway with limited mitigation efforts. These scenarios provide a realistic range of future climate conditions, making it possible to evaluate watershed responses and the effectiveness of best management methods in both moderate and extreme climate change scenarios. The Spatial analysis, hotspot identification, and sub-watershed comparisons were performed using ArcGIS 10.5. The temporal scope of the study covers the baseline period (1995–2023) and future climate projections for the near-future (2030–2059) and far-future (2060–2089) periods. The baseline analysis was based on observed climate data, while the future assessments were driven by selected CMIP6 climate projections. The findings are intended to support climate adaptation planning and sustainable watershed management in the study area.

1.6.2 Limitations of the Study

This study has several limitations that should be considered when interpreting the results. First, observed records of wind speed, relative humidity, and solar radiation were unavailable for the study area. These variables were simulated using the SWAT weather generator based on the default long-term weather statistics provided in the SWAT weather generator database. Although this approach is widely adopted when complete meteorological records are unavailable, the simulated weather variables may introduce uncertainties into evapotranspiration, hydrological simulations, and sediment yield estimates. Second, the assumption of constant land use during the simulation period fails to account for potential future changes in land use, which could affect the accuracy of the projection. Increases in agricultural expansion, urbanization, and deforestation may lead to underestimation of future sediment yield, whereas expanded conservation measures or reforestation may result in overestimation of future sediment yield. Third, CMIP6 climate projections were bias-corrected before being used in the SWAT model, with Distribution Mapping applied to temperature and Power Transformation applied to precipitation to reduce systematic biases relative to the observed climate data. However, bias correction cannot completely eliminate uncertainties arising from climate model structure, coarse spatial resolution, and the representation of localized extreme events, which may affect the simulated hydrological and sediment responses. Finally, although SWAT is widely used for watershed and erosion studies, different hydrological models may produce varying results due to differences in model structures and assumptions.

CHAPTER TWO

LITERATURE REVIEW

2.1 Soil Erosion and Sedimentation

Soil erosion is a major environmental problem that plays a key role in accelerating land degradation. The process involves the depletion of surface soil at a pace that exceeds its replenishment by inherent environmental agents like water and wind, or by human activities such as agricultural methods like plowing. Accelerated soil erosion depletes fertile topsoil, reduces agricultural productivity, degrades ecosystem services, and threatens long-term food security (Jenny et al., 2019; FAO, 2020). Soil erosion is a major challenge, particularly in tropical and sub-tropical regions, resulting from intense rainfall and land use pressures for agriculture. Land degradation affects large areas of agricultural lands and contributes significantly to economic losses ($8 billion), reduced crop yields, and reduced soil fertility (FAO, 2020). These indicate that soil erosion impacts go beyond environmental issues because it leads to economic challenges that undermine sustainable development.

Sedimentation is a direct consequence of soil erosion and has a significant impact on water resource management. The transported sediment from upland areas is deposited in water bodies, irrigation canals, and reservoirs. This leads to reducing storage capacity, impairing water quality and affecting hydropower generation and irrigation performance (Friedman et al., 2018; Gurmu et al., 2021). In Africa, erosion and sedimentation are identified as major constraints to water resource and sustainable land management, mainly from cultivated lands (Kroese et al., 2020). In sub-Saharan Africa, the soil erosion rate ranges from 0 to 650 Mg/ha/year in different basins (Tamene, Lulseged & Bao, 2015).

In Ethiopia, soil erosion is one of the causes of land degradation, particularly in the highland areas where steep slopes, intense rainfall, and high population pressures interact to increase soil loss. Evidence from previous studies showed erosion rates vary with agro-ecologies (Tamene et al., 2022) and lead to a decline in soil fertility and agricultural productivity (Tilahun & Desta, 2021), as a result, agricultural GDP reduced by 10% to 11% (Tsegaye, 2019). Sedimentation from upstream catchments affects irrigation infrastructure and hydropower facilities (Friedman et al., 2018).

Climate change is expected to further influence erosion and sedimentation risks due to increased rainfall. Extreme events can enhance soil detachment and transport, whereas increased temperature may reduce the protection capacity of vegetation when intense storms occur. These process-based interactions indicate that future soil erosion responses will depend on changes in climate, watershed characteristics, and land management practices. Therefore, understanding these dynamics helps to develop effective soil and water conservation strategies under changing climatic conditions.

2.1.1 Previous Studies in the Beressa Watershed

The study watershed is an ideal area for study because of the availability of weather and hydrological stations, and it represents most areas of the Ethiopian highlands. Existing studies mainly focused on land use land cover (LULC) dynamics, hydrological responses, and socio-economic aspects of watershed management. LULC analyses in the Beressa watershed showed significant changes in vegetation cover, agricultural expansion, and ecosystem services within the watershed (Amsalu et al., 2007; Worku et al., 2016; Yohannes et al., 2020; Yohannes, Soromessa, Argaw, & Warkineh, 2021). These studies enhance understanding of the impact of landscape changes on watershed processes; however, interactions with climatic factors have not been well studied. Similarly, agricultural expansion and unsustainable land management practices increased runoff generation and sediment yield (Worku et al., 2017; Yohannes, Soromessa, Argaw, & Dewan, 2021). However, these studies mainly focused on land use impacts and did not clearly evaluate the impact of climate change on hydrological and erosion processes. Lastly, socioeconomic studies have also been conducted, including farmers' perceptions of land degradation (Meshesha & Tripathi, 2017), the influence of population growth on landscape transformation (Yohannes et al.,2020) , and the contribution of tree planting to rural livelihoods (Worku et al., 2018). Although these studies give important insights into local management practices and human-environment interactions, the interaction between climate variability, socioeconomic drivers, and erosion processes is not well understood. Overall, previous studies in the Beressa watershed emphasize LULC impacts, but neglect climate-socioeconomic interaction. This knowledge gap highlights the need for studies integrating climate change impacts on watershed hydrology and erosion processes and evaluating the effectiveness of BMPs under varying climatic conditions.

2.2. Climate Change Effects on Soil Erosion

Climate change is a change in climate caused directly or indirectly by human activities that alter the composition of the global atmosphere, in addition to natural climate variability observed over comparable periods. The average global temperature over land areas has increased by 1.59°C over the last decade compared to the pre-industrial period (IPCC, 2021). Climate change contributes to increased sediment yield by intensifying soil erosion processes. Empirical evidence from the Elbe River Basin indicates that climate change is contributing to increased erosion rates and sediment transport, with projections showing up to a 14% rise by the end of the century (Uber et al., 2022) . Soil erosion is likely to become worse globally, threatening ecosystem services and human well-being (Eekhout & Vente, 2022); particularly significant impacts are expected in semi-arid regions.

In Africa, 62.5% of the causes of land degradation are related to climate change (Sivakumar, 2011). For example, a study conducted in the Kagera basin of the Eastern African Highlands by Li et al. (2021) found that 90.32% of the region was more impacted by climate change than by human activity. This highlights the importance of taking into account both human and climate change impacts when promoting sustainable development. Similarly, research conducted in West Africa has shown that soil erosion is likely to increase under future climate scenarios, with the highest increases predicted to occur in Benin and Nigeria (Adeyeri et al., 2024). Other studies in South Africa show an annual increase in sediment yield of up to 10% throughout the century (Theron, 2021). Additionally, the study in Côte d’Ivoire indicates that climate change could increase sediment fluxes by 14.42% -17.95% (N’dri, Pistre, Kouamé, & Jourda, 2021). Finally, Kenyan-based studies show increases in soil loss rates between 29% and 60% as a consequence of climate change (Watene et al., 2021). Overall, evidence from Africa also shows that climate change is a significant factor in aggravating on-site and off-site erosion risks. This highlights the need for agroecology-based soil and water conservation measures.

In Ethiopia, Future projections based on CMIP5 climate data show an increasing trend of soil loss caused by changes in rainfall patterns and land use (Belay & Mengistu, 2021; Moges et al., 2020). Although various studies addressed climate change and land use change impacts on soil erosion and sediment yield (Mohammed, 2020; Jilo et al.,2019; Chimdessa et al.,2019; Sirikaew et al.,2020; Girmay et al.,2021), they did not evaluate the performance of BMPs under changing climate conditions, incorporate CMIP6 climate projections, and clearly address climate uncertainty. Climate change affects soil erosion processes through various interacting processes. For instance, high intensity of rainfall produces greater runoff and erosive energy (Alavinia, Saleh, & Asadi, 2019), whereas temperature rising influences soil moisture conditions and infiltration capacity, weaken the structure of soil, increases organic matter decomposition (Reinsch et al., 2024; Dowdeswell-Downey et al., 2023). Additionally, a reduction in vegetation cover can further reduces the soil protection capacity and increases its vulnerability to climate driven erosion.

A small number of extreme rainfall events contributes large proportion of annual erosivity (Bezak, Mikoš, Borrelli, Liakos, & Panagos, 2021), which are expected to become more frequent and intense under projected climate conditions. Due to this sediment yield exhibits nonlinear response, with disproportionately high sediment yield happed on years having more extreme rainfall events than the years having normal rainfall conditions (Chen et al., 2025). Overall, previous studies highlight the need for studies that integrate CMIP6 climate projections and BMPs evaluation under changing climatic conditions for reducing climate driven sediment dynamics.

2.2.1 Sediment Delivery Ratio (SDR)

The Sediment Delivery Ratio is defined as the proportion of eroded soil transported to a watershed outlet, which connects gross soil erosion occurring within the watershed and sediment yield measured at the outlet (Gelagay, 2016; Rajbanshi & Bhattacharya, 2020). As not all eroded material reaches the watershed outlets, SDR is widely used to estimate gross soil erosion from the SWAT model sediment yield. Watershed characteristics such as drainage area, slope, vegetation cover, and hydrological connectivity influence sediment transport (Halder, 2023), specifically during high-intensity rainfall events. A large amount of sediment export during a few extreme storm events indicates the role of event-based sediment transport in watershed sediment dynamics. The occurrence of extreme rainfall events integrated with changes in hydrological conditions may increase the amount of eroded sediment reaching the watershed outlet (Zhang et al., 2024).

Various approaches have been applied to estimate SDR, including area-based empirical relationships (Williams & Berndt, 1972), relief length ratio methods (Renfro & Waldo, 1983) , spatially distributed approaches (Ferro & Porto, 2000) and connectivity based methods using sediment connectivity indices (Yigez et al., 2023). Among these, area based empirical equations remain widely used in data scarce regions because of its relatively low data requirements and their simplicity (Bhattacharya, Chatterjee, & Das, 2020; Saygın et al., 2014). In the SWAT model, sediment yield is estimated at the watershed outlet, and the SDR is required to relate modeled sediment yield to gross soil erosion occurring across the watershed. Therefore, SDR are important to convert SWAT simulated sediment yield into total soil erosion for more comprehensive understanding of erosion process in the watershed under changing climate conditions.

2.2.2 Future Climate Model Selection

The Coupled Model Intercomparison Project Phase 6 (CMIP 6) is the most recent generation of global climate models (GCMs) used for understanding climate change impacts on hydrological and environmental systems (Carvalho et al., 2022). Compared to CMIP5, CMIP6 offers higher spatial resolutions, better representation of climate processes, and updated socioeconomic scenarios (Stouffer et al., 2017; Bayar et al., 2023; Martel et al., 2022), which enhances the reliability of future climate projections. However, uncertainties remain among climate models because different models simulate atmospheric and land surface processes differently (Guo et al., 2022). To reduce these uncertainties, the use of multiple climate models and uncertainty analysis, and also using accurate bias correction techniques, is important to enhance confidence in climate change studies. CMIP6 contains Shared Socioeconomic Pathways (SSPs), which combine future socioeconomic development pathways and greenhouse gas emissions trajectories (Riahi et al., 2017). Among five scenarios, SSP2-4.5 (Middle of the Road with Intermediate Emissions) and SSP5-8.5 (Fossil-fueled Development with High Emissions) (Welch, 2024) are widely used to assess the range of possible future climate conditions and associated environmental impacts.

As Climate data from GCMs are too coarse for watershed-scale studies, regional downscaling and bias correction are important to capture local climatic characteristics and to use the data for hydrological modeling. Additionally, selecting an appropriate model is also important because the performance of climate models varies across regions. In Ethiopia, various statistical performance metrics such as coefficient of determination(R^2), root mean square error(RMSE), and percent bias are used to evaluate the performance of several GCMs under CMIP6 in reproducing observed temperatures and precipitation patterns (Alaminie et al., 2021). Among the evaluated GCM models, the MRI-ESM2-0 model showed better performance for temperature simulation, whereas the BCC-CSM-2MR model performed best for precipitation simulation in the upper Blue Nile Basin (Alaminie et al., 2021).

2.3 Soil Erosion and Sediment Hotspot Areas

Soil erosion hotspots are locations within a watershed that experience disproportionally high soil loss rates, whereas sediment hotspots are areas that contribute the largest amount of sediment transport to the watershed outlet. The interaction of topography, rainfall characteristics, soil properties, land use, and human activities influences the shifts in erosion and sediment hotspots (Guo et al., 2021). Identifying hotspot areas is important for targeting conservation measures and optimizing watershed management interventions.

Various techniques were used to identify erosion hotspot areas in different watersheds. The revised universal soil loss equation(RUSLE) is widely used because of its simplicity and less data requirements (Munye,2022), but it estimates average annual soil loss and does not simulate sediment yield within the watershed. The water erosion prediction project (WEPP) model gives a more detailed representation of erosion hotspots (Admas et al.,2022), but its applicability in data-scarce regions is limited (Brazier, Beven, Freer, & Rowan, 2000). SWAT simulates sediment yield at sub-watershed level and specifically for sediment hotspot area identification. Remote sensing and GIS-based techniques such as multi-criteria decision analysis(MCDA), principal component analysis(PCA), and Google Earth Engine (GEE) are currently useful for spatial mapping of erosion-prone areas but are not effective for hydrological and sediment transport processes (Fentaw & Abegaz, 2024; Usman et al.,2023).

Climate change, particularly increased rainfall intensity, can shifts erosion and sediment hotspots from one sub watershed to another. Future projections of climate impact studies on erosion process provides a basis for ranking sub watershed based on vulnerability to climate driven erosion. This enables conservation resources to be allocated efficiently to areas expected to become more vulnerable under changing climatic conditions. The severity of erosion hotspots for sub watersheds is evaluated by comparing the estimated soil loss with the tolerable soil loss limit (TSL). At this threshold, soil erosion is nearly equal to soil formation. The soil loss tolerance for Ethiopian highlands is less than 11Mg/ha/year (Hurni, 1983). Soil loss exceeding this threshold poses a serious threat to land sustainability and highlights areas requiring priority intervention. Generally, Identifying current and future erosion and sediment hotspots are important to maintain soil productivity, reducing downstream sedimentation, and enhancing climate resilient watershed management strategies.

2.4 Soil Erosion Control Measures

Soil erosion leads to a decline in soil fertility and crop yield due to soil organic matter removal (Pimentel et al., 1995). Conservation methods are essential to reduce erosion risks, ensure long-term food security, and environmental sustainability. The evolution of soil erosion control is summarized into three phases: site erosion control from the 1930s to the 1980s, watershed management from the 1980s to the 2010s, and sustainable management starting in the 2010s. Numerous erosion control strategies have been implemented worldwide. Wen et al. (2023) identified around 183 soil erosion control techniques: 83 engineering techniques, 76 cropping techniques, and 22 biological techniques. The applicability of these measures depends on watershed characteristics such as soil type, climate, topography, and land use type. Soil conservation methods were not managed uniformly in terms of time and space (Wen & Zhen, 2020). Because the performance of physical and biological conservation measures significantly varies across watersheds. Therefore, conservation measures that have better effectiveness in one watershed may not achieve similar performance in another watershed due to variation in biophysical conditions.

Farmers in Africa have reported that physical soil and water conservation (SWC) techniques, such as bunds, improve crop production and decrease erosion (Betela & Wolka, 2021). SWAT-based studies in Ethiopia by Wang and J.Cao (2021) documented that filter strips, stone/soil bunds, and reforestation reduced sediment yield by up to 76% at the watershed level. Similarly, Hu (2022) and Xu et al. (2023) reported that conservation tillage, terracing, and contour farming significantly mitigate soil erosion and sedimentation. For example, contour farming has the potential to decrease sediment yield by as much as 54% (Gathagu, Mourad, & Sang, 2018), and reduced tillage reduces sediment delivery by 61% when compared to conventional tillage (Seitz et al., 2019). Terracing and contouring have also been shown to reduce sediment yield in the Tekeze watershed (Hailu, Mishra, & Jain, 2023). The varying performance of these practices is partly related to their different mechanisms of action. For example, Terraces primarily reduce runoff velocity and sediment transport, whereas conservation agriculture and contour farming enhance infiltration and reduce soil detachment. Therefore, combining two or more BMPs often provides greater erosion control than implementing individual measures alone.

Climate change significantly influences watershed management by altering hydrological processes, runoff magnitude, and sediment yield. Rainfall patterns in Ethiopia are variable and erosive, which deteriorate conservation structures and increase maintenance requirements (Amare & Simane, 2017; Bojago et al., 2022). Beyond reducing soil erosion, effective conservation measures can enhance carbon sequestration within watersheds (Shelar et al., 2023). Conservation measures such as reforestation, reduced tillage, and agricultural land abandonment help to mitigate the climate-driven erosion process (Eekhout & Vente, 2022; Gelete et al., 2019). However, the long-term effectiveness of BMPs may also change under future climate conditions.

For instance, the occurrence of more intense rainfall and more frequent extreme storm events can reduce the effectiveness of some conservation structures by exceeding their design capacity.

To ensure these measures remain effective in the future, incorporating climate change projections during the planning phase is vital for their long-term sustainability and success (Yadeta et al., 2020). Therefore, evaluating BMPs under changing climatic conditions is important for identifying effective conservation strategies under changing rainfall and runoff conditions. Although many studies evaluated the effectiveness of BMPs under current climatic conditions, their long-term performance under future climate conditions remains uncertain. Overall, to address the uncertainties associated with future climate change, evaluating the performance of individual and combined BMPs under projected climatic conditions is important for identifying effective management strategies and prioritizing conservation investments.

2.5 Erosion and Sediment Modeling

Globally, models such as the Soil and Water Assessment Tool (SWAT), the Revised Universal Soil Loss Equation (RUSLE), the Water Erosion Prediction Project (WEPP), and the Integrated Valuation of Ecosystem Services and Tradeoffs (InVEST) are widely employed to evaluate the effects of climate change on the erosion process.

WEPP provides detailed process-based simulations at the small catchment scale, but the requirements of high-resolution input data make it difficult to calibrate for larger watersheds (Brazier et al., 2000). Its data requirements limit its usefulness for climate change studies, especially when future climate projections are used. In contrast, SWAT's semi-distributed structure allows for spatially detailed simulation of large, diverse watersheds by separating them into sub-basins and hydrological response units (HRUs) (Arnold et al., 2012). Therefore, SWAT is more suitable than WEPP for watershed-scale studies, particularly in data-scarce regions such as Ethiopia's highlands and under future climatic scenarios. However, the quality of input data and sensitivity of model performance related to runoff generation, channel routing, and sediment transport may introduce uncertainties into SWAT simulation results (Nguyen et al., 2019).

Unlike InVEST, SWAT simulates the full water balance, which allows identification of the complex interactions between climate variability and hydrological processes that cause sediment transport, offering more reliable insights into future erosion hazards (Van Griensven et al., 2012). Similarly, RUSLE is a popular empirical model for estimating average yearly soil loss using static variables such as rainfall, soil, topography, and land use type (Fernández & Vega, 2018). SWAT, on the other hand, combines hydrology, sediment transport, and nutrient cycling to allow for dynamic simulations of erosion, sediment transport, and BMP effectiveness under future climatic scenarios (Gashaw et al., 2021). This makes SWAT more suitable for assessing watershed responses under changing climatic conditions and evaluating the performance of conservation practices.

While no single model is universally applicable (Bambury et al., 2003), spatially distributed models such as SWAT have many advantages for the simulation of sediment transport dynamics at the watershed level (Pelletier, 2012). The selection of an appropriate model is dependent upon various watershed characteristics, site-specific conditions, and the accessibility of relevant data. The integration of CMIP6 climate projections and the SWAT model is emerging to evaluate future changes in runoff and soil erosion processes under different Shared Socioeconomic Pathway (SSP) scenarios (Lepcha, Pandey, & Pandey, 2026; Waheed, Jamal, Javed, & Muhammad, 2024). Such scenario-based studies help to identify the temporal and spatial vulnerability of the watershed and plan climate-resilient management strategies. However, when interpreting simulated results, uncertainties associated with climate models, emission scenarios, and SWAT parameterization should be considered.

2.5.1 SWAT Model

The Soil and Water Assessment Tool (SWAT) is a hydrological model developed by the United States Department of Agriculture (USDA) Agricultural Research Service. Currently, SWAT is the most widely used watershed modeling tool (Shrestha et al., 2021) and is ideal for conducting in-depth investigations of the soil erosion process and evaluating BMPs under varying climatic conditions (Akoko et al., 2021;

Mukundan et al., 2013; Yesuf et al., 2015). The model supports decision-making for implementing best management practices and aids watershed management initiatives and conservation programs, such as those in Ethiopia's highlands (Yesuf et al., 2015). Sediment yield estimation by SWAT is performed using integrated empirical methods such as MUSLE, which relies on rainfall and surface runoff data (Arekhi, Shabani, & Rostamizad, 2012). The integrated empirical equation (MUSLE) in SWAT helps to estimate soil erosion, sediment yield, and erosion-prone areas at the sub-watershed level (Dutta & Sen, 2018).

SWAT has been widely used in Ethiopian watersheds for climate change impact assessments and the evaluation of best management practices. For example, Gashaw et al. (2021) utilized SWAT to identify erosion hotspot areas and evaluate the effectiveness of BMPs in reducing sediment yield in the Gumara watershed. Similarly, Woldemariam, Ddumba, & Addis (2024) used the SWAT model to assess the impacts of climate change on sediment yield in the Andit Tid Watershed. Recently, Abebe et al. (2025) utilized SWAT to evaluate the performance of BMPs in reducing sediment yield of the Andit Tid watershed. Overall, the studies confirm the suitability of the SWAT model in assessing climate change impacts and evaluating best management practices for Ethiopian highland watersheds.

2.5.1.1 SWAT Model Calibration, Validation, and Uncertainty Analysis

The performance of SWAT is commonly evaluated using statistical indicators such as Nash-Sutcliffe Efficiency (NSE), the coefficient of determination (R^2), and percent bias (PBIAS) (Makumbura et al., 2022). To improve model accuracy and quantify uncertainty, SWAT is frequently calibrated using the SWAT Calibration and Uncertainty program (SWAT-CUP), which integrates several calibration algorithms including SUFI-2, GLUE, ParaSol, PSO, and MCMC (Alegre, Clara, & Franco, 2017). Among these methods, SUFI-2 is one of the most widely applied algorithms because it integrates sensitivity analysis, calibration, validation, and uncertainty analysis within a single framework (Abbaspour et al., 2007) and is more reliable for runoff and sediment simulations with acceptable levels of uncertainty (Boutaleb et al., 2022).

In SUFI-2, parameter uncertainty is initially expressed as a uniform distribution within specified ranges, and model output uncertainty is measured using 95% prediction uncertainty (95PPU) band (Kumar, Singh, Srivastava, & Narsimlu, 2017). The model performance is evaluated using the P-factor, which represents the proportion of observed data that fall inside the upper and lower limits of the 95% Prediction Uncertainty, and the R-factor, which represents the average width of the uncertainty band relative to the standard deviation of the observed data. The higher P-factor values and lower R-factor values indicate better model calibration and reduced prediction uncertainty (Abbaspour, 2015). Overall, the SUFI-2 under SWAT-CUP provides a robust framework for model calibration and uncertainty analysis, especially for hydrological and sediment simulations.

2.6 Summary of Literature Review

Soil erosion is a major contributor to land degradation, sedimentation in water bodies and infrastructure, and the general deterioration of productive lands. Climate change intensify its impacts due to increasing rainfall variability and extreme, and rising of temperature. Evidence from reviewed literature indicates future climate expected to increase runoff, soil erosion, sediment yield and changing the spatial distribution of erosion hotspots across watersheds. Among various models, SWAT is suitable for hydrological and sediment-related studies due to its effectiveness for assessing climate change impacts for erosion process and evaluating best management practices at the watershed scale. The effectiveness of BMPs varies with watershed characteristics, climatic conditions, and the nature of implementation approaches, such as individual or combined.

Most studies in Ethiopia have relied on CMIP5 climate projections shows rising trends in risks of soil erosion under future climate scenarios because of increased rainfall and shifting land cover. However, the application of CMIP6 projections for impact assessments on the soil erosion process remained limited despite their improved representation of future climate conditions. In addition, the performance of individual and combined BMPs for reducing sediment yield under future climate scenarios, potential shifts in erosion and sediment hotspots under changing climate conditions, and the uncertainties associated with climate projections and management interventions have not been well addressed. Therefore, a research gap exists in integrating CMIP6 climate projections with the SWAT model, uncertainty analysis, hotspot identification, and BMPs performance evaluation under changing climate conditions, particularly in the Upper Blue Nile Basin.

2.7 Research Gap

Previous studies mainly used CMIP5 climate projections, but studies using CMIP6 climate models are not well utilized in assessing future soil erosion and sedimentation risks. Although various studies have evaluated BMPs' effectiveness under baseline conditions, there is still a lack of understanding about their long-term effectiveness under future climate scenarios. Moreover, the impacts of climate change on soil erosion and sediment yield have not been comprehensively studied in the Beressa watershed. Therefore, there is a need for studies that integrated CMIP6 climate projections and the SWAT model to quantify soil erosion and sediment yield under changing climatic conditions and evaluate the effectiveness of BMPs for reducing sediment yield for projected climate conditions. Based on the reviewed literature, this study is among the first in the Upper Blue Nile Basin to integrate CMIP6 climate projections with the SWAT model to assess future soil erosion and sediment yield and evaluate the performance of BMPs under future climate conditions.

2.8 Conceptual Framework

The conceptual framework (Figure 2.1) outlines the methodology for assessing the impacts of climate change on soil erosion and sediment yield and for evaluating the effectiveness of Best Management Practices (BMPs) under future climate conditions using the SWAT model. The framework includes static and dynamic inputs. Static inputs include the Digital Elevation Model (DEM), soil data, and land use/land cover data, which characterize the physical attributes of the watershed. Dynamic inputs consist of climate variables, primarily precipitation and temperature. Future climate data from CMIP6 datasets were bias-corrected and downscaled before being incorporated into the model. These inputs were integrated into the SWAT model to simulate hydrological and erosion processes in the watershed. To improve model reliability, calibration and validation were performed using the SUFI-2 algorithm in SWAT-CUP. Model performance was evaluated using statistical indicators, including the NSE, R^2, and PBIAS. The model generated outputs such as water balance components and sediment yield at both the Hydrologic Response Unit (HRU) and sub-watershed levels. The calibrated model was then used to assess the impacts of future climate scenarios on sediment yield and to identify erosion-prone areas requiring conservation intervention. Based on the identified sediment hotspots, BMPs, including contour farming, terracing, conservation agriculture, and their combined application, were implemented and evaluated under different future climate scenarios. Their effectiveness was assessed by comparing simulated sediment yield before and after BMP implementation. The study findings provide a scientific basis for prioritizing conservation measures, reducing sediment yield, and supporting sustainable watershed management under changing climatic conditions.

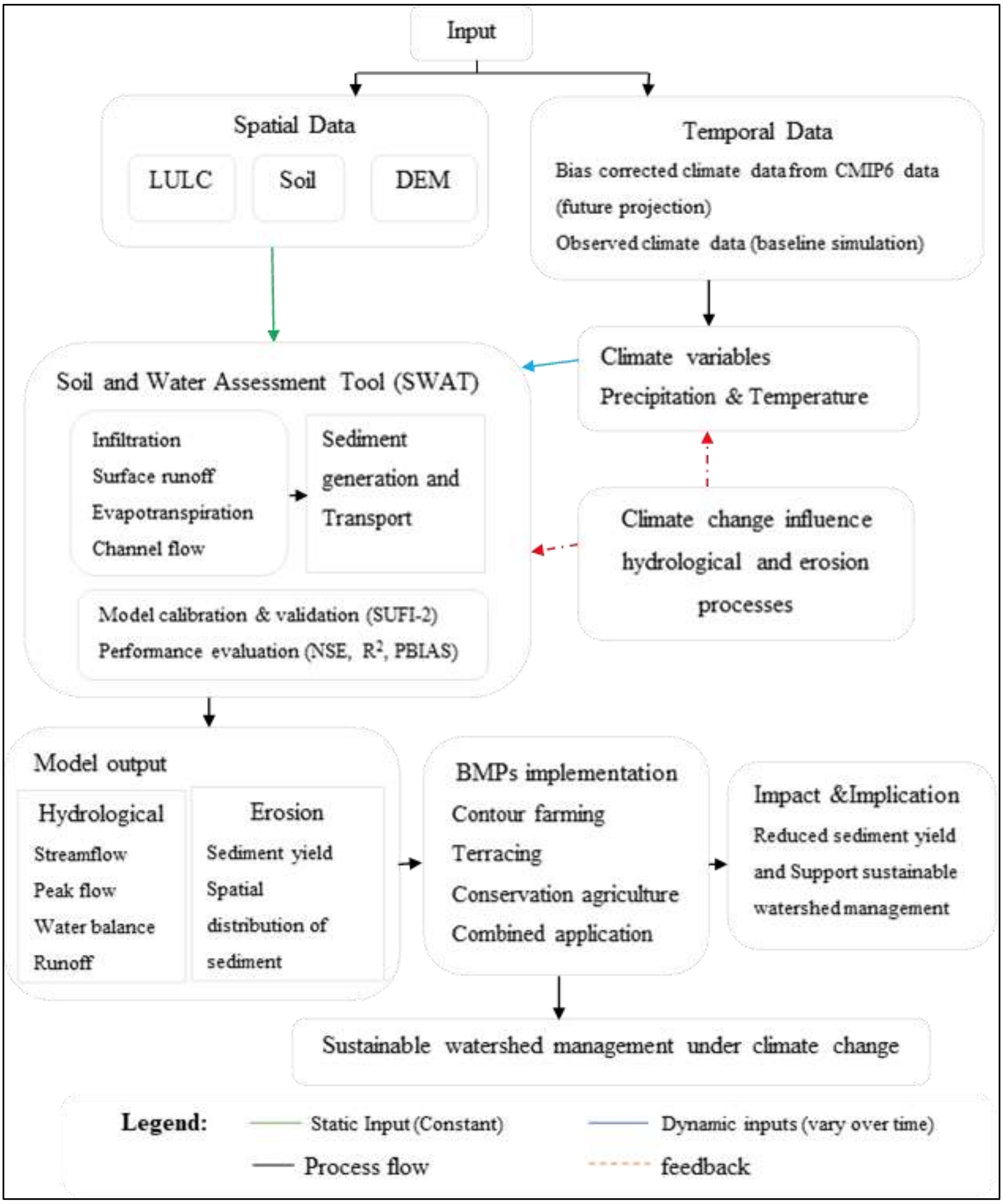

Figure 2.1: Conceptual Framework of the Study

CHAPTER THREE

MATERIALS AND METHODS

3.1 Description of the Study Area

The Beressa Watershed is located in the Upper Blue Nile Basin of Ethiopia, approximately 130 km north of Addis Ababa. It covers an area of 211.64 km^2 and lies between 39.473°E and 39.728°E and 9.535°N and 9.676°N. The topography is mountainous, with elevations ranging from 2732 to 3672 m above sea level (Figure 3.1), resulting in substantial slope variability and complex hydrological responses. The watershed spans four woredas, such as Ankober, Debre Birhan, Angolera Tera, and Basona Werena. Basona Werena and Debre Birhan have the largest share. The Beressa River is a perennial river that drains into the Jemma River, which is the main tributary of the Blue Nile. The watershed experiences a cool highland climate with three seasons: the main rainy season (Kiremt) from June to September, the short rainy season (Belg) from March to May, and the dry season from October to February. The climate is mainly controlled by seasonal rainfall, making the watershed highly dependent on rain-fed agriculture. The mean annual rainfall and temperature of the watershed are approximately 956.8mm and 13.2°C, respectively. The watershed is monitored by three meteorological stations and one river gauge station providing the data required for hydrological and erosion modelling.

The main soil types in the watershed are cambisols, vertisols, andosols, fluvisols, and regosols (Worku et al., 2018). These soils, together with steep slopes, traditional farming influences runoff generation and sediment transport. Land use is predominantly agricultural, with rain-fed farming covering more than 90% of the watershed. The major crops include barley, wheat, and faba bean, while irrigated agriculture in the downstream areas mainly produces carrots and garlic. Smallholder mixed crop-livestock farming is the dominant economic activity (Yohannes et al., 2020). Traditional farming practices and increased population pressure are increasing land use demand, reducing soil fertility, and increasing sediment generation (Amsalu & Graaff, 2006). Although physical conservation measures such as graded bunds, stone-faced bunds, and level soil bunds have been implemented, soil erosion remains a major environmental challenge. The watershed is particularly suitable for assessing climate change impacts because its agriculture is highly dependent on rainfall and its steep slopes and erosion-prone landscapes make it sensitive to rainfall variability. Additionally, the availability of meteorological and hydrological data, together with its representativeness of the Ethiopian highlands, makes the watershed an appropriate case study for assessing climate change impacts on sediment yield and evaluating the effectiveness of best management practices under changing climatic conditions.

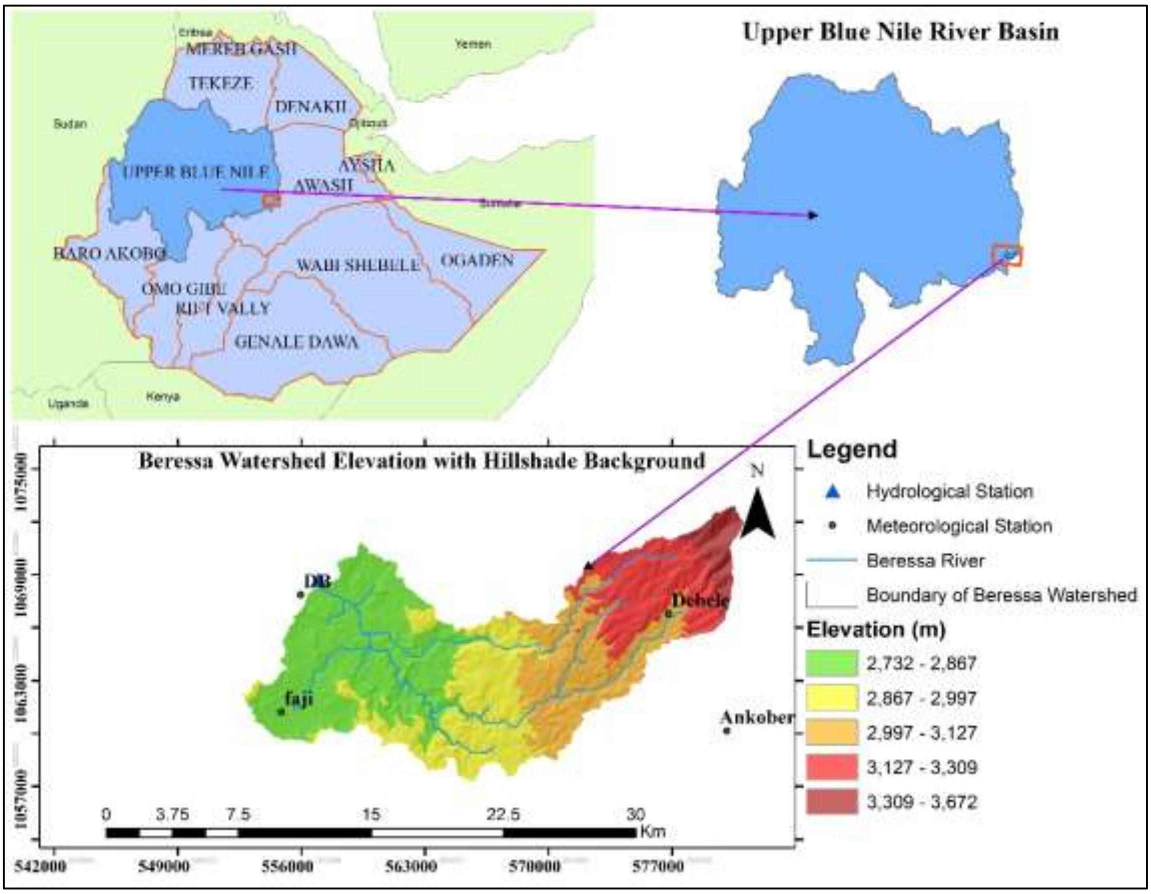

Figure 3.1: Location Map of the Study Area

3.2 Quantifying the Effects of Climate Change on Soil Erosion and Sediment Yield

3.2.1 Data Sources and Method of Data Collection

The input datasets used in this study include DEM, land use/land cover, soil, and climate data (Table 3.1).

Table 3.1: Summary of Spatial Datasets Used in the Study

Dataset	Source	Resolution	Year of data	Purpose
DEM	Alaska Satellite Facility (ASF)	12.5 m	2011	Watershed delineation, slope, and stream network generation.
LULC	ESA/Copernicus - Sentinel-2	10m	2023	Land use classification for SWAT inputs.
Soil Map	FAO/IIASA-HWSD v1.2	~1 km	2009	Define soil texture, hydraulic properties, and erosion-related parameters for the SWAT simulation.
Climate data	Meteorological stations & GCMs	-	-	Weather input

3.2.1.1 Digital Elevation Model (DEM)

The DEM with a spatial resolution of 12.5 m × 12.5 m was obtained from the Alaska Satellite Facility (ASF) DAAC website (https://asf.alaska.edu/datasets/daac/alos-palsar/). The Japan Aerospace Exploration Agency (JAXA) provides this data. This data was used to delineate watersheds, extract stream networks, assess flow accumulation, determine flow direction, and analyze other topographic factors within the SWAT model. The high-resolution (12.5m) DEM was used because it provides a more detailed representation of watershed topography, improving the accuracy of sub-watershed delineation and soil erosion assessments.

3.2.1.2 Soil Map

A key input to the model was the spatial distribution of soil properties obtained from the Harmonized World Soil Database (HWSD v1.2), which is available through the Food and Agriculture Organization (FAO) soil data portal (https://www.fao.org/soils-portal/data-hub/soil-maps-and databases/harmonized-world-soil-database-v12/en/). The database provides soil information at an approximate 1km spatial resolution, which makes it well-suited for watershed-level studies. Important soil characteristics, including bulk density, drainage characteristics, accessible water content, texture, hydraulic conductivity, and soil depth, were extracted and incorporated into the SWAT 2012 database. Additional watershed-specific soil information was included to better represent local conditions. All the input data for SWAT were gathered from FAO soil databases and the water balance model for the Eastern Nile Basin (Hassan, 2012).

Five major soil types occur within the Beressa watershed, namely Vertic Cambisols (CMv.or-6-5ac), Lithic Leptosols (Lpq/Lpe.cm5-bf), Eutric Leptosols (Lpe.or17-4e), Dystric Leptosols (Lpe.or16-4df), and Calcaric Leptosols (Lpe.cm23-4d), as shown in Figure 3.2. These soil types are predominantly characterized by light clay, silt loam, silt loam, loam, and sandy clay textures, respectively. They occupy 39.26%, 2.77%, 4.63%, 17.62%, and 35.71% of the watershed area, respectively. Light clay and sandy clay soils together account for approximately 75% of the watershed area. According to the Natural Resources Conservation Service (NRCS) classification, the dominant soils belong to hydrologic groups B and D. The soil erodibility factor (USLE_K) used in SWAT ranged from 0.2062 to 0.262 (Figure 3.3). These soil properties were used in Hydrologic Response Unit (HRU) delineation and subsequent SWAT model simulations.

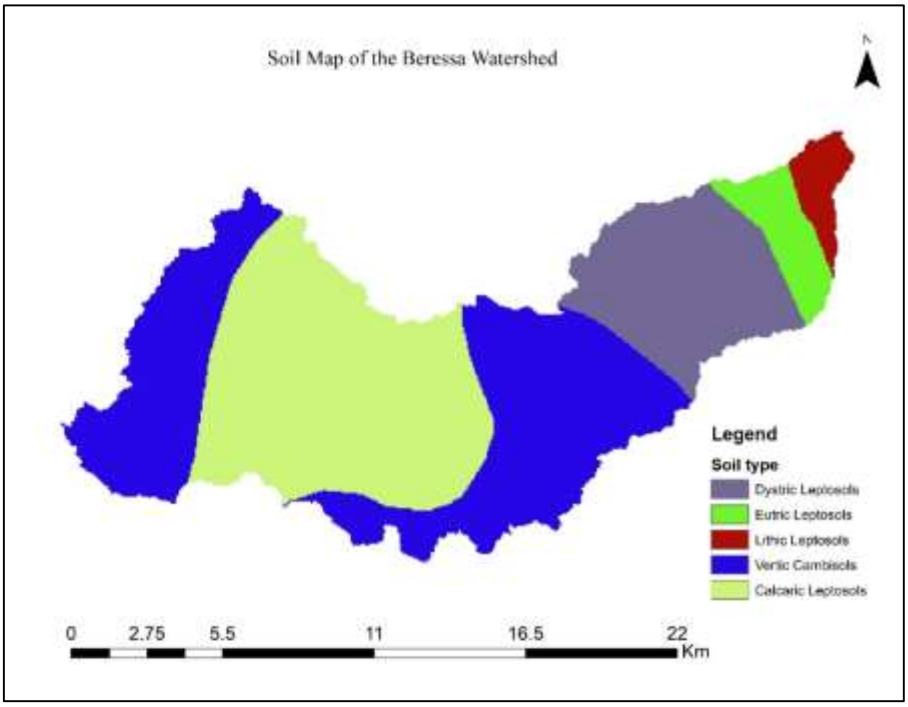

Figure 3.2: Soil Map of the Beressa Watershed

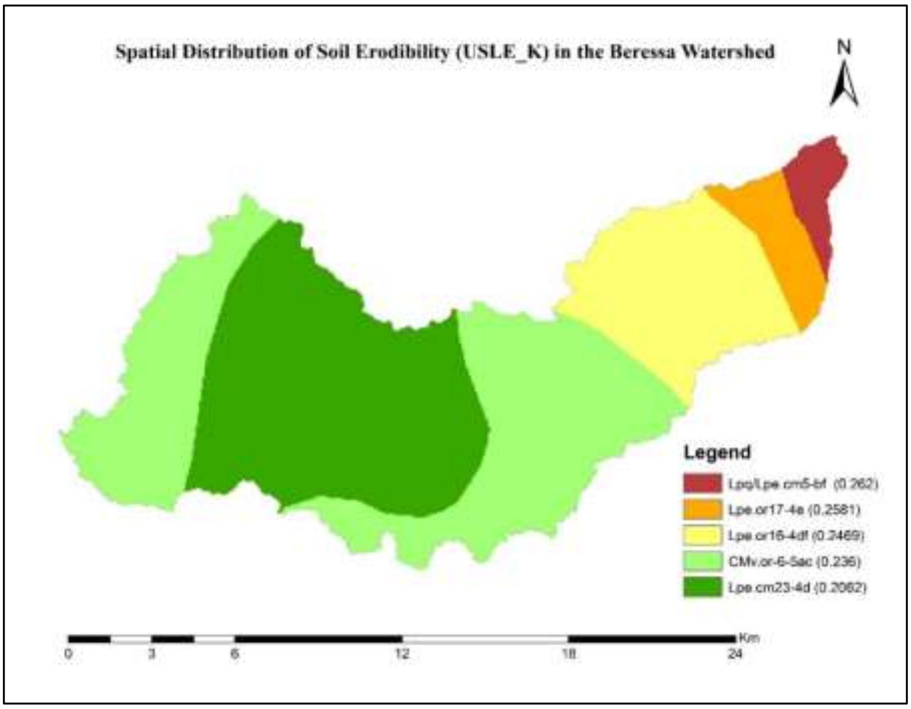

Figure 3.3: Spatial Distribution of Soil Erodibility (USLE_K) Map

3.2.1.3 Land Use and Land Cover (LULC) Map

The LULC map for the Watershed was created using cloud-free Sentinel-2 images (collected on December 28, 2023) that were managed by the European Space Agency (ESA). This information was gathered from the Copernicus Open Access Hub website (https://scihub.copernicus.eu/dhus/#/home). The 2023 LULC map was used to represent current watershed conditions, support conservation planning, and isolate climate change impacts. Sentinel-2 imagery was selected due to its higher spatial resolution to represent current land use categories compared to Landsat data. ArcGIS 10.5 was used for image pre-processing, including band composition and supervised classification. Ground truth points and high-resolution Google Earth imagery were used for accuracy assessment. Major land use types were classified using the technique (Tadese, Soromessa, & Bekele, 2021). The identified LULC classes were agricultural land, forestland, grassland, built-up areas, barren land, water bodies (Table 3.2), and their spatial distribution is presented in Figure 3.4. The final LULC classification achieved an overall accuracy of 95.2% with a kappa coefficient of 0.89, indicating excellent agreement between the classified image and reference data (Islami et al., 2022). The classified land-use categories were converted into corresponding SWAT land-use codes for model development.

Table 3.2: Land Use Classification, Area Coverage, and Description

No	SWAT_Code	LU Name	area_km^2	Percentage	Description
1	GARS	Grass Land	12.26	5.79	Land covered by grass and used for grazing purposes.
2	URBN	built area	12.92	6.10	Land covered by settlements and roads
3	AGRL	Agricultural land	170.82	80.72	Land used for crop production (perennial and fallow land)
4	FRST	Forest land	14.98	7.08	The land has 0.5 ha or more coverage.
5	BARR	Barren land	0.40	0.19	An area with little to no vegetation

6	WATR	Water body	0.25	0.12	Natural or man-made water sources

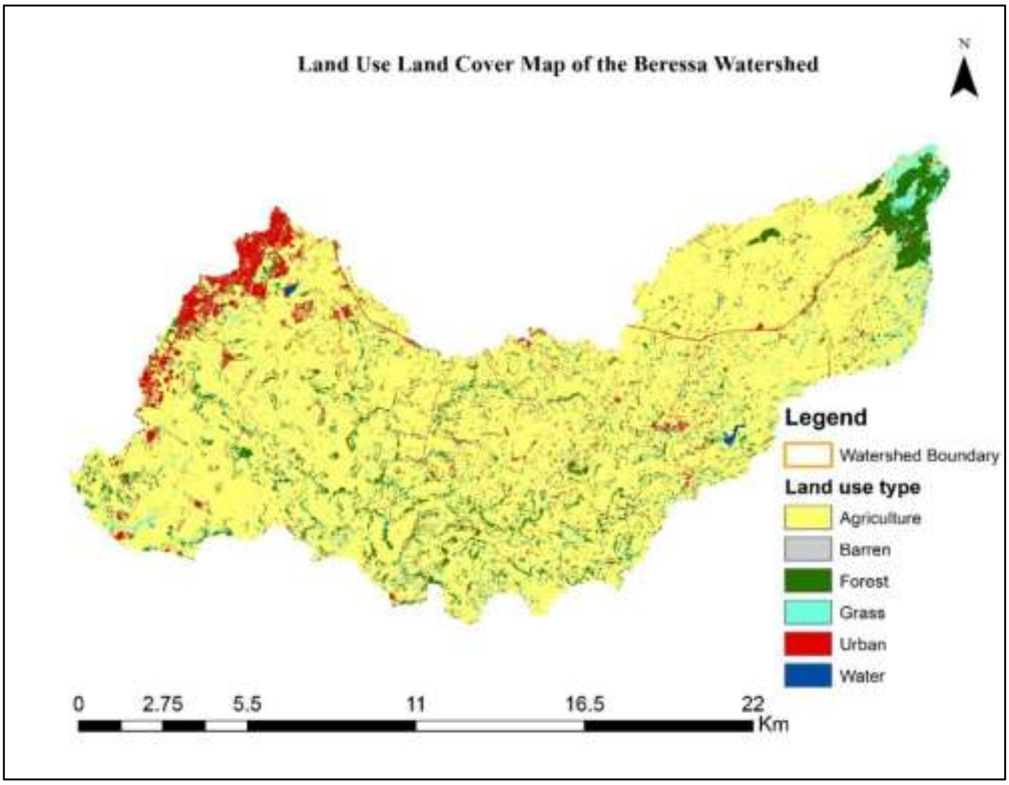

Figure 3.4: Land Use and Land Cover Map of the Beressa Watershed

3.2.1.4 Slope Map

The slope map was derived from the 12.5 m DEM using ArcGIS 10.5. The slope was categorized into five classes, such as 0–5% (flat to nearly flat), 5–10% (gentle slope), 10–15% (moderate slope), 15–30% (steep slope), and >30% (very steep slope), as shown in Figure 3.5. Slope classes greater than 10% account for 57.14% of the watershed area (Table 3.3). The classified slope map was used for Hydrologic Response Unit (HRU) definition within the SWAT model.

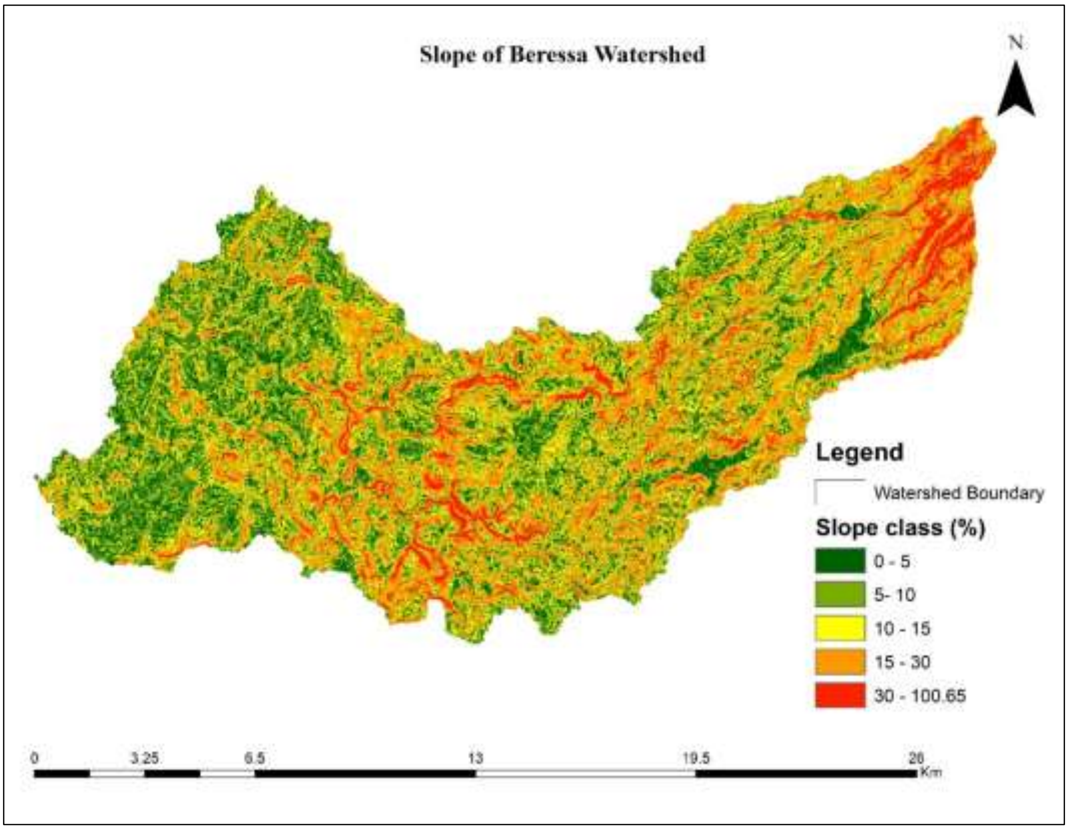

Figure 3.5: Slope Map of the Beressa Watershed

Table 3.3: Area Percentage Distribution of Slope Classes in the Study Watershed

Slope class (%)	Area_km^2	Area (%)
0-5	31.31	14.79
5-10	59.4	28.07
10-15	43.09	20.36
15-30	62.4	29.48
>30	15.44	7.30
total	211.64	100

3.2.1.5 Observed Climate Data (1993-2023)

The daily rainfall, minimum, and maximum temperatures were collected from the Ethiopian national meteorological agency office. The SWAT model used data from three stations in the Beressa watershed (Debre Birhan, Faji, and Debele) and three neighboring stations (Ankober, Gudoberet, and Mendida) (Figure 3.6). The SWAT model incorporated precipitation data from all six stations and temperature data from five stations. The SWAT model's weather generator simulated wind speed, relative humidity, and solar radiation using long-term climatic data from the nearest meteorological station. Climate inputs were compiled with the SWAT-weather database v01803 to ensure simulation suitability.

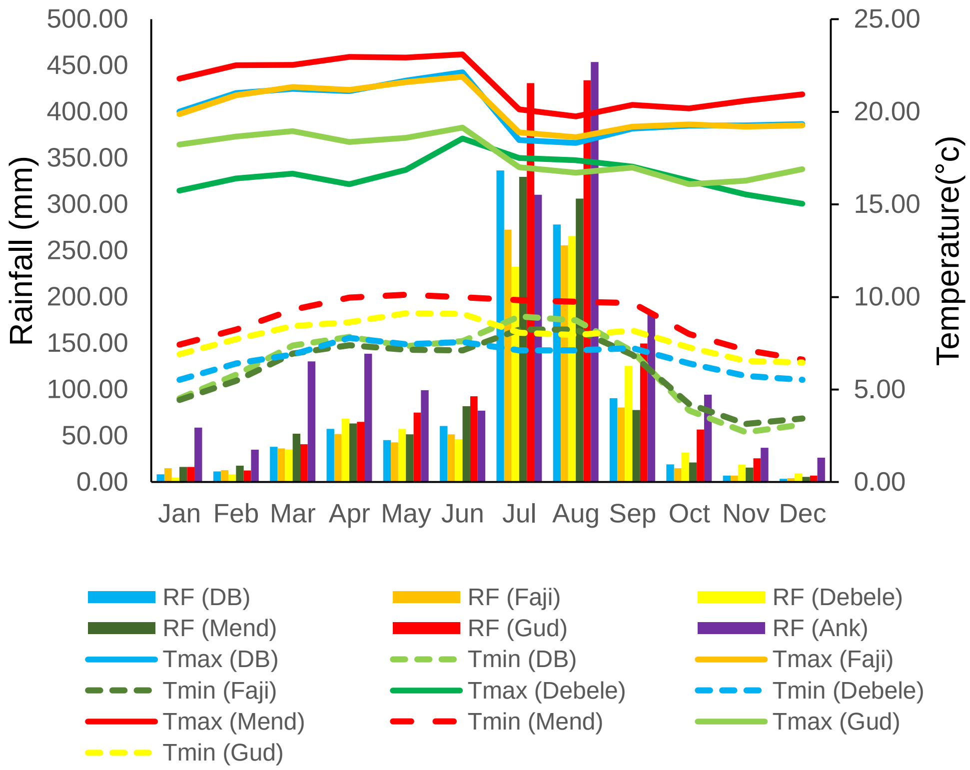

Figure 3.6: Monthly climate data for the study area stations

Table 3.4: Summary of Observed Climate Data Used in the Study

location category	station	parameter	period	data length (years)	Missing data (%)	Source
within	Debre Birhan	RF, Tmax, & Tmin	1993-2023	31	3.02	NMA
within	Faji	RF, Tmax, & Tmin	1993-2023	31	0	NMA
within	Debele	RF, Tmax, & Tmin	2002-2023	22	14.6	NMA
Adjacent	Mendida	RF, Tmax, & Tmin	1993-2019	27	0.92	NMA
Adjacent	Ankober	RF	1997-2023	27	7.5	NMA
Adjacent	Gudoberet	RF, Tmax, & Tmin	1993-2018	26	5.5	NMA

3.2.1.6 Data Checkup and Gap Filling

The data quality of observed climate data, such as daily rainfall, maximum temperature, and minimum Temperature, was checked using Excel to confirm that the maximum temperature is greater than the minimum temperature and the rainfall value is zero or above; additionally, the presence of non-numeric records was checked for each station before starting the missing data filling process. The time series data's consistency was checked using the double mass curve technique. The missing daily values were filled using the SWAT weather generator tool (https://swat.tamu.edu/software/). Filling missing data using SWAT is better than other methods to reduce uncertainty (Schuol & Abbaspour, 2007). A negative 99.0 (-99.0) value was added for missing data, indicating days of data generation (Felix & Jung, 2022).

3.2.1.7 Projected Climate Data

CMIP6 climate scenarios for historical and future daily-based shared socioeconomic pathways such as SSP2-4.5 (Middle of the Road with Intermediate Emissions) and SSP5-8.5 (Fossil-fueled Development with High Emissions) (Riahi et al., 2017) were used. The GCM climate models, the MRI-ESM2-0 model for temperature, and the BCC-CSM-2MR model for precipitation were obtained from the Earth System Grid Federation data node hosted by the Institut Pierre-Simon Laplace (IPSL) website (https://esgf-node.ipsl.upmc.fr/projects/cmip6-ipsl/). BCC-CSM2-MR and MRI-ESM2-0 climate models are relatively best in predicting the future climatic conditions of the upper Blue Nile basin (Alaminie et al., 2021). Two future periods, namely the near term (2030–2059) and the far term (2060–2089) under SSP2-4.5 and SSP5-8.5 climate scenarios were considered.

3.2.1.8 Observed Streamflow and Sediment Data

The calibration, validation, and sensitivity analysis with SWAT-CUP required continuous streamflow and sediment data. Data from the Beressa gauging station (1995–2014) were collected from the Ethiopian Ministry of Water and Energy. Observational data beyond 2014 were unavailable because hydrological and sediment monitoring at the station ceased after the monitoring project was completed. Daily streamflow records were continuous from 1995 to 2014. In contrast, observed suspended sediment concentration (SSC) data (mg/L) were scarce, with only 3 to 50 measurements recorded per year. To address this limitation, daily sediment load data were generated using sediment rating curves, following the method of Asselman (2000)(Eqn.3.1). A power-law regression equation was fitted to the logarithmic values of streamflow and sediment load.

$$SSL = xQ^y \quad \text{..........(3.1)}$$

Where: SSL = suspended sediment Load (ton/day), Q=streamflow rate (m^3/s), x and y are regression constants, which were used to estimate the relationship between available streamflow and sediment load at the Beressa gauging station. The value of y is usually between 1 and 2.

For this study, separate sediment rating curves were developed for the wet season (July-September) and dry season (October-June) using available sediment and streamflow data (Asselman, 2000; Gashaw et al., 2021). The resulting relationships from observed sediment–streamflow pairs achieved strong fits (R^2 = 0.75 for the dry season and 0.91 for the wet season). Using these equations, daily sediment loads were extrapolated from the complete daily streamflow records. The estimated daily sediment loads were evaluated against observed values for the same measured days using statistical metrics such as Nash–Sutcliffe efficiency(NSE) and Percent Bias (PBIAS) (Asselman, 2000). After this, the daily streamflow and sediment data were aggregated to monthly values for SWAT calibration and validation. Monthly data from 2002 to 2013 were selected for this purpose.

Uncertainty in sediment load estimation from a rating curve is unavoidable because of the non-linear nature of sediment discharge relationships, temporal variability and sparse sediment sampling. To minimize this uncertainty, seasonal sediment rating curves were used, which can capture diverse sediment transport dynamics during wet and dry periods and enhance the reliability of sediment load estimates in the watershed.

3.2.1.9 GCM Data Extraction and Bias Correction

Climate model output data are frequently skewed when compared to observable time series, needing correction actions (Christensen et al., 2008). There are numerous approaches to studying statistical bias correction (Teutschbein & Seibert, 2012). For this study, the CMhyd tool was used for bias correction of CMIP6 global climate model (GCM) data. It is widely used for correcting temperature and precipitation biases in climate datasets (Khalaf et al, 2022). The Power transformation was chosen for precipitation bias correction, whereas distribution mapping was utilized for temperature bias correction. These methods were chosen due to their suitability for complex topographic and mountainous regions where climate variability is high

(Enyew et al., 2024; Mukheef et al., 2024). This is especially important for the study area, where topography strongly affects precipitation and temperature distribution.

Power transformation was chosen for precipitation bias correction over delta change and distribution mapping because it adjusts both the mean and variance, which are critical for accurately reflecting precipitation variability and extremes (Leander et al., 2008). This makes it more appropriate than the delta change method, which only adjusts monthly means and assumes constant variability (Anandhi et al., 2011). Distribution mapping can perform well under ideal settings, but it is subject to biases in raw RCM results, especially in regions where models tend to misrepresent wet-day frequency (Teutschbein & Seibert, 2012).

For temperature, distribution mapping was chosen because it adequately corrects mean, variance, and quantiles, resulting in improved representation of temperature extremes (Londhe, Katpatal, & Bokde, 2023) . Simpler techniques, such as delta change and linear scaling, while keeping the general climatic indication, frequently fail to account for higher-order statistical features and may mislead temperature extremes (Beyer, Krapp, & Manica, 2020).

To ensure reliability, model evaluation techniques (Geleta & Ameja, 2022), including root mean square error (RMSE), percent bias (PBIAS), coefficient of determination (R^2), and Nash-Sutcliffe efficiency (NSE), were used for a statistical comparison between the observed and simulated datasets. Overall, the bias correction procedure was evaluated to ensure that the corrected climate variables accurately represent observed hydroclimatic conditions before being used as inputs to the SWAT model.

3.2.2 Extreme Climate Event Analysis

For this study, the 95th and 99th percentiles of the long-term daily rainfall data were used to determine severe rainfall events (Chervenkov & Slavov, 2019; Hong & Ying, 2019) . In relation to the local rainfall distribution, the 99th percentile represents uncommon and extreme rainfall occurrences, while the 95th percentile indicates intermediate intensity rainfall events. For both the baseline period (1995–2023) and future climatic scenarios under SSP2-4.5 and SSP5-8, the frequency of exceeding the

95th and 99th percentile thresholds was computed. These measurements were employed to describe variations in the frequency of intense rainfall under various climatic conditions.

3.2.3 Climate Trend Analysis

The Mann-Kendall (MK) trend test and Innovative Trend Analysis (ITA) were used to detect long-term trends in temperature and rainfall. This study adopts a hybrid trend analysis that combines MK and ITA to improve the reliability and interpretability of results. The approach combines the statistical accuracy of the MK test with the graphical clarity and distribution-free nature of ITA. The MK test provides statistical significance of monotonic trends, while ITA offers a graphical and distribution-free visualization of hidden and non-monotonic patterns. This combined use improves trend detection robustness because MK is strong in statistical hypothesis testing, whereas ITA detects sub-period variations that MK may not detect. Therefore, both methods complement each other in identifying consistent and hidden hydroclimatic trends.

3.2.3.1 Mann-Kendall (MK) Trend Analysis

The Mann-Kendall (MK) trend test is a non-parametric method used to detect monotonic trends in hydrological and climatic time series without requiring normally distributed data (Asfaw, Simane, Hassen, & Bantider, 2018). The analysis was conducted using XLSTAT software. The MK test statistic (S) was computed using Equation (Eqn. 3.2) by comparing all possible pairs of observations (Yu, Zou, & Whittemore, 1993). Positive differences increase S, and negative differences decrease it. The final S value indicates the direction of the trend, where a positive value indicates an increasing trend and a negative value indicates a decreasing trend. The variance of S (Eqn. 3.3) was calculated to account for tied values in the dataset, thereby improving the robustness of the test for hydrological and climatic time series. The statistical significance of the detected trend was then evaluated using the standardized test statistic (Z) (Eqn. 3.4) under the null hypothesis of no monotonic trend. For this study, the MK test was used to determine the presence, direction, and statistical significance of trends in precipitation and temperature.

$S = \sum_{i=1}^{n-1} \sum_{j=i+1}^{n} sign(X_j - X_i)$..
(3.2)

Where n indicates the total number of data, X_j and X_i represent the data points of time j and i.

$VAR(S) = \frac{1}{18}\{n(n-1)(2n+5) - \sum_{j=1}^{g} t_j(t_j-1)(2t_j+5)\}$..............................
(3.3)

Where t_j is the number of data points in the j^{th} tied group, g is the number of tied groups in the data, and n is the total number of observations.

$$Z = \begin{Bmatrix} \frac{S-1}{\sqrt{VAR(S)}}\ if\ s > 0 \\ 0\ if\ s = 0 \\ \frac{s+1}{\sqrt{VAR(S)}} if\ s < 0 \end{Bmatrix} \text{..(3.4)}$$

Where: Z= 0 indicates no trend, a positive Z indicates an increasing trend, and a negative Z indicates a decreasing trend.

3.2.3.2 Innovative Trend Analysis (ITA)

To supplement the Mann-Kendall (MK) test, the Innovative Trend Analysis (ITA) technique, which is proposed by Şen (2012), was used. ITA can detect both monotonic and non-monotonic trends in time series data without assuming normality or linearity (Güçlü, 2020). The time series data were divided into equal parts, sorted in ascending order, and plotted against a1:1 reference line. Points above the reference line indicate increasing trends, while those below indicate decreasing trends, and those along the line reflect no trend (Şen, 2012).

Unlike MK, ITA offers a visual interpretation of trend behavior and can show hidden trends within sub-periods that may not be indicated in the MK test. The slope of the ITA method was determined using Das et al. (2021) equation (Eqn. 3.5). In this study, ITA was used to validate and visually support the results from the MK test, ensuring consistency between statistical significance and graphical trend behavior.

$$S = \frac{1}{n}\sum_{i=1}^{n}\frac{10(X_j - X_k)}{\bar{X}} \quad \text{(3.5)}$$

Where S represents the ITA slope, n is the number of individual sub-series, X_j and X_k represent the values of the second and first half series, respectively, and $\bar{x}$ represents the means of the first half series.

3.2.4 SWAT Model Setup

3.2.4.1 Watershed and Sub-Watershed Delineation

Before starting spatial data analysis in ArcSWAT, all spatial data, including the soil map, LULC map, and DEM, were projected into the same projection, UTM zone 37°N, which is the standard projection used in Ethiopia. Once the projection has been corrected, the first step in preparing the SWAT model input is watershed delineation from digital elevation model. The main steps for watershed delineation using SWAT include DEM setup, stream definition, outlet and inlet definition, watershed outlet selection, and calculation of sub-basin parameters. The SWAT model delineated watersheds of 211.64 km^2 and 23 sub-watersheds, with a minimum flow accumulation threshold area of 500ha. This threshold was selected based on standard small watershed delineation criteria applied in Ethiopia, ensuring an appropriate balance between spatial detail and computational efficiency. From the 23 sub-watersheds, sub-watersheds 2, 8, and 9 were the smallest, whereas sub-watersheds 10,17,19,23 were the largest, covering each greater than 17 km^2.

3.2.4.2 Hydrological Response Unit (HRU) Definition

To include all potential combinations, HRUs were defined using the multiple HRU method with default thresholds for land use, soil, and slope. The selected threshold provided a reasonable balance between representing watershed heterogeneity and maintaining computational efficiency. This helps to preserve the key landscape characteristics influencing runoff, erosion, and sediment yield. The slope classification (0-5, 5-10, 10-15, 15-30, >30%) indicates lower options when considering the deposition of soil materials and nutrients during sediment transport (Zone et al.,2019; Gitima., 2022). These five slope classes were used to reflect differences in runoff and sediment transport potential within the watershed. Land use, soil, and slope maps were reclassified to match the SWAT database. A total of 1031 HRUs were created for 23 sub-watersheds.

3.2.4.3 SWAT Model Sediment Yield Computation

Once HRU creation was completed, the climate data were incorporated into the model to simulate hydrological processes and sediment yield under historical and future climate conditions. SWAT simulates the hydrological cycle based on the water-balance equation (Neitsch et al., 2009) (Eqn.3.6), which links precipitation, evapotranspiration, surface runoff, percolation, and groundwater flow. Changes in climatic variables, particularly precipitation and temperature, directly influence runoff generation and sediment transport within the watershed. Potential evapotranspiration was estimated using the Hargreaves method because it requires limited meteorological data and is suitable for data-scarce regions (Aouissi et al., 2016).

Surface runoff was estimated using the SCS Curve Number method (Eqn. 3.7), in which the retention parameter (S) was determined using Equation (Eqn. 3.8). Lastly, the sediment yield for each HRU was computed using the Modified Universal Soil Loss Equation (MUSLE) (Williams & Berndt, 1977) (Eqn. 3.9). Because MUSLE incorporates runoff volume and peak runoff rate, projected climate-driven changes in rainfall intensity and runoff influence simulated sediment yield. The MUSLE outputs were aggregated at the sub-watershed level to identify erosion-prone areas and evaluate future sediment yield responses under varying climatic conditions.

$$\mathrm{SW_t} = \mathrm{SW_0} + \sum_{i=1}^{t}\left(\mathrm{R_{day}} - \mathrm{Q_{surf}} - \mathrm{E_a} - \mathrm{W_{seep}} - \mathrm{Q_{gw}}\right) \quad \ldots\ldots\ldots\ldots\ldots\ldots\ldots\ldots\ldots\ldots(3.6)$$

Where: SW_t is the final soil water content (mm), SW_0 is the initial soil water content (mm), t is time in days, R is precipitation (mm/day), Q_{surf} is surface streamflow (mm/day), E_a is the actual evapotranspiration (mm/day), $Wseep$ is percolation (mm/day), and Q_{gw} is return flow (mm/day).

$$Q_{surf} = \frac{(R_{day} - 0.2s)^2}{(R_{day} + 0.8s)^2} \qquad \text{(3.7)}$$

Where: Q_{surf} = accumulated runoff/rainfall excess (mm), R_{day} = daily rainfall depth (mm), and S = retention parameter (mm).

$$S = \frac{25400}{CN} - 254 \qquad \text{(3.8)}$$

Where: CN represents the curve number, which is affected by land use and soil type.

$$Sed = 11.8(Q_{surf} * q_{peak})^{0.56} * K * LS * C * P \qquad \text{(3.9)}$$

Where: K=Soil erodibility factor (dimensionless), LS=slope length and steepness factor (dimensionless), C=Cover management factor (dimensionless), P=management practice factor (dimensionless)

3.2.5 Sensitivity Analysis, Calibration, and Validation

The Sequential Uncertainty Fitting version 2 (SUFI-2) algorithm under SWAT-CUP version 5.1.6.2 was used for model sensitivity analysis, calibration, and validation. SUFI-2 was chosen because of its capacity to handle uncertainty in both the conceptual model and the input data (He et al., 2021), as well as its shown applicability for streamflow and sediment modeling (Abbaspour et al., 2007; Gassman et al., 2007). Initial SWAT simulation outputs were not used for analysis. Because it may overestimate or underestimate real-world data. Therefore, sediment yield predictions were assessed through a structured process, such as sensitivity analysis, calibration, and validation.

The calibration steps followed a generally accepted approach, starting with streamflow calibration to ensure accurate water balance, followed by sediment calibration (Abbaspour et al., 2007; Arnold et al., 2012). Sensitivity analysis is performed using both automated and manual methods (Arnold et al., 2012). In the beginning, the manual method was used to define appropriate parameter ranges based on watershed characteristics and expert hydrological knowledge. Then, automatic method was conducted using SUFI-2 to optimize multiple parameters and minimize the difference between observed and simulated values (Abbaspour et al., 2007). This approach is particularly important in diverse hydrological systems (Moriasi et al., 2007).

Sensitivity analysis was carried out using the global sensitivity analysis function in SWAT-CUP. For this study, 13 parameters for streamflow and 17 parameters for sediment yield were chosen based on previous research in similar agro-ecological zones (Gashaw et al., 2021; Woldemariam et al., 2024; Worku et al., 2017; Yesuf et al., 2015). T-statistics and p-values were used to rank parameter sensitivity, with highly sensitive parameters having large absolute t-values and p-values near zero (Abbaspour, 2015). The results helped to narrow the number of parameters for the calibration and validation process and reduce computational burden.

The calibration was performed in a two-step process. Initially, a limited number of parameters was calibrated and then expanded to include all sensitive parameters. A two-year warm-up period (1993-1994) was used to reduce the impact of non-equilibrium initial conditions like soil moisture and residue cover (Addis et al., 2016). Monthly streamflow and sediment yield data from 2002 to 2009 were used for calibration, and data from 2010 to 2013 were used for validation based on the availability and continuity of reliable hydrological records. Although the validation period covers four years, it captures a range of hydrological conditions representative of watershed behavior.

3.2.5.1 SWAT Model Uncertainty Analysis

Uncertainty analysis in the SWAT model is important for quantifying the confidence in simulated outputs by considering uncertainties arising from model parameters, input data and model structure. In this study, uncertainty analysis was performed using the Sequential Uncertainty fitting version 2(SUFI-2) algorithm implemented in the SWAT CUP interface. The performance of SUFI-2 uncertainty analysis was evaluated using the P-factor and R-factor. The P-factor represents the percentage of observed data bracketed by the 95PPU band, indicating the degree of model reliability. Higher P-factor (closer to 1) indicates better model performance and stronger agreement between observed and simulated values. The R- factor measures the thickness of the 95PPU band relative to the variability of observed data. A lower value indicates higher precision of the simulation.

Mathematically,

The P-Factor calculated using the formula

$$P - Factor = 1 - \frac{\sqrt{\sum(Qi - Si)^2}}{\sqrt{\sum(Qi - Qmean)^2}} \quad \text{……………………..……………….………(3.10)}$$

Where: Qi represents the observed data, Si represents the simulated data, and Qmean is the mean of the observed data

The R- factor mathematically calculated as

$$R - Factor = \frac{\sum|\mathrm{Qi - Si}|}{\sum Qi} \quad \text{………………………………………………….….… (3.11)}$$

Where: where Qi represents the observed data and Si represents the simulated data

3.2.5.2 The Fitness of the Goodness of the Model

Evaluation statistics (Moriasi et al., 2007; Waseem et al., 2017) such as coefficient of determination (R^2), percent bias (PBIAS), Nash-Sutcliffe efficiency (NSE), and magnitude of the error (RSR) were used to evaluate model performance. The NSE evaluates the residual variance's relative magnitude in relation to the observed data. It also shows how closely the 1:1 line is followed by the presentation of observed versus simulated data. NSE values can range from -∞ to 1, with a value close to 1 indicating a better fit between observed and simulated data. The R^2 measures the proportion of variance in observed data that is explained by the model. It has a value between 0 and 1. A value close to 1 indicates a high degree of correlation and smaller error variance between observed and simulated data. The PBIAS determines the average tendency of simulated data to differ from observed data. An accurate model simulation is indicated by low magnitude values, and its ideal value is 0.0. Positive values indicate underestimation bias in the model, while negative values indicate overestimation bias. The standard deviation of the observed data is used to compute the root mean square (RSR). A value near 0 indicates better model performance, and a value greater than 0.7 indicates unsatisfactory model performance.

Mathematically,

$$NSE = 1 - \frac{\sum_{i=1}^{n}(Q_i - Q_{si})^2}{\sum_{i=1}^{n}(Q_i - Q_{mean})^2} \quad \ldots\ldots(3.12)$$

$$R^2 = [\frac{\sum_{i=1}^{n}(Q_i - Q_{mean})(Q_{si} - \text{Qsmean}Qs_{mean})}{\sqrt{\sum_{i=1}^{n}(Q_i - Q_{mean})^2 \times \sum_{i=1}^{n}(Q_{si} - Qs_{mean})^2}}]^2 \quad \ldots\ldots(3.13)$$

$$PBIAS = 100 \times \frac{\sum_{i=1}^{n}(Q_i - Q_{si})}{\sum_{i=1}^{n} Q_i} \quad \ldots\ldots(3.14)$$

$$RSR = \frac{\sum_{i=1}^{n}(Q_i - Q_{si})^2}{\sum_{i=1}^{n}(Q_i - Q_{mean})^2} \quad \ldots\ldots(3.15)$$

Where: Q_i=observed discharge, Q_{si} =simulated discharge, Q_{mean} =mean of observed discharge, Qs_{mean}=mean of simulated discharge, n=number of observations.

3.2.6 Baseline and Projected Sediment Yield Simulation

After achieving acceptable calibration and validation results, the fitted parameter values were incorporated into the SWAT model. Parameters available in the Manual Calibration Helper were adjusted directly. The parameters not listed in the manual calibration helper were edited under the SWAT input files. To ensure that changes were applied, the SWAT input files were modified once all calibrated values had been entered. Before running the simulation, the input database was checked to ensure that the fitted values were properly included.

After that, the calibrated SWAT model was used to simulate sediment yield throughout the baseline period. Future sediment yield projections were conducted under the SSP2-4.5 and SSP5-8.5 climate scenarios after the baseline simulation was completed. For these projections, the climate input files were modified to reflect projected conditions for both the near-term and far-term periods, while keeping the calibrated parameters constant. To isolate climate change impacts on sediment yield, land use was assumed to remain constant throughout all future simulation periods. Accordingly, the baseline land use map was used for both historical and future SWAT simulations.

3.2.7 Sediment Delivery Ratio and Soil Erosion Estimation

In this study, soil erosion was estimated by converting simulated sediment yield from the SWAT model into gross soil loss using the SDR (Eqn. 3.17). The SDR calculates the proportion of eroded soil carried to the watershed outlet while accounting for deposition and filtering activities along the flow channel. In the Beressa watershed, all slope classes (0–100%) are represented across the 23 sub-watersheds, with differences primarily in size rather than slope type. Due to a lack of spatially distributed observed soil loss data, the empirical relationship derived by Williams & Berndt (1972) was used to estimate SDR.

This equation is widely used in locations with limited data, especially for medium to large watersheds (Bhattacharya et al., 2020; Saygın et al., 2014). The study by Abebe, Lemma, & Meshesha (2025) used this equation in similar agroecologies to estimate the SDR for the Andit Tid Watershed.

Although the empirical SDR technique is widely used in data-scarce watersheds, it may not accurately reflect the temporal and spatial variability of sediment transport processes, which can add uncertainty to soil erosion predictions. Other methods, especially physically based sediment routing models, can explicitly quantify sediment transport and deposition processes (Basile et al., 2010); however, the requirements of extensive field observation and calibration data make it inapplicable for the study watershed. Therefore, the empirical SDR method was the best alternative based on the available data conditions.

$$Eg = \frac{SY}{SDR} \quad \text{...(3.16)}$$

$$SDR = 0.3481 * (A)^{-0.211} \quad \text{...(3.17)}$$

Where, Eg=gross soil erosion (Mg/ha/year), SY=Sediment yield (Mg/ha/year), and A = the area of the watershed in square kilometer (km^2).

3.2.8 Methodological Framework

The methodological framework provides graphic representations of how soil erosion and sediment yield are affected by climate change using the SWAT model (Figure 3.3). The framework integrates observed climate data (1993–2023), historical (1993–2014), and future (2030–2059 and 2060–2089) CMIP6 GCM data under SSP2-45 and SSP5-85 scenarios. Bias correction was applied to precipitation, maximum temperature, and minimum temperature from GCMs and used for future simulations. Other climatic variables, including solar radiation, wind speed, and relative humidity, were stochastically generated using the SWAT weather generator based on long-term observed climate statistics. Model inputs include DEM, soil, LULC, and observed streamflow and sediment data. The model validation and calibration were done using SWAT-CUP. The calibrated model is then applied to simulate future erosion and sediment yield.

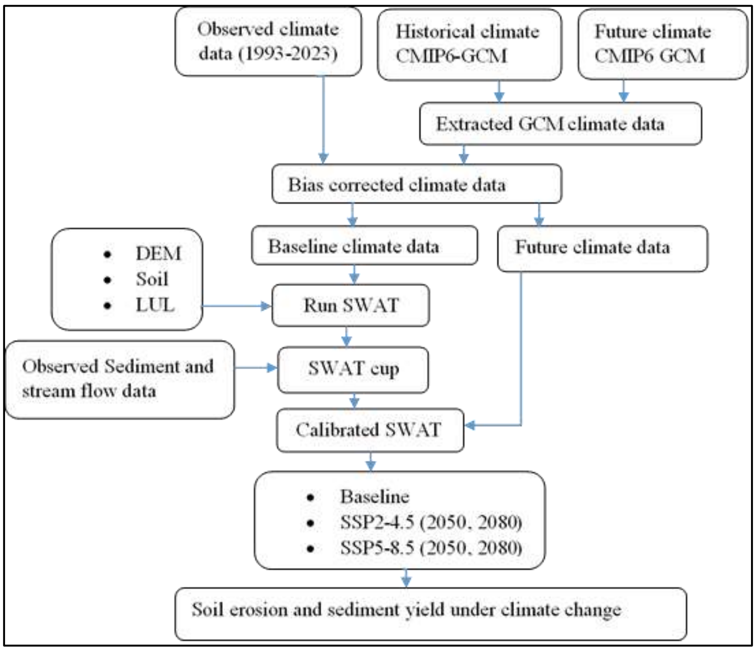

Figure 3.7: Soil Erosion and Sediment Yield Analysis under Climate Change using SWAT

3.3 Analysis of the Spatial and Temporal Dynamics of Erosion and Sediment Hotspots in the Beressa Watershed under Future Climate Scenarios.

3.3.1 Data Preparation

The results from the first objective were converted to an ArcGIS-compatible format in Excel. The soil erosion and sediment yield from each sub-watershed were analyzed for the baseline, near-term, and far-term periods under the SSP2-4.5 and SSP5-8.5 climate scenarios. The sub-basin and boundary shape file of the Beressa watershed were used to prioritize areas for conservation practices.

3.3.2 Erosion and Sediment Hotspot Identification Procedures

The identification and analysis of erosion and sediment hotspots were conducted using ArcGIS 10.5 software. Soil erosion rates and sediment yield data were imported into ArcMap and spatially linked to the sub-watershed shapefile to enable visualization of the results across the watershed. After the data were successfully joined, classification and mapping of gross erosion and sediment hotspots were performed. For this study, five severity classes adopted from previous studies conducted in the region were used to classify soil erosion (Sinshaw et al., 2021) and sediment yield (Gashaw et al., 2021; Tamene et al., 2017) (Table 3.5).

The adoption of these thresholds is used to compare the results from previous studies conducted under similar biophysical conditions and supports consistent identification of priority management areas. These categories were developed based on the Ethiopian highlands' tolerable soil loss limit, and they were used to identify priority conservation and management interventions.

Table 3.5: Soil Erosion and Sediment Yield Severity Classes Used in This Study

Severity class	**Sediment yield (Mg/ha/year)**	**Soil erosion (Mg/ha/year)**
Very low	< 5	<15
Low	5-11	15-30
Moderate	11-18	30-50
High	18-25	50-100
Very high	>25	>100

3.3.3 Analysis of the Evolution of Erosion Hotspot Areas

Variations in mean gross erosion and sediment yields (Mg/ha/year) were presented as percentage increases or decreases relative to the baseline period. Furthermore, comparative assessments were conducted between the SSP2-4.5 and SSP5-8.5 scenarios for both the near and far term periods. The spatial distribution of erosion and sediment severity classes was investigated to see how areas that were previously classified as stable under baseline conditions changed to moderate, high, or very high severity classes. These shifts were presented in tabular format. In addition, the hotspot transition analysis was performed by comparing the severity class of each sub-watershed between baseline and future periods to identify areas that remained stable and increased hotspots.

3.4 Effectiveness of Selected Best Management Practices (BMPs) in Reducing Sediment Yield under Projected Climate Conditions in the Beressa Watershed.

3.4.1 Sub-Watershed Selection for BMPs Implementation

The mean exported sediment from the Beressa watershed for both SSP2-4.5 and SSP5-8.5 climate scenarios was higher than the tolerable soil loss limit for Ethiopian highlands. The acceptable soil loss rate, which does not affect sustainable economic activity and optimum productivity, is below 11 Mg/ha/year (Woldemariam et al, 2024; Hurni, 1983). According to Gashaw et al. (2021), applying BMPs in sub-watersheds with very low and low erosion severity classes unknowingly resulted in higher sediment yield than the baseline. However, applying BMPs in areas with moderate to very high erosion severity significantly reduces sediment yield. Therefore, to ensure cost-effectiveness, this study applied and evaluated BMPs using the SWAT model only in sub-watersheds where soil loss rates were higher than the acceptable soil loss limit.

3.4.2 Implementation of BMPs

For this study, four BMPs, such as conservation agriculture (CA), contour farming (CF), Terracing, and their combined use, were selected based on their relevance to the biophysical and socio-economic conditions of the watershed. To evaluate the effectiveness of these measures on reducing sediment yield, modification of the calibrated values was conducted in the SWAT model. These practices were applied to the near and far terms of SSP2-4.5 and SSP5-8.5 climate scenarios.

Slope classes were used to represent the spatial variation in BMP effectiveness throughout the study area. The selected MPs were implemented at the Hydrologic Response Unit (HRU) level by changing specific management and hydrological parameters in the SWAT model. BMP implementation in this study was primarily carried out by adjusting the support practice factor (USLE_P.mgt), which was assigned values according to slope classes to capture variations in effectiveness across different topographic settings. Additional modifications were made to the curve number (CN2.mgt), slope length factor (SLSUBBSN.hru), and Manning’s roughness coefficient (OV_N.hru) to account for changes in runoff generation and surface friction resulting from the adoption of BMPs. This parameter-based strategy was chosen because detailed field-level management records were not readily available. Therefore, BMP parameter values were selected from previously validated SWAT studies and SWAT documentation to ensure realistic representation of contour farming, terracing, and conservation agriculture under local watershed conditions. The selected parameter modifications fall within ranges commonly reported in the literature and were applied consistently across all climate scenarios.

The description of each scenario is shown as follows.

I. Scenario 0 (Baseline)

The baseline scenario from Objective 1 was used as a reference to evaluate near-term and far-term projections under SSP2-4.5 and SSP5-8.5 climate scenarios. This baseline data was obtained from the calibrated SWAT model before implementing any management practices. It was used to quantify the percentage reduction in sediment yield resulting from applying best management practices for future climate conditions.

II. Scenario 1 (Terracing)

A terrace is a large earthen embankment that is designed to reduce soil erosion and surface runoff (Uniyal et al., 2020). Terraces help to reduce slope length and angle, minimize gullies, and decrease sediment content in runoff water at the watershed outlet (Arnáez et al., 2015). In this study, terracing was implemented in the SWAT by modifying relevant parameters for agricultural land, bare land, and grassland land uses. Field observations indicated that grasslands in the Beressa watershed are highly degraded, with sparse and short grasses, no shrub cover, and visible gully formation due to overgrazing, unlike well-managed grasslands with protective vegetation cover. These land uses are the most vulnerable to soil erosion in the study watershed due to minimal plant cover and significant soil disturbance. For this study, the Calibrated curve number (CN2.mgt) value decreased by 3, the slope length factor (SLSUBBSN.hru) parameter was reduced by 50%, and the support practice factor (USLE-P.mgt) factor was set to 0.12 for slopes less than 10% and 0.32 for slopes greater than 10% (Regasa & Nones, 2024; Gashaw et al., 2021; Zantet et al., 2023; Mequanient & Kebede, 2023). Other land use types, such as forest, urban areas, and water bodies, were excluded from terracing implementation for this study because forestland has natural protection against erosion, urban areas contain impervious surfaces, and water bodies do not contribute to sediment yield.

III. Scenario 2 (Contour Farming)

This practice uses the natural contour lines for tilling, planting, and harvesting. This helps to reduce the erosive ability of surface runoff and successfully minimize rill and sheet erosion formation (Dibaba, Demissie, & Miegel, 2021). In SWAT, the calibrated parameters, such as USLE_P (.mgt), were replaced by 0.5 for slopes less than 5% and 0.6 for slopes ranging between 5-10%, and the calibrated curve number(CN2.mgt) was reduced by 3 based on (Uniyal et al., 2020; Regasa & Nones, 2024; Zantet et al, 2023; Mequanient & Kebede, 2023; Dibaba, Demissie, & Miegel, 2021). Contour farming was simulated on slopes <10% because these areas are commonly recommended for contour-based agricultural practices. The practicality of CF decreases with increasing slope due to operational constraints and higher erosion risks. The agricultural lands having slopes higher than 10% and other land uses are left as the calibrated value.

IV. Scenario 3 (Conservation Agriculture)

Conservation agriculture is a tillage practices that help reduce soil erosion (Araya et al. ,2011) and improve soil physicochemical properties (Mitiku et al., 2024). In the framework of SWAT, conservation tillage has unique characteristics regarding mixing efficiency (EFFMIX), which specifies the proportion of materials (residue, nutrients, and pesticides) located on the soil surface that are uniformly incorporated throughout the soil profile, indicated by DEPTIL (the depth of mixing induced by the tillage procedure). Based on the recommendations of Uniyal et al. (2020) and Tuppad et al. (2010), the calibrated CN2 (.mgt) value was reduced by 2. To simulate the no-till condition, DEPTIL (.mgt.till.dat) was set at 25mm, EFFMIX (.mgt.till.dat) were set at 0.05 and also the overland flow Mannings roughness coefficient(OV-N) was increased to 0.3 from the model's default of 0.14 based on residue levels ranging from 2 to 9 Mg/ha, as suggested by Lamba et al., (2016). This scenario was designed to evaluate the potential effects of CA on sediment yield under improved management conditions rather than to replicate existing farmer practices. This management practice was applied to agricultural land use types, and other land use types were kept as calibrated values because it is less applicable to other land use types.

V. Scenario 4 (Combined Measures)

For the combined measures, the following configurations were applied: contour farming integrated with conservation agriculture on agricultural lands with slopes <10%, terracing integrated with conservation agriculture on agricultural lands with slopes >10%, and terracing alone on grasslands and barren lands. The influence of these measures on sediment yield reduction was evaluated by modifying calibrated values of USLE_P.mgt ,CN2.mgt , EFFMIX (.mgt.till.dat), DEPTIL (.mgt.till.dat), SLSUBBSN.hru, and OV_N.hru , according to land use and slope class. This configuration was designed as an optimization approach that allocates BMPs according to slope conditions and land use characteristics to enhance erosion control, minimize implementation cost and land occupied by structural interventions. This measure aimed to achieve a balance between the effectiveness of sediment reduction and practical feasibility by reducing the need for terracing on relatively flat agricultural lands while maintaining effective erosion control on steeper slopes. All parameter modifications followed the same rules defined in the individual scenarios, ensuring consistency across BMP configurations.

3.4.3 Effectiveness of BMPs

After modifying the relevant parameters according to each best management practice, the measures were applied under near-term and far-term projections for both SSP2-4.5 and SSP5-8.5 climate scenarios. The effectiveness of BMPs, such as contour farming, terracing, conservation agriculture, and their combined implementation, was assessed by comparing sediment yield before and after BMP application across the four future periods. These comparisons were performed separately for each measure and time period. The findings were reported using both tables and figures. A total of 16 SWAT model simulations were run, accounting for the four measures across two climate scenarios and two timeframes. The percentage reductions in sediment yield due to each measure were visualized using spatial maps. Spatial changes in sediment severity, specifically shifts from moderate, high, and very high classes to low sediment severity classes, were mapped using ArcMap. In addition, the increase in stable areas (zones with erosion rates within the tolerable soil loss limit for the Ethiopian highlands) was quantified and presented in tabular form. The response of each sub-watershed to the applied measures was assessed by determining the percentage reduction in sediment yield caused by each measure. The effectiveness of BMPs was quantified using Equation 3.18.

$$Sediment\ reduction(\%) = \left(\frac{X_1 - X_2}{X_1}\right) * 100 \qquad (3.18)$$

Where X1 represents sediment yield before applying BMPs X2 refers sediment yield after BMPs are applied.

CHAPTER FOUR

RESULTS AND DISCUSSION

4.1 Quantifying the Effects of Climate Change on Soil Erosion and Sediment Yield

4.1.1 Spatial Characteristics of the Watershed

The spatial distribution of land use/land cover (LULC), soil types, and slope classes as presented in Chapter 3 provides the physical basis for the spatial variability of climate-driven soil erosion and sediment yield in the Beressa watershed. Cultivated lands are generally more vulnerable to soil erosion because continuous cultivation and leaving soil uncovered during peak rainy seasons increase Vulnerability to runoff, particularly on sloping lands. Agricultural land, which covers more than 80% of the watershed area, contributed the largest share of simulated soil loss in the watershed. Comparison with the 2015 land use map reported by Worku et al. (2017) indicates that agricultural land expanded by approximately 26.91 km² by 2023, primarily at the expense of forestland and grassland. The observed land use change in the Beressa watershed suggests greater vulnerability to erosion and sediment transport under future climate change conditions.

Soil characteristics of the watershed further influence the spatial variation in erosion susceptibility. Silt-rich soils exhibit weaker particle cohesion, making them more prone to detachment by raindrop impact than clay-rich soils (Taharin et al.,2026). In contrast, clay-rich soils generally possess stronger aggregation and greater resistance to soil detachment despite their relatively low infiltration capacity (Uddin, 2021).

The slope further increases erosion risk, particularly during high-intensity rainfall events. More than 57% of the watershed has slopes higher than 10%, and extensive agricultural activities occur on these steeper slopes. On steeper slopes, runoff velocity and erosive energy increase considerably, enhancing the detachment and transport of soil particles (Shi et al., 2012). Similarly, Setyawan, Lee, & Prawitasari (2019) documented that farming practices on slopes higher than 15% substantially increase soil erosion. Overall, the interaction of extensive cultivated land, erodible soils, and steep slopes explains the spatial variability in simulated soil erosion and sediment yield in the Beressa watershed under changing climate conditions.

4.1.2 Performance Evaluation of Bias-Corrected Climate Data

The bias correction for precipitation (Prc), maximum temperature (Tmax), and minimum temperature (Tmin) across the three meteorological stations (Debre Birhan, Faji, and Debele) in the Beressa watershed performed well for all variables (Figure 4.1). High R^2 and NSE values, low RMSE, and small percent bias (Table 4.1) indicate strong agreement between observed and bias-corrected datasets.

The precipitation bias-corrected data achieved an R^2 value of approximately 0.999, and the NSE value exceeded 0.997 at all stations, indicating excellent agreement with observations. The percent bias was below ±5% at all stations. However, the Faji and Debele stations exhibited slight overestimation, while slight underestimation was observed at Debre Birhan station after bias correction.

Similarly, bias-corrected minimum and maximum temperatures showed strong performance with $R^2 > 0.95$ and NSE > 0.89. The PBIAS values indicate minor systematic deviations between observed and bias-corrected climate variables. A negative PBIAS value suggests a slight overestimation, whereas positive values indicate an underestimation of bias-corrected data as compared to observed data.

Table 4.1: Performance Evaluation of Bias Correction for Three Stations in the Beressa Watershed

Station	variables	R^2	RMSE	PBIAS	NSE
Debre Birhan	Prc.	0.999	5.3	0.028	0.997
	Tmax	0.9616	0.2	0.0057	0.96
	Tmin	0.984	0.234	-0.1326	0.98
Faji	Prc.	0.997	6.64	-1.46	0.995
	Tmax	0.9502	0.2887	-0.419	0.945
	Tmin	0.977	0.408	-2.84	0.962
Debele	Prc.	0.997	6.32	-2.81	0.995
	Tmax	0.9616	0.167	0.0128	0.898
	Tmin	0.975	0.116	-0.891	0.957

Note: Negative PBIAS values indicate overestimation, whereas positive PBIAS values indicate underestimation relative to the observed data

a) b)

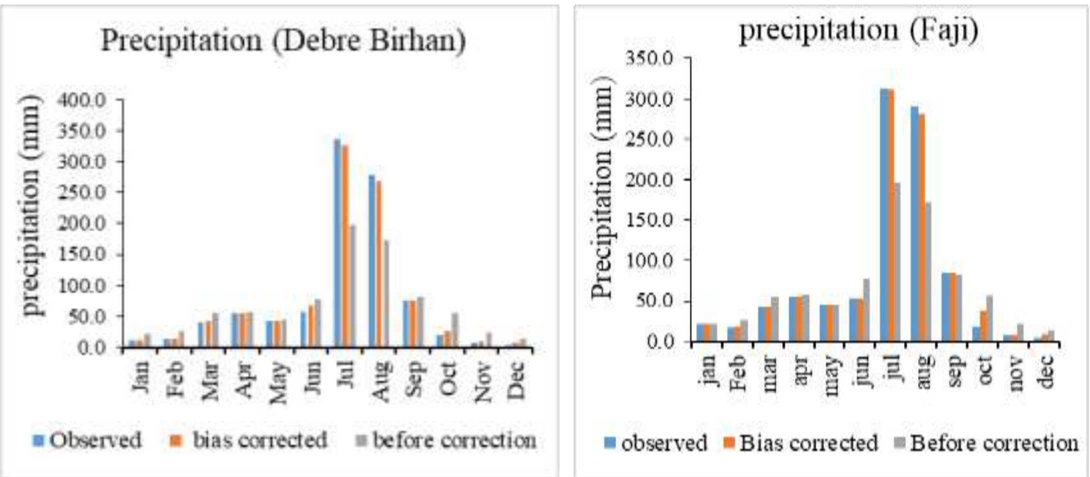

c)

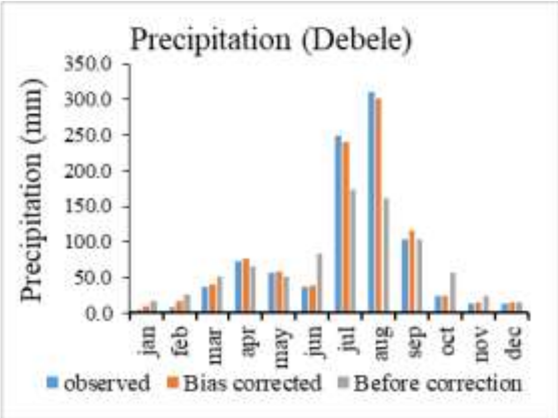
Precipitation (Debele)
Precipitation (mm)
350.0
300.0
250.0
200.0
150.0
100.0
50.0
0.0
jan feb mar apr may jun jul aug sep oct nov dec
observed
Bias corrected
Before correction

d)

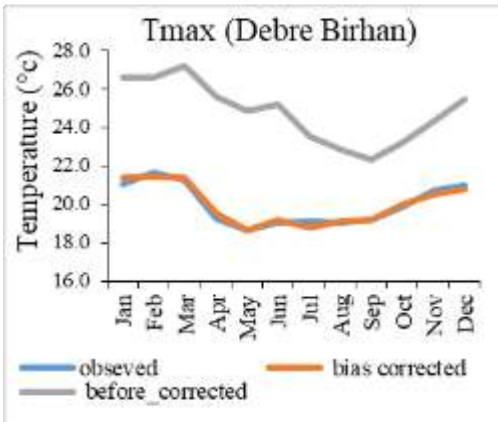
Tmax (Debre Birhan)
Temperature (°c)
28.0
26.0
24.0
22.0
20.0
18.0
16.0
Jan Feb Mar Apr May Jun Jul Aug Sep Oct Nov Dec
obseved
bias corrected
before_corrected

e)

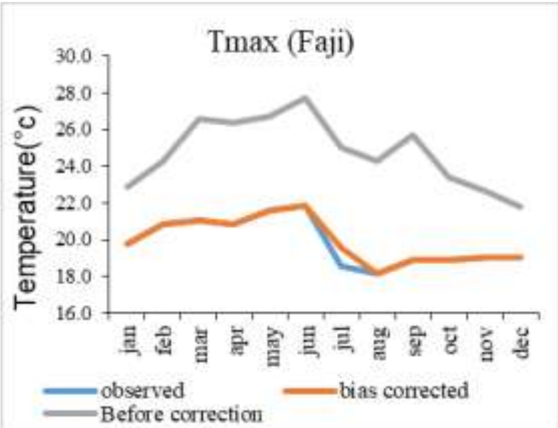
Tmax (Faji)
Temperature(°c)
30.0
28.0
26.0
24.0
22.0
20.0
18.0
16.0
jan feb mar apr may jun jul aug sep oct nov dec
observed
bias corrected
Before correction

f)

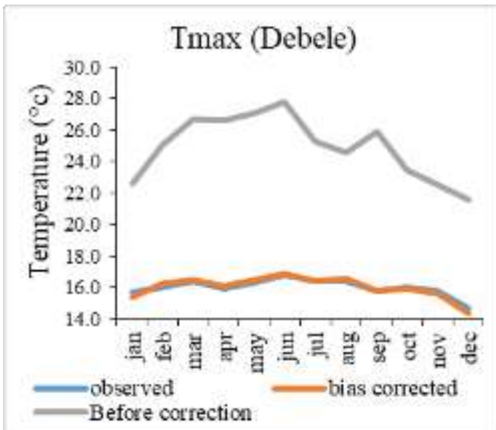
Tmax (Debele)
Temperature (°c)
30.0
28.0
26.0
24.0
22.0
20.0
18.0
16.0
14.0
jan feb mar apr may jun jul aug sep oct nov dec
observed
bias corrected
Before correction

g)

h)

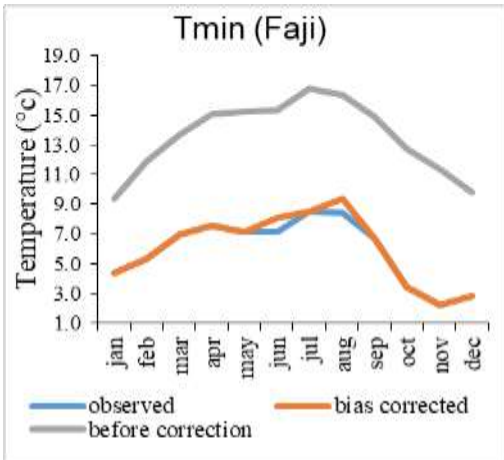
Tmin (Faji)
Temperature (°c)
19.0
17.0
15.0
13.0
11.0
9.0
7.0
5.0
3.0
1.0
jan feb mar apr may jun jul aug sep oct nov dec
observed
bias corrected
before correction

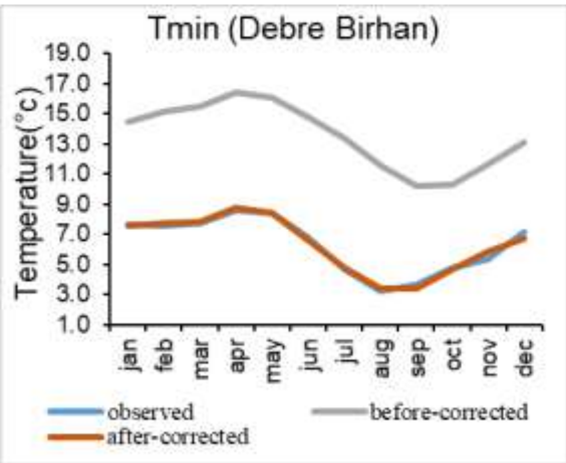

i)

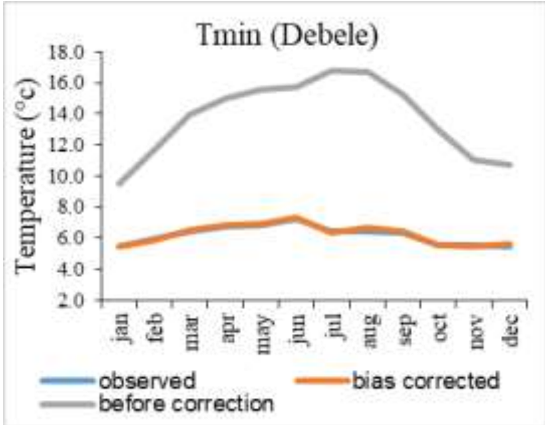

Figure 4.1: Comparison of Monthly Mean Values of Observed, Before Bias Correction, and After Bias Correction Climate Data for Precipitation, Maximum Temperature, and Minimum Temperature at Three Meteorological Stations within the Watershed. Bias Correction was Performed Using Power Transformation for Precipitation and Distribution Mapping for Temperature Variables

The higher R^2 and NSE value, together with low RMSE and PBIAS values, indicates the applied bias correction techniques importantly reduced systematic errors in both precipitation and temperature datasets (Siabi et al., 2023; Mukheef et al., 2024). Similar findings have been reported in previous studies. In the upper Blue Nile basin, for instance, Alaminie et al. (2021) applied quantile mapping and reported R^2 and NSE values of 0.98 and 0.93, respectively. Similarly, Enyew et al. (2024) used a power transformation technique and obtained an R^2 value of 0.77 for precipitation in highland areas. Additionally, Mukheef et al. (2024) utilized the power transformation method and reported R^2 values exceeding 0.97 for bias-corrected precipitation in Iraq. Similar performance for minimum and maximum temperature bias correction has been reported by Alaminie et al. (2021) using the Quantile Mapping method and by Enyew et al. (2024) and Mukheef et al. (2024) using distribution mapping techniques.

The satisfactory statistical performance achieved using the Power Transformation method for precipitation and the Distribution Mapping method for temperature indicates that both approaches were effective in reducing systematic biases in the climate model outputs. These findings indicate that the effectiveness of bias-correction techniques is influenced by data characteristics and the spatial heterogeneity of the study area. For instance, Alaminie et al. (2021) identified Quantile Mapping as a suitable approach for CMIP6 climate data because it effectively represents extreme events by correcting the entire distribution of climate variables. However, the excellent performance achieved in this study demonstrates that alternative bias-correction methods can also provide reliable results for climate impact assessments when appropriately matched to local conditions.

Despite the overall excellent performance, the slight overestimation and underestimation observed for some variables across the meteorological stations in the Beressa Watershed indicate the presence of residual biases, suggesting that the applied bias-correction techniques were not able to completely remove all model errors. Such residual biases in bias correction of the climate model may arise from local topographic impacts, spatial variability in rainfall processes, variations in station elevation, and constraints in the climate model's representation of localized atmospheric conditions (Argüeso, Evans, & Fita, 2013; Zahedipour & Gallus, 2026). Future studies could further quantify the remaining uncertainties using confidence intervals or uncertainty bands around the corrected climate variables to better characterize the robustness of the bias-correction procedure.

4.1.3 Climate Trend Analysis

i. The Mann-Kendall (MK) Trend

The Mann-Kendall (MK) trend analysis for precipitation, minimum and maximum Temperature for the period 2015–2100 under SSP2-4.5 and SSP5-8.5 scenarios showed a statistically significant increasing trend ($\alpha = 0.05$) for all climate variables (Table 4.2 ; Figure 4.2). Under SSP2-4.5, the highest annual precipitation value of 2756mm was projected for 2074, whereas under SSP5-8.5 scenarios, the maximum annual precipitation value of 1900mm expected in 2033. Under the SSP2-4.5 scenario, annual precipitation exhibited a significant increasing trend during the near-term period (MK = 0.338, p = 0.009), with a Sen's slope of 13.737 mm/year. In contrast, the far-term period showed no statistically significant trend (MK = 0.01, p = 0.943), and Sen's slope decreased to 0.74 mm/year, indicating a substantially weaker rate of change than in the near term.

For temperature, under SSP2-4.5 climate scenarios, the trend shows an annual increase in maximum temperature by 0.021°C/year, reaching 21.31°C by 2092, while the minimum temperature rises at 0.034°C/year, reaching 10.19°C by 2091. Under the high-emission SSP5-8.5 scenario, the maximum temperature increases by 0.041°C/year (peaking at 23.02°C by 2099) and the minimum temperature rises by 0.073°C/year, reaching 13.65°C by 2100.

Table 4.2: MK Trend Analysis of Simulated Climate under SSP2-4.5 and SSP5-8.5

Scenario	Period	Precipitation			Maximum temperature			Minimum temperature		
		MK	sen	p-value	MK	sen	p-value	MK	sen	p-value
SSP2-4.5	2030-59	0.34	13.74	0.009*	0.31	0.04	0.02*	0.48	0.05	0.00***
	2060-89	0.01	0.74	0.94	0.29	0.02	0.025*	0.33	0.02	0.011*
	2015-2100	0.21	2.63	0.01*	0.55	0.02	0.00***	0.67	0.03	0.00***
	2030-59	0.18	5.69	0.18	0.49	0.04	0.00***	0.6	0.065	0.00***

SSP5-	2060-89	0.03	1.39	0.81	0.61	0.06	0.00***	0.729	0.084	0.00***
8.5	2015-2100	0.15	1.75	0.05*	0.77	0.04	0.00***	0.869	0.073	0.00***

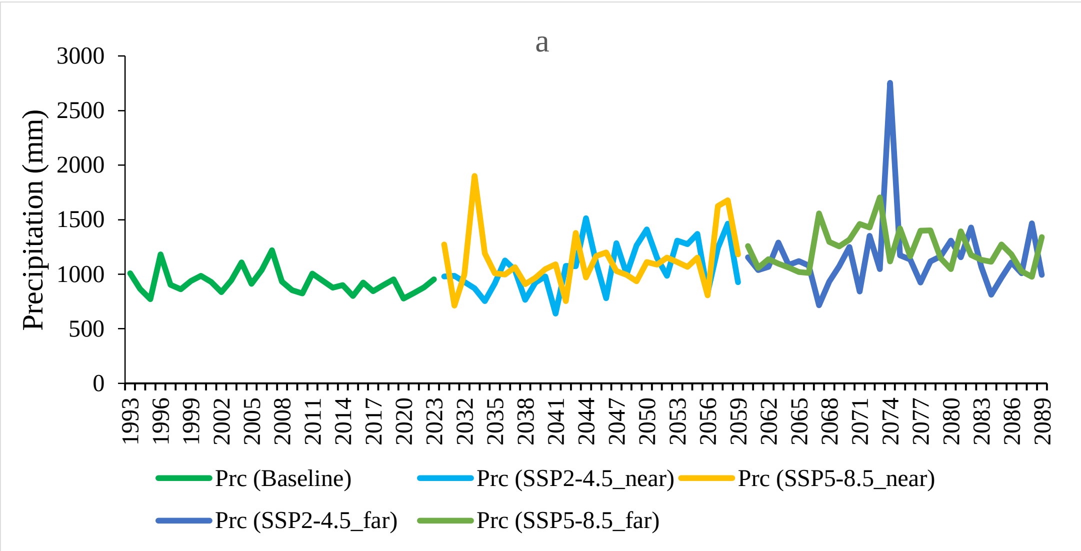

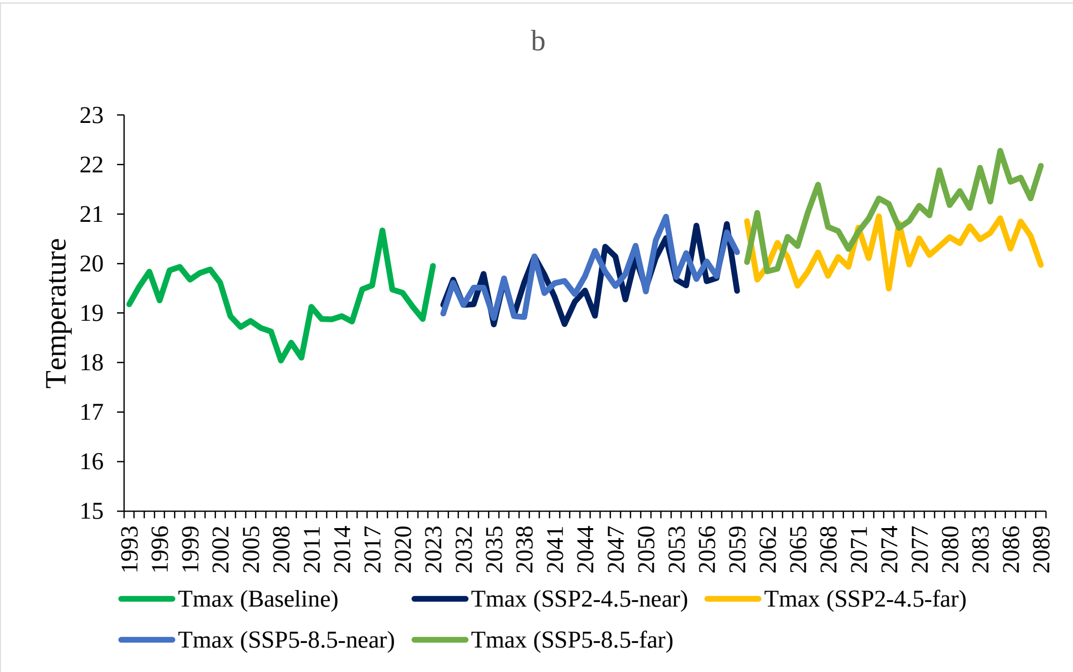

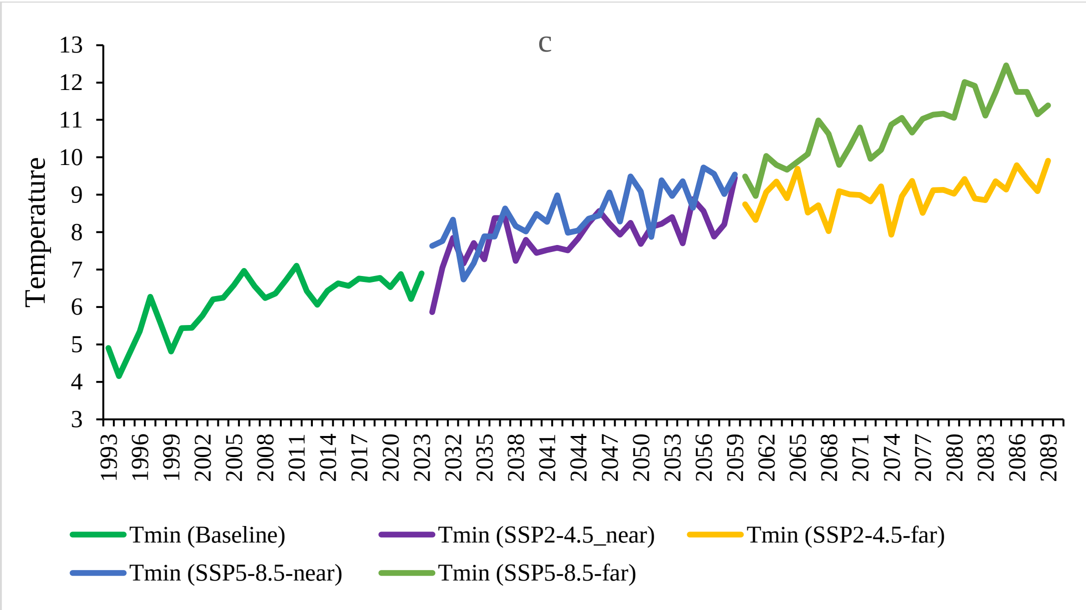

Figure 4.2: Mann-Kendall (MK) Trend Analysis of Precipitation (a), Maximum Temperature (b), and Minimum Temperature (c) for the Baseline Period, Simulated Near Future, and Far Future under SSP2-4.5 and SSP5-8.5.

ii. Innovative Trend Analysis (ITA)

The Innovative Trend Analysis (ITA) of annual precipitation (prc), minimum temperature (Tmin), and maximum temperature (Tmax) for the period 2015–2100 under the SSP2-4.5 and SSP5-8.5 climate scenarios showed that most data points are above the 1:1 trendless line (Figure 4.3), indicating increasing trends in all climate variables. However, for precipitation under the SSP5-8.5 scenario, a few data points were observed below the trendless line, suggesting some decreasing trends within the overall increasing trend. The corresponding ITA slope values shown in Figure 4.3 quantify the magnitude of these trends.

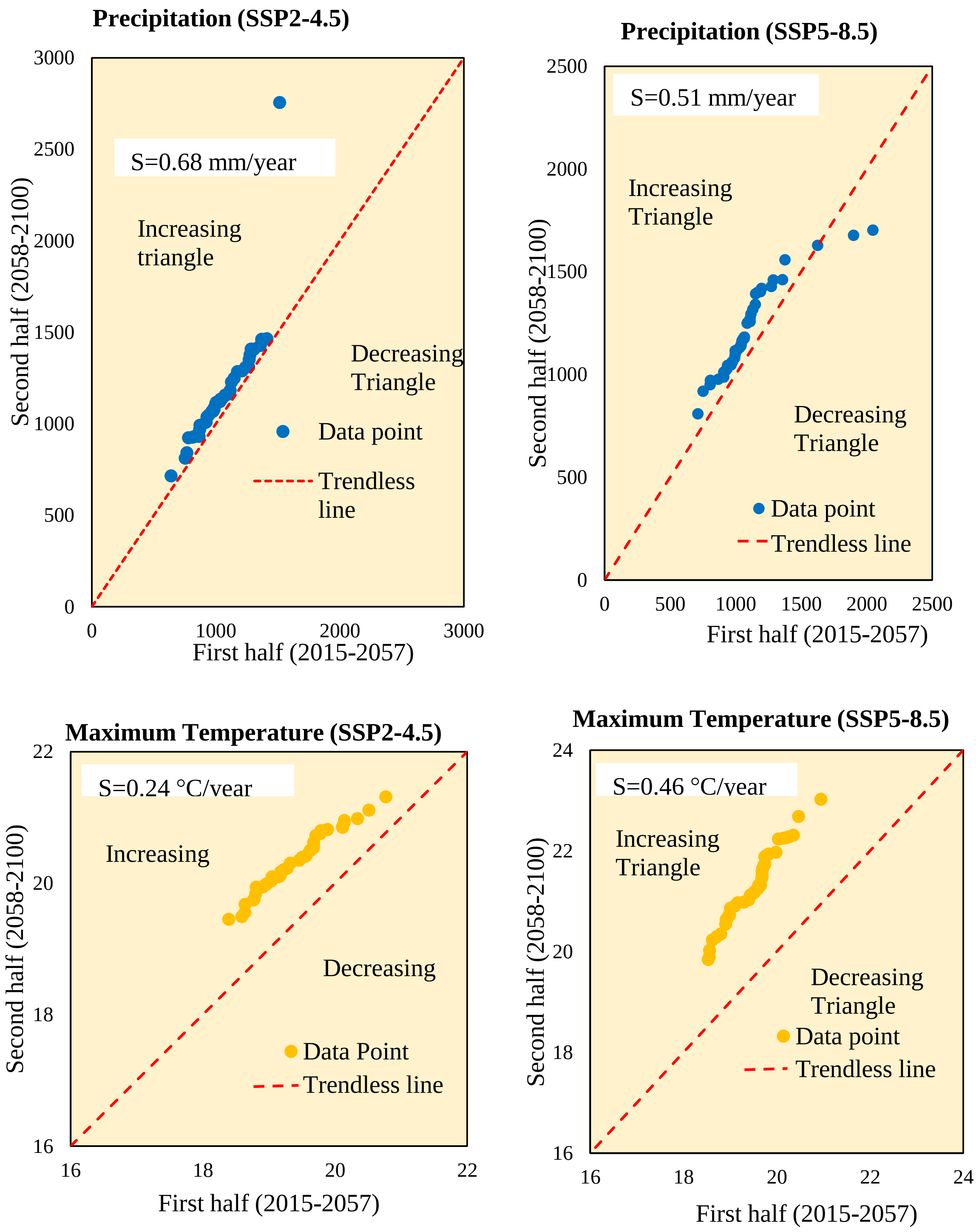
Precipitation (SSP2-4.5)
S=0.68 mm/year
Increasing triangle
Decreasing Triangle
Data point
Trendless line
Second half (2058-2100)
First half (2015-2057)
0
500
1000
1500
2000
2500
3000
Precipitation (SSP5-8.5)
S=0.51 mm/year
Increasing Triangle
Decreasing Triangle
Data point
Trendless line
Second half (2058-2100)
First half (2015-2057)
Maximum Temperature (SSP2-4.5)
S=0.24 °C/year
Increasing
Decreasing
Data Point
Trendless line
Second half (2058-2100)
First half (2015-2057)
16
18
20
22
Maximum Temperature (SSP5-8.5)
S=0.46 °C/year
Increasing Triangle
Decreasing Triangle
Data point
Trendless line
Second half (2058-2100)
First half (2015-2057)
24

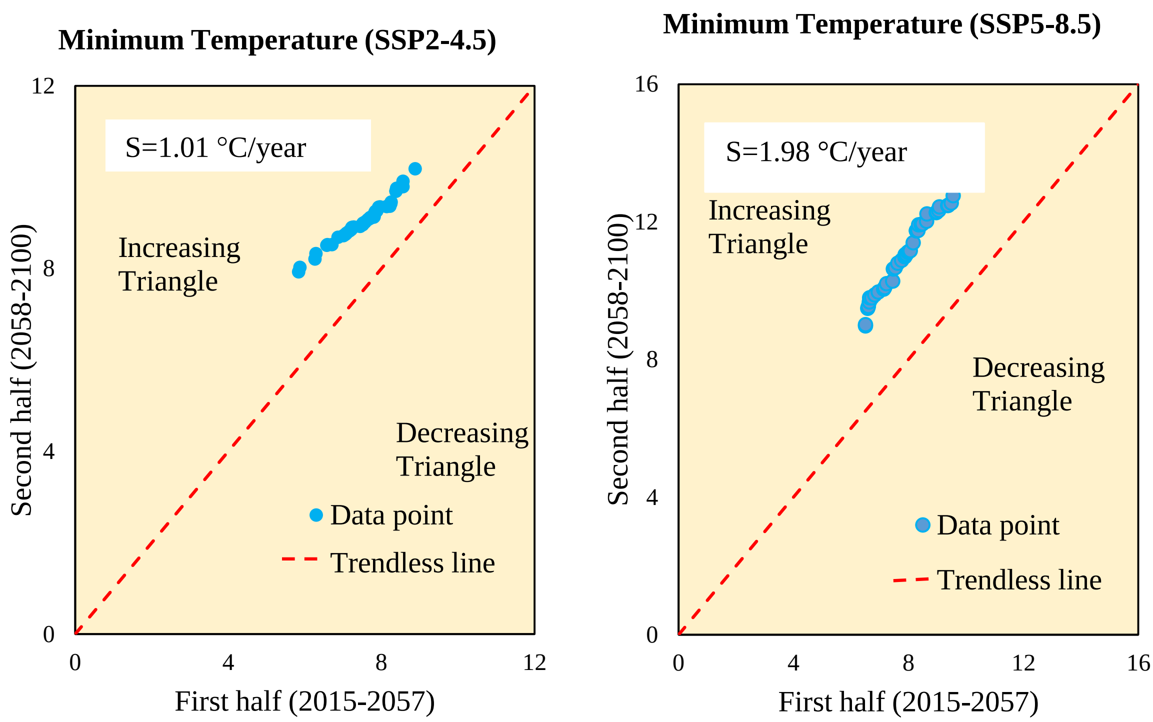

Figure 4.3: Innovative Trend Analysis (ITA) Plots of Annual Precipitation, Minimum Temperature, and Maximum Temperature under SSP2-4.5 and SSP5-8.5 Climate Scenarios.

iii. Extreme Rainfall Indices (P95 and P99) under SSP2-4.5 and SSP5-8.5 Scenarios

The projected extreme rainfall indices results showed P95 rainfall decreases across all future periods, whereas P99 rainfall exhibits substantial increases under both SSP2-4.5 and SSP5-8.5 (Table 4.3). This indicates that the most extreme rainfall events are projected to increase significantly, particularly under the SSP5-8.5 scenario, which may increase the risk of soil detachment and transport in the Beressa watershed.

Table 4.3: Percentage Changes of Extreme Rainfall Indices (P95 and P99) under CMIP6 Climate Scenarios (SSP2-4.5 and SSP5-8.5) for Near-Term and Far-Term Periods Relative to the Baseline

Scenarios	Time period	P95 rainfall (mm)	% change (P95)	P99 rainfall (mm)	% change (P99)
baseline	1995-2023	14.55		27.95	
SSP2-4.5 (near term)	2030-2059	12.85	-11.68	35.23	26.05
SSP2-4.5 (far term)	2060-2089	13.26	-8.87	44.38	58.79
SSP5-8.5 (near term)	2030-2059	13.01	-10.58	45.13	61.46
SSP5-8.5 (far term)	2060-2089	14.14	-2.82	51.19	83.16

Note: P95 represents the 95th percentile of daily precipitation to characterize moderate extreme rainfall conditions. P99 represents the 99th percentile of daily precipitation, used to characterize extreme rainfall

The stronger precipitation trend during the near-term SSP2-4.5 period suggests that most projected increases occur during the early decades of the projection, whereas precipitation becomes relatively stable in the far term, with interannual variability dominating the long-term trend. Furthermore, the occurrence of higher precipitation under SSP2-4.5 than SSP5-8.5 during some periods is consistent with the nonlinear nature of regional precipitation responses to climate change. Unlike temperature, precipitation is controlled not only by greenhouse gas forcing but also by atmospheric circulation, moisture availability, and internal climate variability. Consequently, a lower-emission scenario may temporarily produce higher precipitation than a higher-emission scenario. Similar findings have been reported in previous studies within the Upper Blue Nile Basin. Enyew et al. (2024) and Alaminie et al. (2021) reported significant increasing trends in both precipitation and temperature under future climate scenarios. Furthermore, the ITA results obtained in the present study are consistent with the findings of Lyu et al. (2025), who observed that although overall precipitation exhibits an increasing trend, some periods may show decreasing tendencies, particularly in regions characterized by complex topography.

Projected increases in precipitation and temperature are expected to enhance detachment and transport of soil particles in the Beressa watershed by increasing rainfall erosivity. Rising temperature reduces soil infiltration and weakens soil structure (Reinsch et al. 2024), accelerates organic matter decomposition (Downey et al. 2023), which increases vulnerabilities to erosion. The analysis of extreme rainfall events further highlights the potential for increased soil detachment, sediment transport, and erosion under future climate conditions. In the SSP2-4.5 scenario, the most extreme daily rainfall occurrences above the 99th percentile occurred on 14 days in 2074, with six events having rainfall that was more than double the 99th percentile value, suggesting abnormally severe storms. Similarly, under the high-emission SSP5-8.5 scenario, nine daily rainfall events exceeded the 99th percentile in 2033 and 2058, and ten events in 2067. These results indicate an increase in the frequency and magnitude of extreme rainfall events that can increase runoff volume and erosive energy and lead to a dramatic increase in sediment output compared to other years.

Although such extreme events occur in a few days per year, they may contribute disproportionately to annual soil loss and sediment yield because intense rainfall increases raindrop impact, runoff generation, and sediment transport capacity. The increases in the P99 index under both future climate scenarios, particularly under SSP5-8.5, confirm the higher risks of erosion and sediment yield in the future. The findings are consistent with the study by Bezak et al. (2021) found that a limited number of severe rainfall events contribute significantly to yearly erosivity. Other studies by Jiang et al. (2024) found that climate change is likely to increase the frequency and intensity of rainfall extremes.

In the study watershed, cultivated lands covered more than 80% of the watershed, and slopes exceeding 10% occupy a large portion of the watershed, and the projected increases in extreme rainfall events may increase the vulnerability of the watershed to climate-driven erosion and sedimentation risks. A limited number of high-intensity storms controlled the annual sediment yield more than changes in average rainfall alone. Therefore, effective soil and water conservation measures will be essential to mitigate the anticipated increase in climate-driven erosion and sediment transport within the watershed

4.1.4 Sensitivity Analysis of Streamflow and Sediment Parameters

Among 13 parameters, 10 were used for streamflow calibration and validation, whereas among 17, 9 were considered for calibration and validation of sediment, as shown in Table 4.4. The P-value and t-stat value were used to determine the rank of sensitive parameters. The calibration was conducted by adjusting the parameter range to enhance model performance for low flow and peak flow.

Sensitivity analysis for streamflow simulation in the Beressa watershed revealed that ALPHA_BF.gw, CH_K2.rte, and CN2.mgt were the most sensitive parameters at the $P < 0.05$ level of significance. GW_REVAP.gw, GW_DELAY.gw, GWQMN.gw, CANMX.hru, SOL_AWC.sol, EPCO.hru, and ESCO.hru all showed low to moderate sensitivity. In terms of flow regimes, ALPHA_BF.gw, GWQMN.gw, GW_DELAY.gw, GW_REVAP.gw, SOL_AWC.sol, and ESCO.hru had the greatest influence on managing low flows. On the other hand, CN2.mgt, CH_K2.rte, EPCO.hru, and CANMX.hru were the primary parameters affecting peak flows.

Following streamflow calibration and validation, sediment-related parameters were assessed. SOL_K.sol, CH_N2.rte, HRU_SLP.hru, and CH_COV2.rte were the most sensitive parameters for sediment simulation, indicating that they play a significant role in erosion and sediment transport dynamics. Other Parameters, such as USLE_K.sol, SLSUBBSN.hru, USLE_C(AGRL).plant.dat, SPCON.bsn, and USLE_P.mgt showed moderate to low sensitivity, indicating a secondary influence on sediment output in the current model setup. USLE_K.sol, HRU_SLP.hru, and SLSUBBSN.hru were the main factors influencing low sediment yield, Whereas High sediment yield was strongly associated with CH_COV2.rte, CH_N2.rte, SPCON.bsn, USLE_P.mgt, and USLE_C(AGRL).plant.dat.

Table 4.4: Sensitive Parameters for Streamflow and Sediment

Flow/sediment	Parameter	P value	t-stat	Rank	fitted value	parameter space
streamflow	V__ALPHA_BF.gw	0.00	8.97	1	0.535	0-1
	V__CH_K2.rte	0.00	-3.57	2	21.523	5-130
	R__CN2.mgt	0.02	2.38	3	-0.008	-0.1-0.1
	V__GW_REVAP.gw	0.19	1.32	4	0.035	0.02-0.17
	V__EPCO.hru	0.30	-1.04	5	0.590	0.5-1
	V__GW_DELAY.gw	0.31	1.01	6	10.256	0-251.15
	V__CANMX.hru	0.36	0.92	7	3.833	0-100
	R__SOL_AWC(..).sol	0.45	-0.76	8	0.059	-0.1-0.1
	V__ESCO.hru	0.46	-0.74	9	0.829	0.35-0.95
	V__GWQMN.gw	0.55	0.59	10	1800.5	0-4500
Sediment	V__SOL_K(..).sol	0.00	6.47	1	532.96	0-651.936
	V__CH_N2.rte	0.00	5.28	2	0.0138	0-0.3
	V__HRU_SLP.hru	0.00	2.88	3	0.463	0.385-0.795
	V__CH_COV2.rte	0.01	-2.12	4	0.378	0.11-0.51
	V__USLE_K(..).sol	0.09	1.68	5	0.447	0.32-0.47
	V__SLSUBBSN.hru	0.10	-1.64	6	55.63	32.036-96.24
	V__USLE_C{AGRL}.plant.dat	0.12	-1.56	7	0.326	0.235-0.348
	V__SPCON.bsn	0.47	-0.73	8	0.0057	0.005-0.0065
	V__USLE_P.mgt	0.52	-0.65	9	0.998	0.752-1

Where "R_" represents adding 1 from the fitted value and multiplying the result by the parameter's initial value; "V_" indicates changing the initial value with the fitted value.

The sensitivity analysis identified ALPHA_BF.gw, CH_K2.rte, and CN2.mgt as the most influential parameters controlling streamflow simulation in the Beressa watershed. The high sensitivity of these parameters indicates that groundwater dynamics, channel hydraulic conductivity, and runoff production are the most significant hydrological controls in the Beressa watershed. The sensitivity ranking also shows that the biggest impact on streamflow prediction may arise from uncertainties in runoff generation, channel hydraulic conductivity, and groundwater response. This highlights the need for accurate representation of these processes to enhance model reliability.

A calibrated value of ALPHA_BF.gw (0.535) indicates moderate groundwater response to variations in recharge. This highlights the importance of base flow contribution in sustaining dry-season flows in the Watershed. Similarly, the high sensitivity of CH_K2.rte (21.52 mm/hr) indicates that infiltration losses through channel alluvium play a significant role in regulating streamflow. The sensitivity of CN2.mgt (-0.008) indicates a considerable overestimation of initial runoff potential because the watershed has mixed land use and moderate slopes. In the Beressa watershed, as more than 80% of the watershed is cultivated land and a large portion of the watershed slopes exceed 10%, surface runoff is a major contributor to streamflow response. Similar findings have been reported in Ethiopian watersheds and the Upper Blue Nile Basin, where CN2.mgt, CH-K2.rte, ALPHA_BF.gw were consistently identified as the most influential parameters affecting streamflow simulations (Abebe et al., 2025; Gashaw, Dile, et al., 2021; Woldemariam et al., 2024).

For sediment simulation, SOL_K.sol, CH_N2.rte, HRU_SLP.hru, and CH_COV2.rte were the most sensitive parameters, indicating soil hydraulic properties, channel characteristics, topography, and channel cover are the primary controls on sediment yield in the watershed. The high sensitivity of SOL_K.sol (532.96 mm/hr) demonstrates the importance of soil permeability in regulating infiltration, runoff generation, and soil detachment. The calibrated value indicates the existence of moderately porous soils, which might exacerbate erosion processes, especially after heavy storms. Similarly, the fitted value of CH_N2.rte (0.0138) indicates that smoother channel surfaces encourage quicker flow velocities, which improve sediment transport. This represents the watershed's relatively deep and sparsely vegetated channels, which provide minimal barrier to flowing water. The high sensitivity of HRU_SLP.hru (0.463) confirms that steep slopes in the Beressa watershed contributes significantly increased sediment yield through increased runoff energy and soil detachment. The channel cover factor (CH_COV2.rte) was the fourth most sensitive (fitted value = 0.378), indicating that increased channel vegetation or residue cover lowers channel erosion. Similar findings have been reported in Ethiopian watersheds, for example, (Woldemariam, Ddumba, & Addis, 2024) identified USLE-k.sol, SOL-K.sol, and SOL_AWC.sol as the most sensitive parameters for sediment in the Andit Tid watershed. Similarly, Yesuf et al. (2015) identified HRU_SLP. hru, USLE-K.sol as the most sensitive parameters in the Mybar watershed. This highlights the need for site-specific calibration, which may change in response to changing environments (Cibin, Sudheer, & Chaubey, 2010). Identifying which parameters are most sensitive simplifies the calibration procedure, especially in data-scarce areas (Mihret et al., 2025).

The high sensitivity ranking for sediment simulation indicates that slight changes in their values can result in significant changes in simulated sediment yield. Accurate representation of these processes is essential for better climate change impact assessment and evaluating BMP effectiveness. Uncertainties in soil hydraulic conductivity, channel roughness, slope characteristics, and channel vegetation have a greater influence on sediment predictions. The dominance of cultivated lands and moderate to steep slopes in the Beressa watershed further highlights that erosion processes are strongly controlled by runoff generation and slope-driven sediment transport processes. Therefore, erosion control measures such as improving soil structure, stabilizing stream channels, decreasing slope gradients, and increasing channel vegetation might be the most effective solutions in the Beressa watershed.

4.1.5 Calibration and Validation Results

The graphical comparison between observed and simulated streamflow (Figure 4.4) showed the model's ability to represent both peak and low flows with reasonable accuracy during both periods. Similarly, the sediment yield simulation (Figure 4.5) effectively captured the temporal variations in both low and high sediment loads across the two periods.

Model performance statistics showed acceptable results (Table 4.5). For streamflow, the calibration period resulted in $R^2 = 0.83$, NSE = 0.78, PBIAS = -4.7%, RSR = 0.47, and KGE=0.67; during validation, performance slightly improved to $R^2 = 0.88$, NSE = 0.85, PBIAS = -0.4%, RSR=0.39 and KGE = 0.76. For sediment yield, calibration resulted in $R^2 = 0.73$, NSE = 0.69, PBIAS = 10.4%, RSR = 0.55, and KGE = 0.63, while validation showed $R^2 = 0.75$, NSE = 0.68, PBIAS = 18%, RSR = 0.56, and KGE=0.56.

Table 4.5: Model Performance Statistics for Streamflow and Sediment Calibration (2002-2009) and Validation (2010-2013)

Simulated variable		**Model performance statistics**				
		R^2	**PBIAS**	**NSE**	**RSR**	**KGE**
streamflow	calibration	0.83	-4.7	0.78	0.47	0.67
	validation	0.88	-0.4	0.85	0.39	0.76
Sediment	calibration	0.73	10.4	0.69	0.55	0.63
	Validation	0.75	18.0	0.68	0.56	0.56

Note: PBIAS: Percent Bias. Positive values indicate underestimation; negative values indicate overestimation.

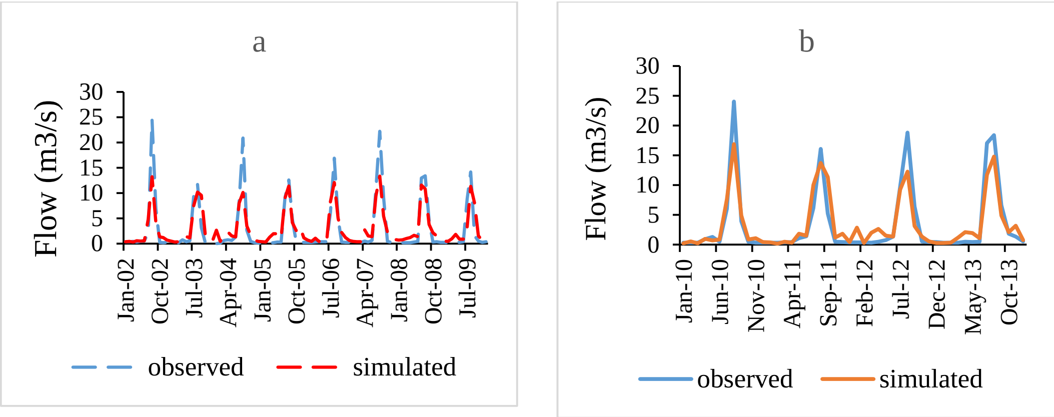

Figure 4.4: The Monthly Streamflow Hydrograph for Calibration (a) and Validation (b) period

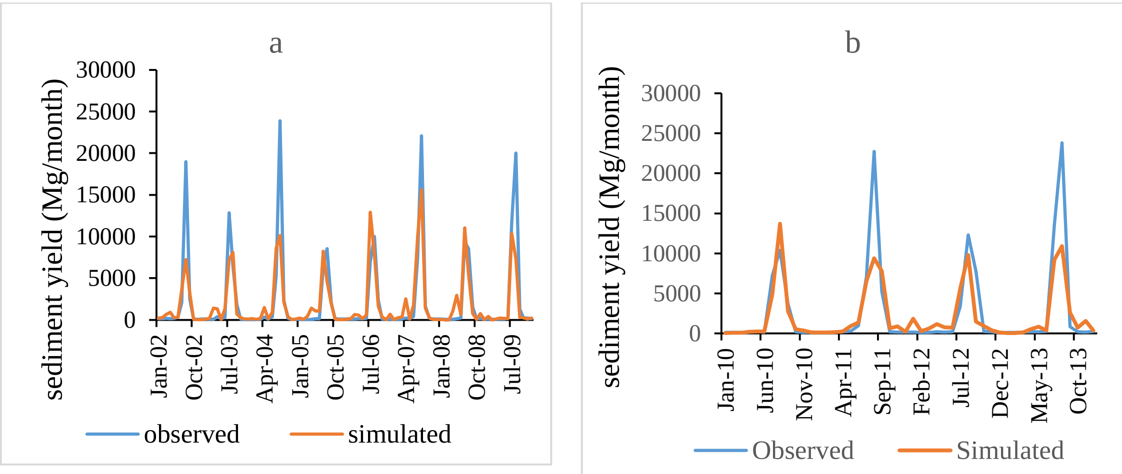

Figure 4.5: The Monthly Sediment Hydrograph for the Calibration (a) and Validation (b) periods

The model performance for streamflow and sediment meets acceptable performance standards recommended by Moriasi et al. (2007), which specify NSE > 0.5, RSR < 0.7, and PBIAS < ±15% for streamflow and < ±30% for sediment. For both variables, Validation results exhibited slightly better performance than during the calibration period. This result may be due to more stable hydrologic situations throughout the validation period, such as constant rainfall-runoff correlations and less extreme occurrences, which can improve model performance. Furthermore, when hydrologic variability is simpler, a well-calibrated model performs better during validation. These could lead to higher efficiency measures such as NSE and R2 in validation versus calibration (Dakhlalla & Parajuli, 2019; Quamar et al., 2025).

The slightly higher percent bias during the sediment validation period could be attributed to model parameters that were modified during the calibration phase but not further changed for validation. This shows that the model's predicted accuracy is slightly lower when applied to independent data. Additionally, validation involves testing the model on independent data, which may introduce new sources of error, particularly for sediment, which is highly sensitive to measurement uncertainties and extreme events (Dakhlalla & Parajuli, 2019). In addition, PBIAS may rise in validation compared to calibration because sediment transport depends on land use and rainfall intensity (Quamar et al., 2025). These results are consistent with earlier hydrological research conducted in the region (Gashaw et al., 2021; Worqlul et al., 2018).

The PBIAS value of 18% indicates moderate bias in sediment yield simulation, which may arise from the sediment-rating curve used to estimate observed sediment loads. Extrapolated sediment loads from rating curves may not adequately represent sediment transport in the watershed, leading to disagreement between simulated and observed sediment yields. Additionally, watershed characteristics such as land use, soil, and slope influence erosion processes and may introduce additional uncertainty into sediment predictions. Compared to streamflow simulation, sediment simulation showed weaker performance because sediment yield is influenced by runoff generation, soil detachment, transport, and deposition processes within the watershed, unlike streamflow. Additionally, uncertainties from rainfall variability, land use, and channel conditions influence sediment accumulation, which leads to greater prediction uncertainty for sediment than for streamflow. In the Beressa watershed, the dominance of cultivated land and moderate to steep slopes, together with limited observed sediment data records, makes an accurate representation of erosion and sediment transport processes challenging.

Despite these limitations, satisfactory calibration and validation performance metrics indicate that the model is suitable for quantifying climate change impacts on sediment yield and evaluating BMP performance. The results indicate that sediment yield in the

Beressa watershed is significantly influenced by runoff-driven erosion, mainly from cultivated lands and sloping areas. Therefore, implementing BMPs like terracing, contour farming, and conservation agriculture can reduce sediment production from the watershed. These findings provide useful information for watershed management and policy development targeted at decreasing land degradation and sustaining agricultural productivity under changing climatic conditions.

The streamflow model performance is consistent with previous studies conducted in the region. For instance, Gashaw et al. (2021) found the Gumura watershed model's performance for streamflow calibration (R2=0.86, NSE=0.81, PBIAS=10.7%, RSR=0.43) and validation (R2=0.93, NSE=0.86, PBIAS=13.5%, RSR=0.38). Similarly, Woldemariam et al. (2024) examined the Andit Tid model performance results for streamflow calibration (R2=0.83, NSE=0.72, KGE=0.53) and for validation (R2=0.73, NSE=0.65, KGE=0.59). Additionally, Worku et al. (2017) found streamflow model performance calibration results (R2=0.72, NSE=0.67, PBIAS=3.9%) and validation period results (R2=0.68, NSE=0.64, PBIAS=7.6%) in a similar region.

The sediment calibration and validation model performance results are consistent with previous research in the region. For example, the study conducted by Gashaw et al. (2021) on the Gumura watershed found calibration results (R2=0.68, NSE=0.67, PBIAS=-6.1%) and validation period results (R2=0.70, NSE=0.69, PBIAS=-11.2%). In addition, sediment studies by Abebe et al. (2025) on the Andit Tid watershed model performance found calibration results (R2=0.72, NSE=0.68, PBIAS=-19.4%) and validation period results (R2=0.69, NSE=0.67, PBIAS=-4.3%).

4.1.6 Uncertainty Analysis of Sediment Yield Simulation

The uncertainty analysis of sediment yield simulation (Figure 4.6) resulted in a P-factor of 0.44 for both calibration and validation, with corresponding R-factor values of 0.54 and 0.52, respectively. The relatively low R-factor indicates a narrow uncertainty band. Furthermore, the similarity of uncertainty measures between calibration and validation suggests consistent model performance across both periods.

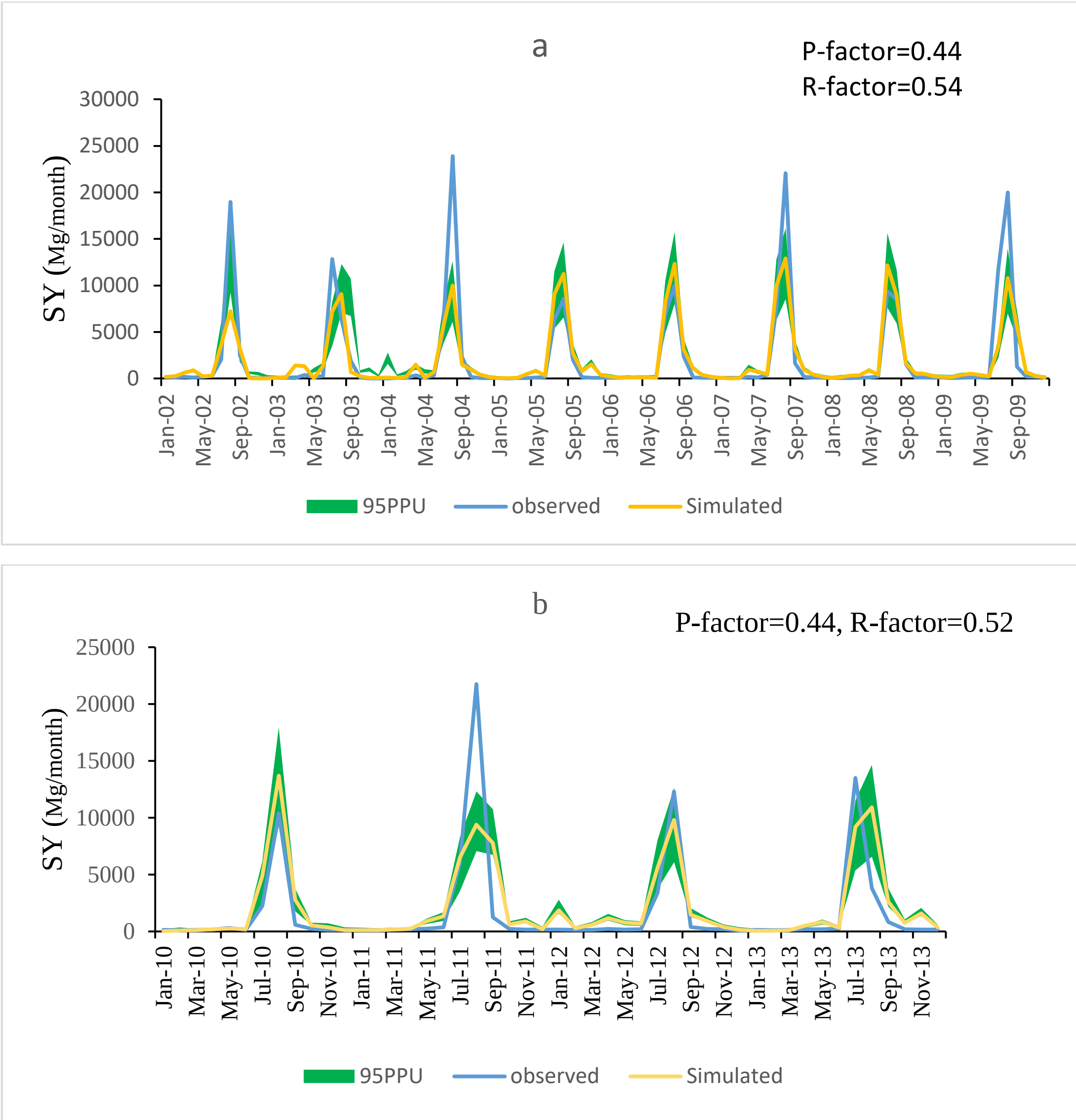

Figure 4.6: Observed and Simulated Sediment Yield with the 95% Prediction Uncertainty (95PPU) Band during (a) the Calibration Period and (b) the Validation Period.

The uncertainty analysis result indicates that 44% of the observed data were enclosed within the relatively narrow 95% prediction uncertainty (95PPU) band. The relatively low P-factor (0.44) may arise from high temporal variability of the sediment transport process, which is highly influenced by rainfall variability and land cover conditions. Additionally, due to a lack of continuous sediment measurements, the sediment data were extrapolated from sediment rating curves. As rating curves are derived from limited sediment sample records, they may not adequately capture sediment movement during extreme runoff episodes, hence introducing uncertainty into the observed sediment dataset. Similar findings have been reported in Ethiopian watersheds for sediment modeling studies; for instance, in the Genale watershed, Negewo & Sarma (2021) reported a p-factor of 0.48 for calibration and 0.43 during validation periods. A lower p-factor value (0.23) was reported for the Maybar watershed during the calibration period (Yesuf et al., 2015). Therefore, the uncertainty measures obtained in this study are within the range reported for sediment simulations in previous studies. Despite this uncertainty, the satisfactory performance statistics ($R^2 = 0.73$ and NSE = 0.69) and consistent calibration and validation results indicate that the model is reliable for assessing climate change impacts and BMP effectiveness in reducing sediment yield.

4.1.7 Sediment Delivery Ratio of the Beressa Watershed

The SDR values for sub-watersheds within the Beressa watershed ranged from 0.153 to 0.525 (Figure 4.7). The lowest SDR value was among sub-watersheds 10, and the highest was from sub-watersheds 2, 8, 9, and 16. The SDR value for the Beressa watershed was obtained as 0.26. This indicates 74 % of the total eroded soil was deposited within the watershed before reaching the watershed outlet, and the remaining 26% of the eroded soil was transported from the origin to the watershed outlet and left the Beressa watershed.

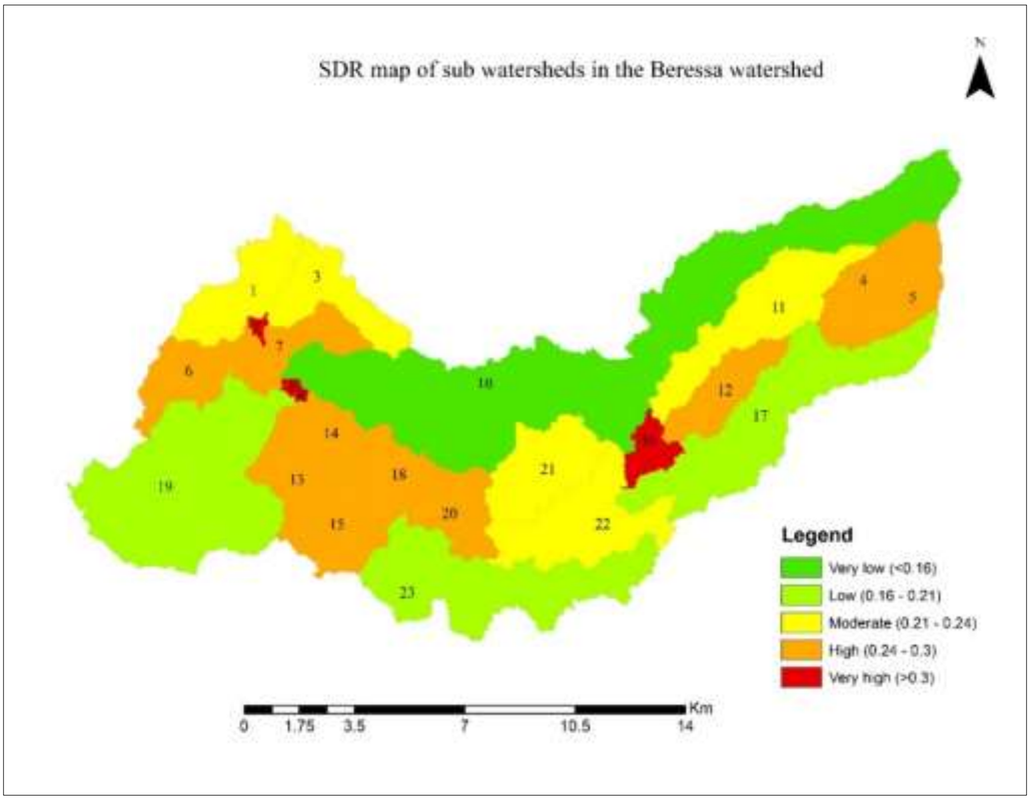

Figure 4.7: Sediment Delivery Ratio at the Sub-Watershed Level of the Beressa Watershed

The estimated SDR for the Beressa watershed indicates that a higher amount of eroded soil settled with the watershed before reaching the outlet. This indicates moderate sediment connectivity but also the presence of important sediment storage areas such as hillslopes, foot slopes, floodplains and stream channels where sediment may be temporarily stored and redistributed. The observed variation in SDR between sub-watersheds indicates variation in sediment transport and deposition due to the inherent characteristics of sub-watersheds. The larger sub-watersheds have lower SDR values because of more opportunities for sediment deposition along longer flow paths and more complex terrain. This inverse relationship between SDR and watershed area is consistent with the study by Abebe et al. (2025), which states that as watershed size increases, sediment delivery efficiency typically declines. On the other hand, smaller sub-watersheds typically have higher SDR values, which indicates a larger fraction of eroded sediment is delivered to the outlet because of shorter flowpaths and little chance for deposition (Woznicki & Nejadhashemi, 2013; Xiao et al., 2024). In addition, Topography and drainage network characteristics affect SDR by controlling runoff concentration, sediment transport capacity, and connectivity between sediment source areas and stream channels (Cho et al., 2023).

The SDR value of the Watershed is aligned with the SDR values of 0.249 and 0.28 reported by Gebre, Belete, & Belayneh (2024) and Gashaw et al. (2021) for the Lake Hawassa sub-basin and Andassa watershed, respectively. On the other hand, the Beressa watershed's SDR value is greater than the Koga watershed's SDR value of 0.14 reported by Gashaw et al. (2021). Other studies by Abebe et al. (2025), Abebe & Woldemariam (2024), and Sinshaw et al. (2021) found higher SDR values of 0.47, 0.48, and 0.44 for the Andit Tid, Aygebre, and Rib watersheds, respectively. The difference may come from watershed characteristics such as land use, topography, parent material, and watershed size (Halder, 2023), all of which influence sediment transport throughout the watershed. The agreement between the estimated SDR for this study and empirical SDR–area relationships reported for neighboring watersheds provides additional confidence in the practicality of the estimated value. In addition, the SDR value was used to convert the SWAT simulated sediment yield into gross soil erosion estimates for a better understanding of the erosion process in the watershed. For conservation intervention, sub watersheds with relatively high SDR value should be prioritized because soil erosion reduction in such areas more likely to translate into sediment reduction at the watershed outlet.

4.1.8 Average Soil Erosion and Sediment Yield under Climate Change

The baseline average sediment yield exceeds the tolerable soil loss limit (<11Mg/ha/year) for Ethiopia highlands, and climate change projections further increase sediment yield and soil erosion under both SSP2-4.5 and SSP5-8.5 scenarios (Table 4.6). The largest increases occur under the SSP5-8.5 far-future scenario. The result indicates that climate change is likely to increase the already unsustainable sediment yield and soil erosion rates in the watershed.

Table 4.6: Baseline and Projected Average Sediment Yield and Soil Erosion (Mg/ha/year), and Their Percentage Changes Relative to the baseline under SSP2-4.5 and SSP5-8.5 Climate Scenarios.

Time period	scenarios	sediment yield	Change (%)	Soil erosion	Change (%)
Baseline (1995-2023)	historical	19.57	-	70.5	-
near future (2030-59)	SSP2-4.5	25.83	31.99	94.9	34.61
near future (2030-59)	SSP5-8.5	23.33	19.21	85.36	21.08
Far future (2060-89)	SSP2-4.5	25.03	27.90	93.48	32.60
Far future (2060-89)	SSP5-8.5	28.45	45.38	105.87	50.17

i. Baseline Sediment Yield and Soil Erosion

In the baseline period, the mean exported sediment (19.57 Mg/ha/year) surpasses the Ethiopian highlands' tolerable soil loss limit. This reveals that soil loss in the Beressa watershed surpasses natural regeneration, resulting in reduced soil fertility, poorer agricultural yield, and long-term land deterioration. The average sediment yield of the watershed is consistent with previous studies. For instance, a mean sediment yield of 17.9 Mg/ha/year for Andit Tid Watershed (Woldemariam, Ddumba, & Addis, 2024), 19.7 Mg/ha/year for Gumura Watershed (Gashaw et al., 2021), and 17.9 Mg/ha/year for Andassa Watershed (Abebe et al., 2022). This consistent value may result from the catchments similar land use nature and traditional farming practices.

However, the Beressa watershed's annual sediment yield is lower than the national average of 26 Mg/ha/year (Tamene et al., 2022), 25.53Mg/ha/year of the Rib watershed (Sinshaw et al., 2021), and 28.57 Mg/ha/year of the Megech watershed (Admas et al., 2022). This difference may be because those watersheds are mountainous compared to Beressa. On the other hand, the Beressa watershed has a larger sediment yield than the Dame watershed in the Omo Gibe Basin, which is 14.35 Mg/ha/year (Mekuria, Derib, & Melesse, 2024), and the Mormora watershed in the Dewa sub-basin, which is 8.54 Mg/ha/year (Tenaw, Tadesse, & Kerebih, 2024). These areas have a smaller sediment yield than the Beressa watershed, most likely due to their flat topography and small agricultural activity.

The gross soil erosion rate of the Beressa watershed lies within the range reported for the Nile Basin, which varies from 0 to 650 Mg/ha/year (Tamene, Lulseged & Bao, 2015). The average annual gross soil loss in the Beressa watershed (70.5 Mg/ha/year) is approximately double the Ethiopian national average of 38 Mg/ha/year (Tamene et al., 2022). It also exceeds erosion rates reported for other Ethiopian watersheds, including 18.74 Mg/ha/year in the Gidabo watershed (Dogiso, Muluneh, & Ketema, 2025), 34.36 Mg/ha/year in the Mugger watershed (Tullu & Tumsa, 2024), and 32.7 Mg/ha/year in the Megech watershed (Admas et al., 2022).

The Beressa gross erosion rate is also comparable to the range reported for Ethiopia's moist agroecological zones from 49.2–64.8 Mg/ha/year (Tamene et al., 2022) and to the Nile Basin's RUSLE-based average of 75 Mg/ha/year (Tamene, Lulseged & Bao, 2015). This comparable value may be due to their similar agricultural activities and weather conditions. On the other hand, the gross erosion rate of the watershed is lower than the Chimango watershed of 80 Mg/ha/year (Bewket & Teferi, 2009), and the Guder watershed in Ethiopia experiences 97.5 Mg/ha/year (Hajisheko et al., 2025). These are likely due to their steeper mountainous terrain, higher average rainfall, and dependency on traditional farming practices. Globally, the gross erosion rate of the Beressa watershed is also lower than erosion rates documented for other erosion-prone basins. For example, the Yangtze River Basin in China averages 138 Mg/ha/year (An et al., 2022), while the Zhuoshui River Basin in Taiwan averages 122.94 Mg/ha/year (Liou et al., 2022). These higher erosion rates in such catchments are mostly due to their having steep and rugged terrain, severe rainfall, mountainous farming, and highly erodible soils compared to the Beressa watershed.

ii. Projected Soil Erosion and Sediment Yield

The projected increases of average sediment yield (19.2%-45.4%) and average soil erosion (21.2%-50.2%) under SSP2-4.5 and SSP5-8.5 scenarios may arise from variation in rainfall intensity and rising temperature in the future periods. The magnitude of the change in sediment yield was greater than that of the change in average rainfall, indicating a nonlinear response of erosion processes to climate forcing. This may arise from the expected intensified precipitation in the future climate conditions, as it is likely to have amplified runoff generation and soil detachment. The study by Gu et al. (2025) also reported that high-intensity rainfall events produce more erosive energy than the same amount of average rainfall over longer periods and lead to disproportionate sediment yield increase. Additionally, antecedent soil moisture conditions may increase sediment production by reducing infiltration capacity during subsequent rainfall events (Lan, Junyou, & Jingjing, 2020). Because under wetter soil conditions, a large amount of rainfall is converted to surface runoff, which facilitates sediment transport.

The findings strongly aligned with studies by Dogiso, Muluneh, & Ketema (2025) in the Gidabo watershed in Ethiopia, who reported the mean soil loss increment by 21.4%,32.2%,23.4%, and 35.7% for near SSP2-4.5, far SSP2-4.5, near SSP5-8.5, and far SSP5-8.5, respectively, compared to the baseline period. Similarly, in China's Loess Plateau, Chen et al. (2024) found that soil loss would rise by 19.11% under SSP2-4.5 and by 35.35% under SSP5-8.5 relative to the baseline. Other studies by Tullu & Tumsa (2024) in the Muger watershed reported an increase in soil loss of 6-8.5% under SSP2-4.5 and 5.6-9.4% under SSP5-8.5 compared to the baseline. In South Asia, the soil erosion rate is expected to increase by 31–39% under future climate and high-erosion zones under SSP5-8.5, expanding by 35% by 2100 (Das, Jain, & Gupta, 2024).

4.1.9 Temporal Variations in Erosion and Sediment

Sediment yield and soil erosion are directly affected by precipitation patterns as shown in Figure 4.8. For example, peak sediment yield occurred in 2074 under SSP2-4.5 and in 2033 under SSP5-8.5, corresponding to higher precipitation events. The highest sediment yield in Mg/ha/year for the baseline, near SSP2-4.5, near SSP5-8.5, far SSP2-4.5, and far SSP5-8.5 were 36.98 in 2007, 48.04 in 2044, 55.88 in 2033, 96.46 in 2074, and 54.59 in 2071, respectively. Similarly, for soil erosion, the highest erosion in Mg/ha/year for the baseline, near SSP2-4.5, near SSP5-8.5, far SSP2-4.5, and far SSP5-8.5 were 142.24 in 2007, 184.77 in 2044, 214.93 in 2033, 371.01 in 2074, and 209.92 in 2071, respectively. In the near future, the peak is expected under SSP5-8.5 compared to SSP2-4.5, while in the far future, the highest peak is expected under SSP2-4.5 compared to SSP5-8.5.

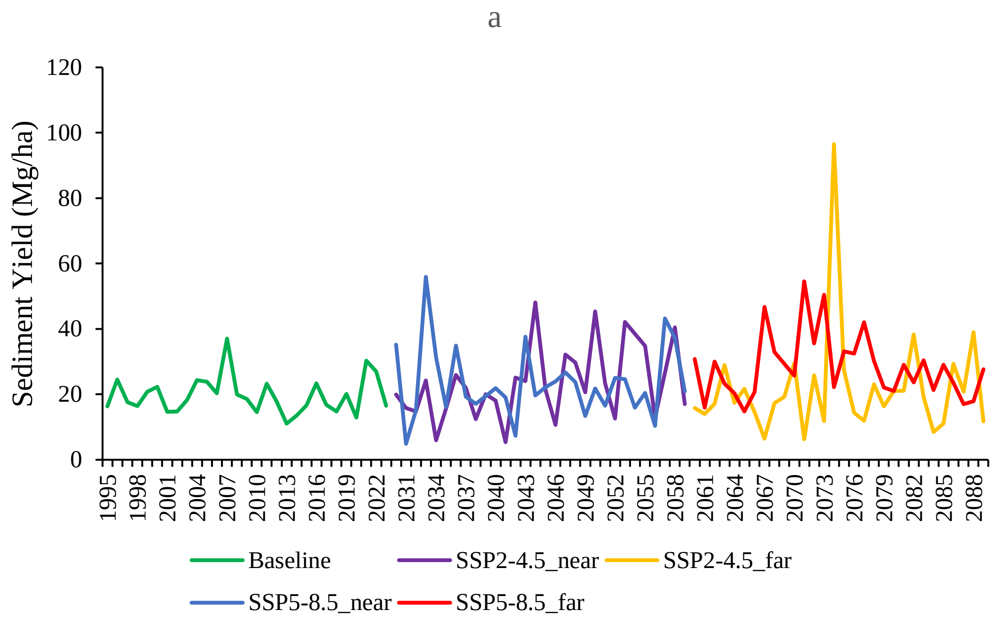

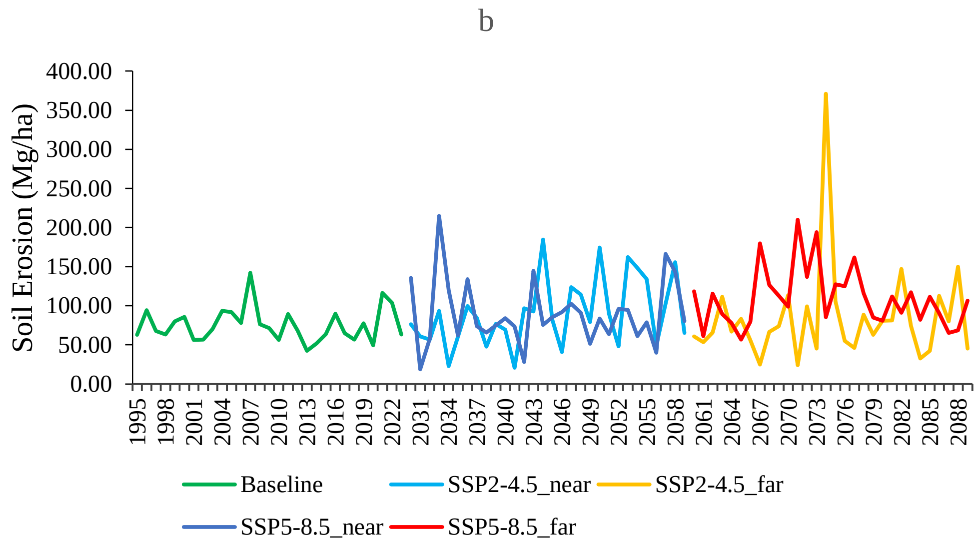

Figure 4.8: Temporal Variation of Sediment Yield (a) and Soil Erosion (b) in the Beressa Watershed under Baseline, Near, and Far Terms of SSP2-4.5 and SSP5-8.5 Scenarios

The year-to-year variability in erosion suggests that extreme years exhibit sudden changes in erosion rates. This dramatic spike in annual soil erosion may have resulted from extreme events, and the size of the droplets was larger than in other years. Similar to the findings, the study by Majewski & Szpikowski (2024) reported that intense, short-duration storm events disproportionately affect soil erosion within a single year by significantly increasing the erosive capacity of precipitation. Additionally, the occurrence of heavy rains in the early season before crops are established results in a sudden shift for specific years (Marcinkowski & Szporak-Wasilewska, 2024). In years with relatively few extreme events, infiltration capacity, vegetation cover, and soil cohesion effectively buffer erosion processes. In contrast, years characterized by frequent climate extremes exhibit a severe increase in sediment yield, reflecting a transition from infiltration-dominated to runoff-dominated erosion processes.

4.1.10 Non-Linear Sediment Response to Rainfall Extremes

Higher intensity rainfall events (P99 and above) explain a significantly larger portion of sediment variability than moderate extreme indices (P95), according to the correlation between annual sediment and daily extreme rainfall indices (Table 4.7). Rather than normal rainfall conditions, the most extreme rainfall events account for nearly half of the interannual variability in sediment. Approximately 29.5% of the total sediment yield in the Beressa watershed comes from the top 20% of years with the highest frequency of P99 rainfall events, highlighting the dominant influence of very intense rainfall events on sediment transport.

Table 4.7: Relationship Between Extreme Rainfall Indices and Annual Sediment Yield

Extreme rainfall indicators	Correlation (r)	Explained Variance (r^2)
Days > P95 rainfall	0.50	0.25
Days > P99 rainfall	0.67	0.45
Days > 2× P99 rainfall	0.71	0.51

The relationship between climate variables and sediment yield appears to be non-linear, with small changes in rainfall parameters causing disproportionately large increases in sediment export. This response illustrates threshold-controlled erosion processes, in which runoff generation, soil detachment, and sediment transport increase as crucial hydrological thresholds are exceeded. The expected increase in sediment yield is likely caused by a small number of high-intensity rainfall events, which account for a disproportionate part of yearly sediment export. These results are consistent with research done throughout mainland China, where roughly 24% of total rainfall erosivity is attributed to the most extreme 20% of rainfall events (Chen et al., 2025). These findings suggest that future sediment management strategies should prioritize preventing runoff and erosion during extreme storms. As a result, best management practices (BMPs) should be designed to resist high-intensity rainfall, and regular checkup and maintenance will be required to ensure their continued effectiveness in increasingly extreme weather conditions.

4.1.11 Sub–Watershed Level Soil Erosion and Sediment Yield under Climate Change Scenarios

Compared to the baseline conditions, the sub-watershed level soil erosion and sediment yield are higher under future scenarios (SSP2-4.5 and SSP5-8.5), as shown in Figure 4.9. Sub-watershed 2 had the highest sediment yield, whereas Sub-watershed 10 had the lowest sediment yield. Similarly, Sub-watershed 10 experienced the least amount of soil erosion, while Sub-watershed 22 experienced the greatest rate of erosion. Despite similar climate conditions, sediment yield and soil erosion varied throughout the 23 sub-watersheds. Notably, smaller sub-watersheds produced more sediment, whereas larger sub-watersheds produced less sediment. Specifically, sub-watershed 10 has been less affected by climate change. This sub watershed have large area and conservation measures compared to the remaining sub-watersheds.

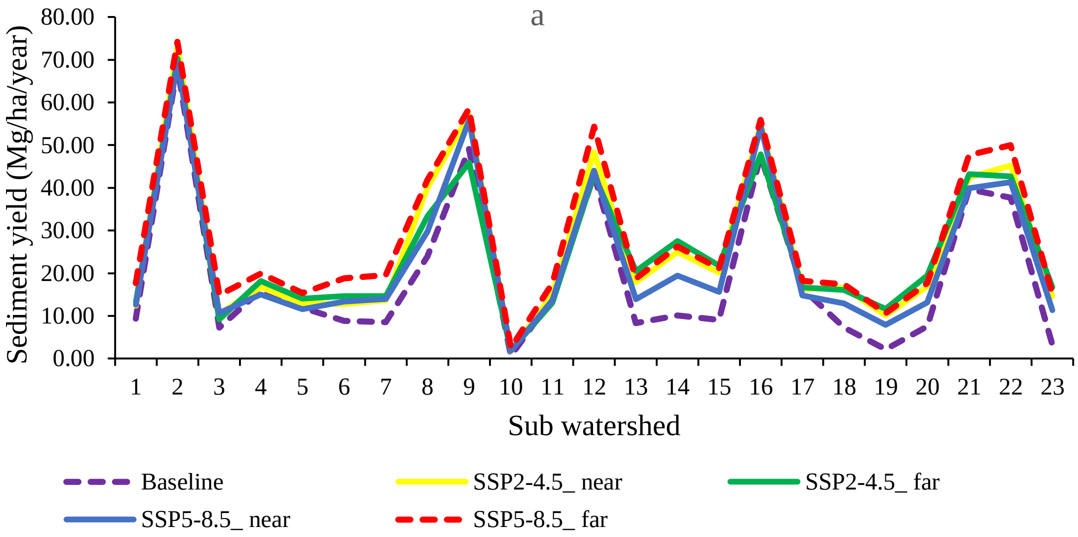

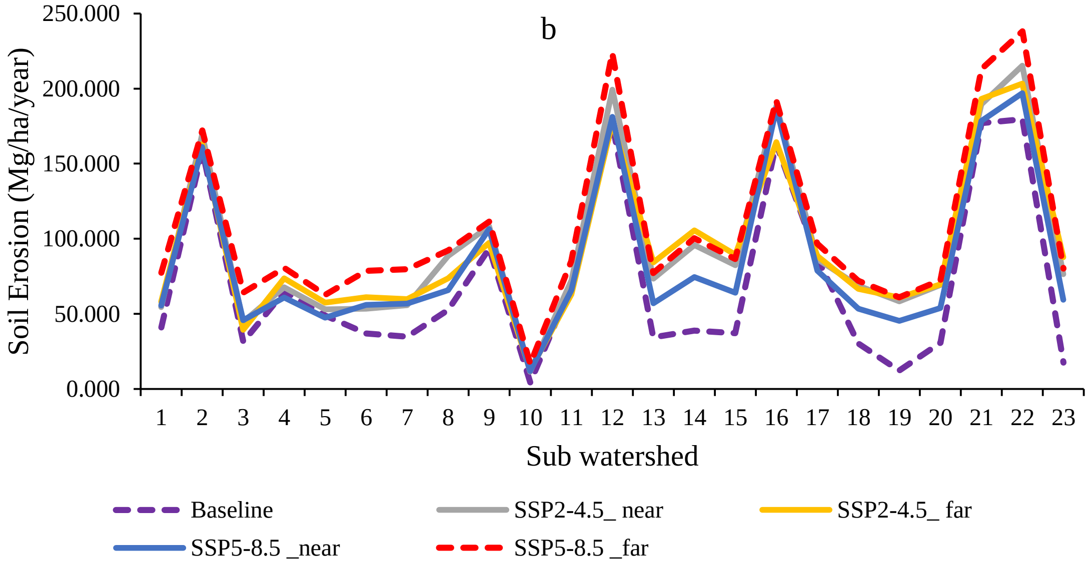

Figure 4.9: Sediment Yield (a) and Soil Erosion (b) at the Sub-Watershed Level under Baseline, Near and Far terms of SSP2-4.5 and SSP5-8.5 Climate Scenarios

The spatial variability shows climate-driven erosion processes strongly influenced by watershed characteristics, such as slope, land use, management practices, soil properties, and watershed size. Smaller sub-watersheds and steeper slopes generally produced higher sediment yield because they lead water to flow more quickly, which increases sediment yield by leaving little chance for sediment deposition. Larger watersheds, on the other hand, possess longer flow paths and more expansive floodplains, which give increased opportunities for sediment deposition before reaching the watershed outlet.

The results were consistent with previous studies by Sedighi et al. (2021), who report that watershed characteristics, such as slope and size, significantly affect soil erosion and sediment yield. Other studies by Arabkhedri, Heidary, & Parsamehr (2021) reported that smaller watersheds typically have higher sediment connectivity and Shorter travel distances, which contributes little chance to sediment depositions and allows more chance for the eroded materials to reach the watershed outlet quickly. Similarly, the study by Sun et al. (2023) documented that smaller sub-watersheds respond more intensely to rainfall events, resulting in sharper peak flows and sediment output. In addition, Panagos, Borrelli, & Meusburger (2015) found that areas with high LS factor values were more susceptible to erosion, due to the combined effect of slope length and steepness.

Furthermore, the observed variability reflected differences in sediment and hydrological connectivity between sub-watersheds. A higher percentage of detached soil was exported to streams in regions with stronger connections between hillslopes and channel networks (Bracken et al., 2015). This spatial heterogeneity supports the HRU-based structure of the SWAT model, which accounts for spatial variations in slope, land use, and soil characteristics across the watershed. Overall, prioritizing erosion-prone sub-watersheds under changing climate conditions is important for targeted best management practices implementation and sustainable natural resource management.

4.2 Spatial and Temporal Dynamics of Erosion and Sediment Hotspots in the Beressa Watershed under Future Climate Scenarios.

4.2.1 Temporal Variability of Erosion and Sediment Hotspot

The severity class shows the shift from the very low and low severity classes to a higher severity class under both SSP2-4.5 and SSP5-8.5 scenarios compared to baseline (Table 4.8). During the baseline period, 67.8% of the watershed had sediment yields within the tolerable soil loss limit (< 11 Mg/ha/year), while the remaining 32.2% exceeded the tolerable limit. However, due to climate change, the area of the watershed generating sediment yields below 11 Mg/ha/year was reduced by 29.3% for the near-term SSP2-4.5 and SSP5-8.5 scenarios, 41.7% for the far-term SSP2-4.5 scenario, and 44.9% for the far-term SSP5-8.5 scenario compared to the baseline.

Under the far-term SSP5-8.5 scenario, the soil erosion severity class showed the complete disappearance of the very low and moderate erosion classes. In contrast, the sediment yield severity classification retained 22.9% of the watershed within the very low severity class. Compared with the far-term SSP2-4.5 scenario, the far-term SSP5-8.5 scenario showed a more pronounced shift toward higher severity classes. Specifically, 3.2% of the watershed remained within the low-severity class under far-term SSP2-4.5, whereas no sub-watersheds remained in this class under the far-term SSP5-8.5 scenarios.

Table 4.8: Shifts in Erosion and Sediment Severity Class Coverage (%) under SSP2-4.5 and SSP5-8.5 Climate Scenarios Relative to the Baseline in the Beressa Watershed.

Sediment severity class (Mg/ha/year)	Baseline	SSP2-4.5_near	SSP5-8.5_near	SSP2-4.5_far	SSP5-8.5_far
Very Low (<5)	43.6	22.9	22.9	22.9	22.9
Low (5-11)	24.2	15.6	15.6	3.2	0.0
Moderate (11-18)	19.1	44.0	46.5	48.7	40.6
High (18-25)	0.1	4.4	1.8	10.2	21.5
Very high (>25)	13.0	13.1	13.1	14.9	14.9
Erosion Severity class (Mg/ha/year)					
Very low (<15)	35.4	22.9	22.9	22.9	0.0
Low (15-30)	8.2	0.0	0.0	0.0	22.9
Moderate (30-50)	26.7	3.2	18.2	3.2	0.0
High (50-100)	16.7	60.9	45.9	59.2	62.3
Very high (>100)	12.9	13.0	13.0	14.7	14.8

4.2.2 Identification and Evolution of Hotspot Areas

The sediment and erosion hotspot map indicated an expansion in severity classes under future climate scenarios compared to the baseline, as shown in Figure 4.10. The baseline period indicated erosion hotspots in steeper, smaller, and less vegetated sub-watersheds, whereas the future projections show widespread high-risk areas. Under the near-term SSP2-4.5 scenario, a greater land area transitioned into moderate and high severity classes relative to the baseline period. In the far-term of SSP2-4.5 scenarios, the southeast portion of the watershed experienced more severe classes. In the near-term SSP5-8.5 scenarios, the emergence of high and very high erosion zones is mainly within the watershed's central, southeastern, and northeastern regions. In the far term, the SSP5-8.5 scenario exhibited the most severe changes, with high to very high severity expanding across the central, northwestern, and southeastern regions.

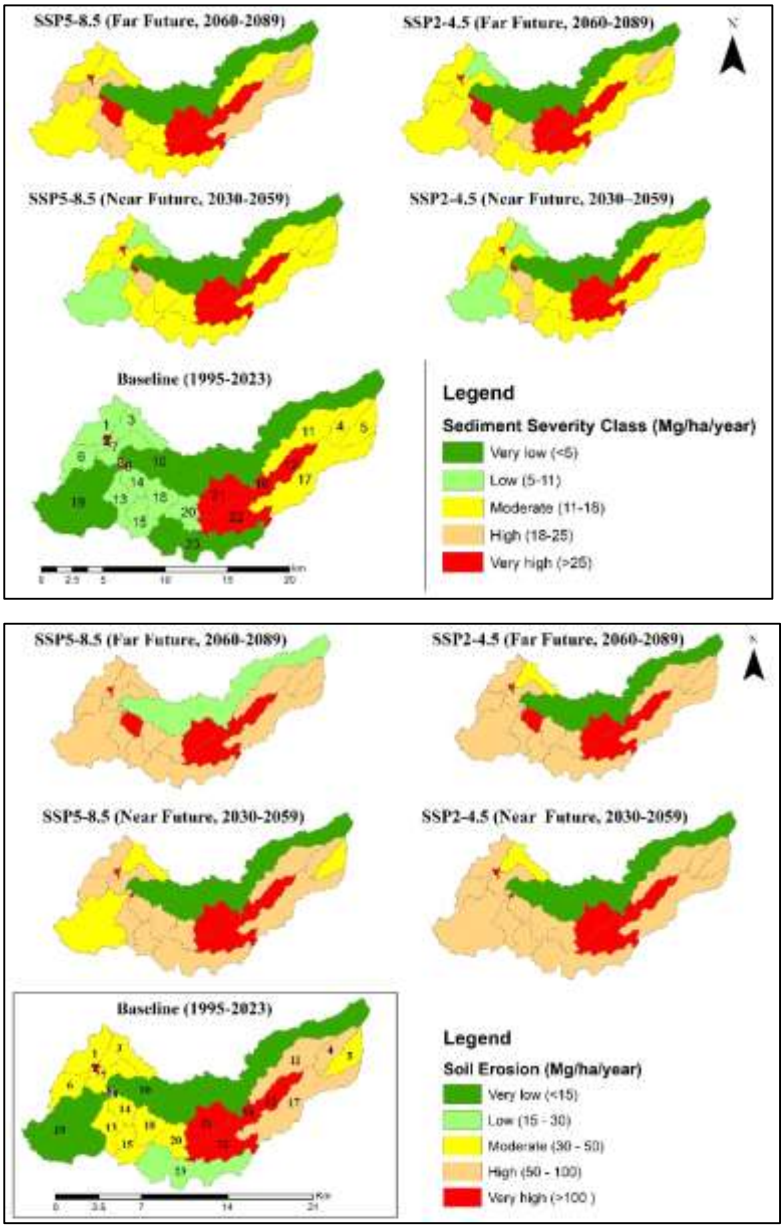

Figure 4.10: Soil Erosion and Sediment Hotspot Map of the Beressa Watershed under Baseline, Near-Term SSP2-4.5, Near-Term SSP5-8.5, Far-Term SSP2-4.5, and Far-Term SSP5-8.5 Scenarios.

The more pronounced shift toward higher severity classes under the far-term SSP5-8.5 scenario is likely attributable to the stronger climate forcing projected for this scenario. Greater increases in extreme precipitation (P99) enhance soil detachment and transport, causing areas previously classified as low severity to shift into higher severity classes. The expected more extreme future climatic conditions will intensify erosion processes and expand erosion hotspots across the watershed. Although the soil erosion map indicates the disappearance of the very low severity class under the far-term SSP5-8.5 scenario, the sediment yield classification retains 22.9% of the watershed within the very low severity class because it uses different threshold values. Therefore, the results are consistent within each classification system and should be interpreted independently. Furthermore, the transition matrix revealed a progressive conversion of low-risk areas to moderate- and high-risk classes, indicating that erosion-prone zones will expand under future climate conditions.

Similar to this finding, the study by Dogiso, Muluneh, & Ketema (2025) found that both SSP2-4.5 and SSP5-8.5 scenarios contributed to shifts in hotspots, the largest increase expected under far future SSP5-8.5 scenarios. The study by Chen et al. (2024) documented that climate change contributed more strongly to erosion processes than land use change, with the biggest impact observed under SSP5-8.5 climate scenarios. Other studies by Das, Jain, & Gupta (2024) found that high-risk zones widespread under climate change, as a result, previously low-risk areas may shift to high severity. The findings highlight the necessity for climate-adaptive watershed management measures in the Beressa watershed to reduce erosion rates under future climate.

The spatial shift of hotspots within the Beressa watershed indicates that climate change not only worsens erosion in current hotspot areas but also encourages the formation of new sediment-producing zones. The areas with the greatest increases in erosion risk were typically linked with steep slopes, continuous farming, and low plant cover, all of which increase susceptibility to rainfall-induced soil detachment and transport. However, some hotspot locations remained consistent across all scenarios, demonstrating that topography, soil properties, and land-use patterns continue to have stronger resistance to soil detachment and transport despite shifting climatic conditions. Overall, the results suggest that future watershed management should focus not only on existing erosion hotspots, but also on places that are expected to become vulnerable under future climate conditions. Climate-adaptive best management practices (BMPs) should be promoted in both existing and new hotspot areas. Regular monitoring and maintenance of these measures will be required to ensure their long-term efficacy as erosion risk grows and worsens under future climatic scenarios.

4.3 Effectiveness of Selected Best Management Practices (BMPs) in Reducing Sediment Yield under Projected Climate Conditions in the Beressa Watershed.

4.3.1 Projected Sediment Yield Reduction with BMPs.

Compared to the baseline (no mitigation measures) condition, all individual practices contributed to sediment reduction, with the combined measures showing the greatest effectiveness, as shown in Table 4.9 and Figure 4.11.

Table 4.9: Reduction in Average Sediment Yield after BMP Implementation

scenarios	Terracing (%)	CA (%)	CF (%)	Combination (%)
SSP2-4.5_near	50.64	32.4	19.74	59.0
SSP2-4.5_far	47.66	29.68	20.05	59.41
SSP5-8.5_near	47.6	30.77	20.4	58.2
SSP5-8.5_far	48.36	32.76	19.65	59.86
Rank	2	3	4	1

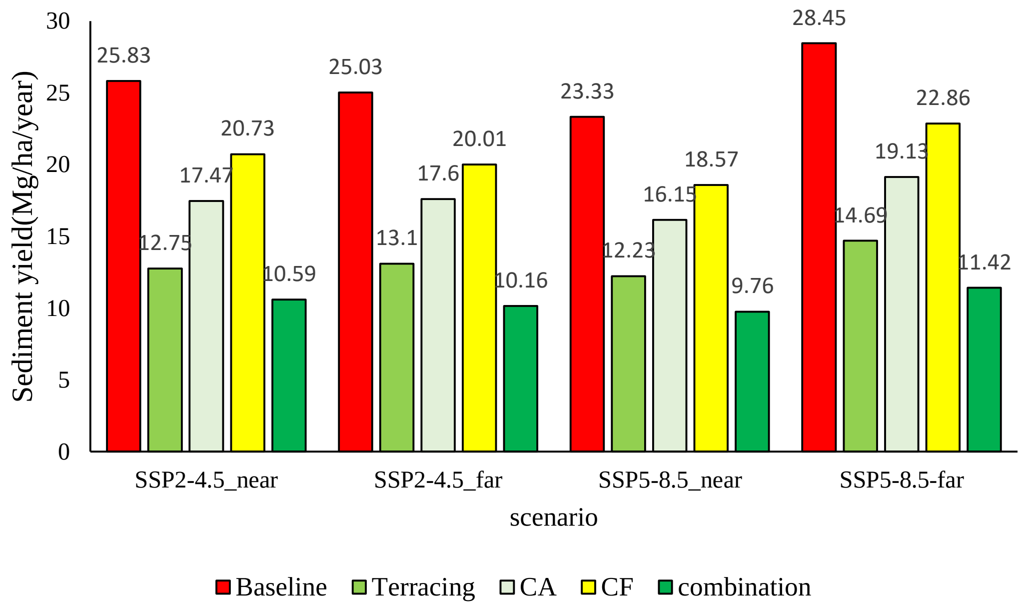

Figure 4.11: Sediment Yield Before and After BMPs under Near and Far Terms of SSP2-4.5 and SSP5-8.5 Climate Scenarios.

The effectiveness of the applied BMPs is discussed in detail below:

a. Terracing

Terracing was effective across all erosion severity classes, especially in very high sediment severity areas, because it creates level steps that disrupt downslope water movement and enhance water infiltration (Chen, Wei, & Chen, 2017; Uniyal et al., 2020). Their effectiveness in high-risk areas of the watershed confirms the need for physical interventions in severe erosion zones. The presence of agricultural activities on higher slope areas (>15%) increases water erosion unless conservation measures such as terraces are implemented. Agricultural land, grassland, and barren land covered more than 86% of the watershed, and implementing terracing on these land uses reduced the sediment yield of the watershed by 47.6-50.64% for SSP2-4.5 and SSP5-8.5 climate scenarios compared to the baseline. This is due to terracing, which reduces slope length and runoff velocity, while also improving infiltration and sediment trapping.

The findings are comparable with previous SWAT-based and field experiment research conducted in similar regions. For example, Mequanient & Kebede (2023) found 45.4% reduction in sediment yield in the upper Gilo watershed after terracing application. Similarly, Regasa & Nones (2024) found that terracing reduced sediment output by 76.32% in future periods in the Fincha Watershed. Furthermore, Lemann et al. (2016) observed that installing Fanaju terraces on 50% of agricultural lands reduced sediment yield by 30%. Finally, Debie, Singhb, & Belay (2018) found that rill erosion was reduced by 53.5% in terraced fields relative to fields without terracing.

b. Conservation agriculture

The observed reduction in sediment yield (29.68-32.76%) under no-till farming methods in SWAT can be due to the shallow soil disturbance (about 25 mm) and low mixing efficiency (0.05) associated with no-till operations. In contrast, conventional tillage methods like generic fall plowing operation and moldboard plow2-way4-6b (mixing efficiency = 0.95; depth = 150 mm) encourage significantly greater soil mixing, potentially leading to higher sediment and nutrient transport. The no-till method reduces soil erosion by maintaining a protective layer of residue on the field's surface. This cover is crucial for protecting bare soil during the early stages of crop growth, a period of heightened susceptibility to erosive forces (Martínez et al., 2020). These practices have been proven to reduce erosion, improve soil health, and enhance farm productivity (Rao et al., 2022).

The findings were consistent with previous field-level and SWAT-based evaluation studies. For example, Araya et al. (2011) found that adopting zero tillage combined with 30% residue retention reduced average sediment yield by 78.5% when compared to traditional farming practices. SWAT-based studies by Martínez et al. (2020) at Pleasant Valley Watershed found 14 to 25% sediment yield reduction due to the implementation of no-till practices. Similarly, the study at the Bosque River watershed by Tuppad (2010) and the study by Uniyal et al. (2020) at the upper Baitarani River basin found 10% and 5.36% reduction of sediment yield due to the implementation of conservation tillage, respectively.

c. Contour farming

The observed sediment reduction (19.65-20.4%) was due to contour farming's effect in reducing slope-length flow pathways and increasing the role of water infiltration. This is consistent with previous studies by Saggau, Kuhwald, & Duttmann (2023), which found that contour farming considerably reduces soil detachment and water movement from cultivated lands. The study in the Fincha watershed by Dibaba, Demissie, & Miegel (2021) found a 17.1% reduction due to contour farming. Similarly, Leta et al. (2023) observed a 39.55% reduction in the Nashe watershed by the use of contour farming on agricultural land. Lastly, Mequanient & Kebede (2023) found a 43.6% reduction as a result of contour farming.

d. Combined measures

Compared to the baseline, combined measures reduced nearly three-fifths (58.2-59.86%) of the average sediment yield. This is because, in this combination, Terracing served as a strong physical barrier by shortening slope length and effectively trapping sediments. Conservation agriculture reduces soil detachment by continuous soil cover, whereas contour farming enhances these measures by directing water along natural contour lines. These methods address key components of the erosion process, including detachment, transport, and deposition, resulting in an effective and integrated erosion control system. The study by Uniyal et al. (2020) reported the advantages of integrating agronomic measures with structural measures on steeper slopes to control the intensity of surface runoff. Other studies by Gashaw et al. (2021), Regasa & Nones (2024), and Zantet et al. (2023) documented that the combined application is more effective in reducing sediment yield than individual measures. Furthermore, the consistent effectiveness of combined measures under a range of projected climates, including moderate (SSP2-4.5) and high-emission (SSP5-8.5) pathways, confirms their role for adaptive land management. The technique remains practical and cost-effective for widespread application by smallholder farmers. Terracing is useful, but may not be cost-efficient for gentle slopes (< 10%). In such flat slope areas, agronomic measures alone have proven effective for controlling erosion. Lastly, these methods contribute to improved soil health, greater water infiltration, and the long-term sustainability of agricultural systems (Cárceles et al., 2022). These findings highlight the importance of using slope-specific and integrated structural and agronomic solutions to improve erosion control and promote climate-resilient land management.

4.3.2 Spatial Variation in Sediment Yield Following BMPs Implementation

Following the application of BMPs, the watershed area that generates soil loss below 11 Mg/ha/year increased significantly across all climate scenarios (Table 4.10). In the near-term SSP2-4.5 scenario, 38.5% of the watershed produced sediment yield within the tolerable limit before BMP application. After BMPs, this area increased by 48.41% with terracing and combined measures, 39.13% with conservation agriculture (CA), and 19.65% with contour farming (CF). Similarly, under the near-term SSP5-8.5 scenario, 38.5% of the watershed generated a sediment yield below 11 Mg/ha/year. The application of BMPS increased by 48.41% with terracing, 46.57% with CA, 44.19% with CF, and 48.55% with the combined measures. In the far-term SSP2-4.5, 26.1% of the watershed exceeded this threshold limit; after BMPs, this area increased by 60.81% with terracing and combined measures, 51.51% with CA, and 32.05% with CF. For the far-term SSP5-8.5 scenario, 22.9% of the watershed generates soil loss within tolerable limits. After applying BMPs, this increased by 61.19% with both terracing and the combined measure, 38.13% with CA, and 23.9% with CF. These results indicate that the applied BMPs are important in the Beressa Watershed. Terracing and the combined use were the most effective in expanding the area of the watershed that maintained sustainable sediment yields under both climate scenarios.

Table 4.10: Percentage Change in Sediment Severity Classes After Applying Best Management Practices under SSP2-4.5 and SSP5-8.5 Climate Scenarios.

climate scenarios	Sediment severity class	Baseline	Terracing	CA	CF	combined measures
	<11	38.5	86.91	77.63	58.15	86.91
	11-18	44	0.14	9.28	28.76	11.75
SSP2-	18-25	4.4	11.61	-	-	-
4.5_near	>25	13.1	1.34	13.09	13.09	1.34
	<11	38.5	86.91	85.07	82.69	87.05
	11-18	46.5	0.14	1.97	4.22	2.58
	18-25	1.9	-	-	0.14	9.03
SS5-8.5_near	>25	13.1	1.34	12.95	12.95	1.34
	<11	26.1	86.91	77.61	58.15	86.91
	11-18	48.7	0.14	9.28	28.76	11.75
	18-25	10.21	11.61	-	-	-
SSP2-4.5_far	>25	15	1.34	12.95	12.95	1.34
	<11	22.9	84.09	61.03	46.8	84.09
	11-18	40.6	2.82	23.5	35.89	11.99
	18-25	21.5	0.14	2.38	4.22	2.58
SSP5-8-5_far	>25	15	12.95	13.09	13.09	1.34

4.3.3 Sediment Hotspot Reduction under Future Climate Scenarios

Across all climate scenarios, the implementation of best management practices (BMPs), including contour farming, conservation agriculture, terracing, and their combined application, significantly reduced sediment yield hotspots compared with the baseline condition (before BMP implementation), as shown in Figure 4.12. This pattern was consistent across the near- and far-future periods under both SSP2-4.5 and SSP5-8.5, indicating the robustness of BMP performance despite increasing climate change impacts. The effectiveness of the BMPs varied, terracing provide the greatest reduction among the individual measures, while conservation agriculture and contour farming were more effective in reducing sediment yield in moderately eroded sub-watersheds. The combined measures, consistently produced the largest reduction in sediment yield under all climate scenarios. This combined application was the most resilient, as it achieved the highest sediment reduction even in the extreme scenario of SSP5-8.5. Because it significantly neutralized sediment hotspots by shifting most sub-watersheds from high sediment yield classes (>18 Mg/ha/year) to low sediment yield classes (<11 Mg/ha/year), while reducing the maximum sediment yield to approximately 29–36 Mg/ha/year. These results demonstrate that combined measures are the most resilient and effective strategy for mitigating sediment yield under both moderate (SSP2-4.5) and high emission (SSP5-8.5) climate scenarios.

a)

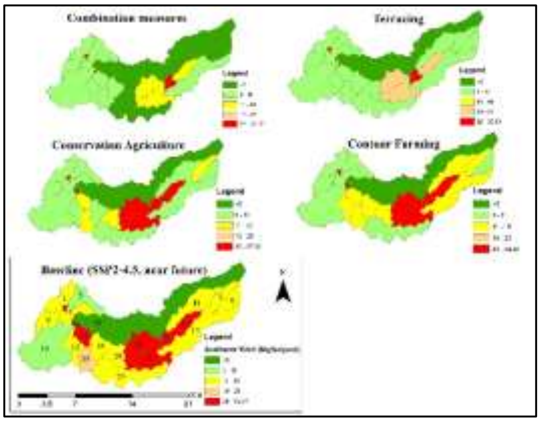

b)

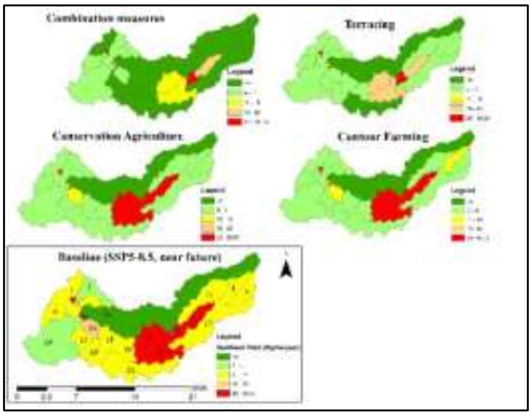

c)

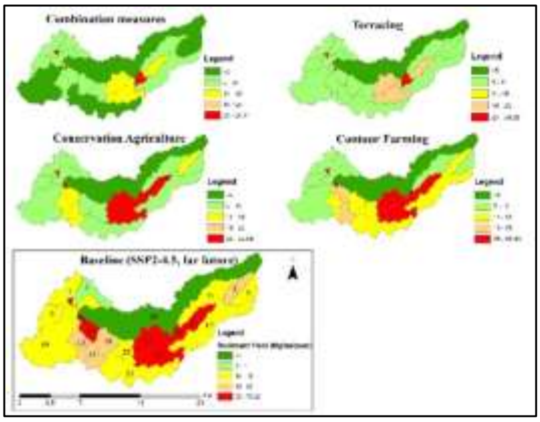

d)

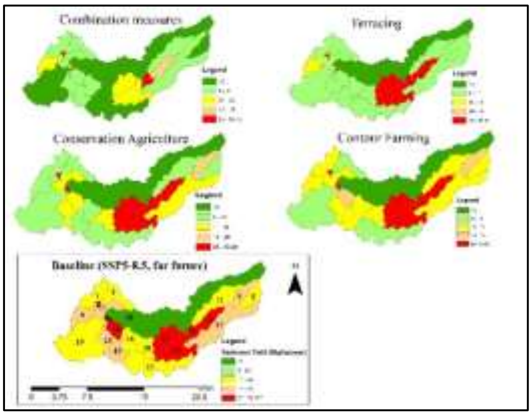

Figure 4.12: Reduction in Sediment Yield Following the Implementation of Terracing, Conservation Agriculture, Contour Farming , and Combined measures Relative to the Baseline (Before BMP Implementation) under (a) Near-Future SSP2-4.5, (b) Near-Future SSP5-8.5, (c) Far-Future SSP2-4.5, and (d) Far-Future SSP5-8.5 Climate Scenarios.

4.3.4 Sub-Watershed Scale Effectiveness of BMPs under Future Climate Scenarios

The effectiveness of the applied measures, such as terracing, conservation agriculture (CA), contour farming (CF), and combined measures, varied across sub-watersheds as shown in Figure 4.13. Among the BMPs, combined measures and terracing showed higher reductions in sediment yield at the sub-watershed level, with combined measures performing better. This shows the advantages of combining structural and agronomic measures on agricultural fields. For example, in sub-watersheds 2, 8, 9, and 12, combined measures and terracing resulted in larger reductions than CA and CF. Under both scenarios, conservation agriculture and contour farming reduced erosion severity more in the moderate class, but terracing and combined approaches were more successful in the high and very high classes. However, after applying individual and combined measures, sub-watersheds 2, 9, and 16 remained in the very high erosion severity class, despite showing reductions from the baseline. This suggests that present methods are important but insufficient to adequately control erosion risk in these locations. This may be due to the limitations of conventional BMPs in high-risk geomorphic settings, where adverse physical characteristics continue to produce excess sediment. Additionally, smaller size, steep slopes, and strong hillslope-to-channel connectivity in such sub-watersheds increase runoff generation and sediment transport, thereby reducing the effectiveness of field-scale BMPs.

Although combined measures considerably reduced sediment yield, they could not completely neutralize erosion hotspots because the underlying geomorphic conditions remained dominant. The physical BMPs are often less effective in smaller watersheds because high edge-to-area ratios intensify boundary effects and reduce the sediment-trapping capacity of structures. To enhance the performance of best management practices in these high-risk sub-watersheds, supportive structures such as diversion ditches to divert upstream runoff will be important (Blanco & Lal, 2023; Dollinger et al., 2015). Additionally, check dams in concentrated flow paths, reforestation in steep and degraded areas, and targeted land-use conversion in highly vulnerable areas (Jain, 2025) may further reduce sediment delivery and improve long-term watershed resilience. Similarly, Regasa & Nones (2024) found that the effectiveness of BMPs varies with watershed factors and land use type. Furthermore, Lee et al. (2025) found similar patterns with sediment reductions ranging from 1% to more than 70%. Therefore, site-specific interventions, such as land use change, may be necessary to reduce erosion to tolerable levels in these sub-watersheds.

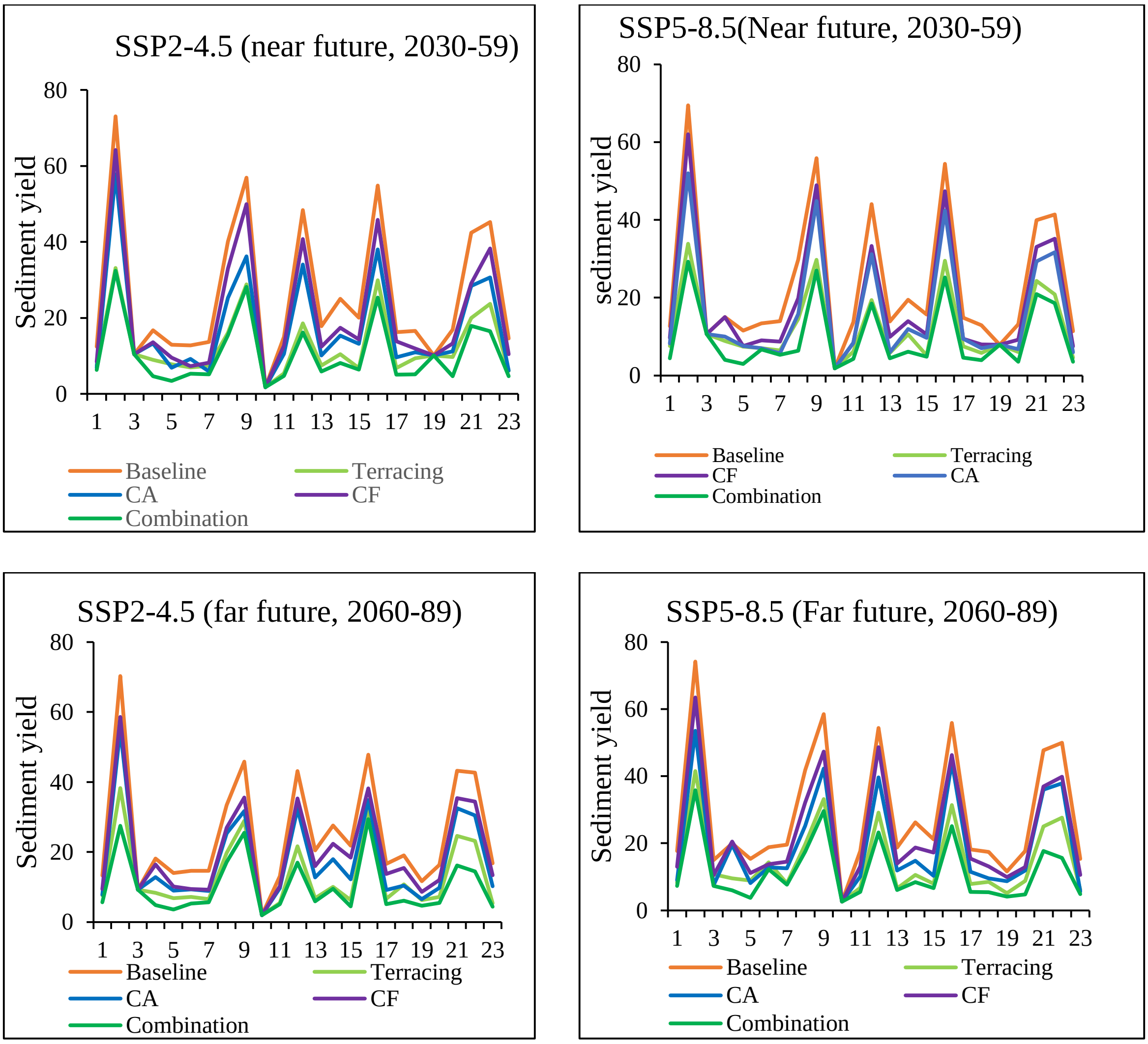

Figure 4.13: Sub-Watershed Level Sediment Yield Reduction due to the Applied BMPs under Near Term (2030-2059) and Far Terms (2060-2089) of SSP2-4.5 and SSP5-8.5 Climate Scenarios.

4.3.5 Economic and Local Feasibility

The findings suggest that implementing combined measures has significant environmental advantages. Their practical implementation will require creating awareness, providing technical assistance, and offering tailored incentives to stimulate stakeholder involvement. A previous study has found that agronomic measures such as conservation agriculture and contour farming can be less expensive than structural interventions like terracing (Tuppad et al., 2010). Contour farming is the practice of aligning land preparation and planting with natural contours. Farmers may readily adopt this method because it does not require any additional inputs. Terracing, on the other hand, takes engineering abilities, although the materials are readily available within the watershed. The choice of physical conservation measures should always align with land-use characteristics and technical standards. Conservation agriculture is a new practice in the watershed. It requires retaining at least 30% of crop stubble during harvesting time. This is challenging because farmers typically collect stubble for livestock feed. Providing incentives, such as negotiating alternative livestock feed sources, could promote adoption. Development agents and trained farmers can conduct the slope classification to ensure effective targeting of these measures. This integrated approach offers a practical and sustainable solution for long-term agricultural productivity in the watershed.

Considering implementation cost, contour farming is likely the most cost-effective measure because it requires minimal additional investment and can be readily adopted by farmers. Conservation agriculture ranks second due to its relatively low implementation cost but greater management requirements, such as crop rotation and residue retention. Combined measures ranked third, due to the requirement for physical structure limited to moderate to higher slopes, making it the most cost-effective strategy for highly erosion-prone watersheds where maximizing erosion control and soil health improvement are the primary objectives. Terracing ranks fourth because it requires greater labor, engineering skills, and maintenance costs.

In years with frequent extreme rainfall events, soil and water conservation measures may subjected to greater stress and reduced efficiency, resulting in increased maintenance demands, resource requirements, and associated costs. Under intensified rainfall extremes, particularly in high-emission scenarios (SSP5-8.5), physical conservation structures are more likely to experience overtopping, structural stress, and reduced trapping efficiency. Consequently, the watershed is expected to face an increasing maintenance burden and potential redesign of conservation measures. In high-risk sub-watersheds, the probability of BMP failure may increase unless design standards are revised to accommodate higher return-period storm events. These findings indicate that the effectiveness of existing BMPs may be reduced by the expected increase in rainfall intensity under future climate conditions. Therefore, periodic maintenance, adaptive design improvements, and awareness creation on expected erosion risks under future climate change enhance sustainable watershed management.

However, uncertainties associated with climate model projections, SWAT model parameterization, future rainfall variability, and assumptions of constant land use should be considered for the interpretation of sediment yield reduction due to the applied BMPs. Therefore, the predicted sediment yield reductions should be interpreted as approximate estimates rather than precise values. Despite these uncertainties, the consistent effectiveness of combined measures under SSP2-4.5 and SSP5-8.5 climate scenarios increases confidence in their effectiveness.

4.4 Uncertainty due to Data Limitations and Model Assumptions

Uncertainties in this study may come from both input data limitations and model assumptions. First, due to gaps in observed climate data, such as wind speed, relative humidity, and solar radiation, were fully simulated using SWAT's built-in weather generator (WGEN). In the absence of observed data records, WGEN is commonly used in SWAT to simulate these variables (Senent-Aparicio et al., 2021). This simulation has impacts on potential evapotranspiration estimation and the runoff process (Haddeland et al., 2011). However, the impacts of uncertainties from generated wind speed, solar radiation, and relative humidity are generally less significant on hydrological model performance than those arising from precipitation and temperature input data uncertainties (Ricard & Anctil, 2019). In data-scarce regions, mainly in Africa, the Hargreaves method is widely used to estimate potential evapotranspiration. Although this technique has known limitations compared to the Penman-Monteith method, it provides a viable alternative for addressing data gaps and enabling hydrological investigations in catchments with limited data (Jung, Lee, & Moon, 2016). Therefore, interpretation of these findings should consider this limitation in the input data, as it may influence sediment yield projections.

Second, daily sediment loads were estimated by applying sediment-rating curves, which were developed from a limited set of sediment and discharge observations. Although separate seasonal rating curves for wet and dry seasons showed explanatory power, they may overestimate sediment yield compared to observed pairs of records (Asselman, 2000). The sediment-rating curve overestimated sediment yield by approximately 15.4% relative to observed data, with an NSE of 0.98 and a PBIAS of -15.4%. The study by Thomas (1985) documented that the limited observational sediment records may have overlooked extreme sediment transport events. This influences the representation of the rating curve for high-magnitude, low-frequency occurrences, leading to skewed estimates of event frequency and total sediment yield. Additionally, the sediment–discharge relationship may not be linear (Crowder, Demissie, & Markus, 2007), which changes over time due to channel adjustments, climatic variability, and land use changes. Therefore, extrapolating sediment data from a few records should account for these uncertainties.

Third, the assumption that land use would remain constant in the future is frequently used to isolate climate change impacts. Such assumptions may cause significant uncertainty in sediment yield projections. In reality, land use within the Beressa watershed is unlikely to remain stable. Agricultural development, urbanization, and deforestation are projected to increase soil erosion and sediment yield, implying that the model underestimates future impacts. In contrast, large-scale reforestation, terracing, and other conservation measures would minimize erosion, causing the model to overestimate future sediment loads. Erosion processes are extremely sensitive to land-use changes. Previous studies have shown that the conversion of forestland to agricultural and urban areas causes increased soil loss and sediment delivery (Aghsaei et al., 2020; Munoth & Goyal, 2020; Roba et al., 2025). When evaluating these findings, it is important to acknowledge this constraint, as future estimations of erosion and sediment yield could vary in any way from the model's projections.

Finally, climatic data from the CMIP6 model have inherent uncertainties due to model selection, emission scenarios, and internal climate variability (Doi & Kim, 2022) . While bias correction was used to increase accuracy, future climate estimates remain uncertain, which may affect the precision of simulated hydrological and sediment responses. Although bias correction increases accuracy, it cannot remove uncertainty (Di et al., 2024). Despite these limitations, the findings are strong and useful for guiding erosion control and watershed management under changing climate conditions.

CHAPTER FIVE

CONCLUSIONS AND RECOMMENDATIONS

5.1 Conclusions

This study assessed the impacts of climate change on soil erosion and sediment yield, analyzed the spatial and temporal dynamics of erosion and sediment hotspots, and evaluated the effectiveness of selected best management practices (BMPs) in the Beressa watershed using the Soil and Water Assessment Tool (SWAT). The conclusions are summarized according to the study's specific objectives.

i. **Quantify the effects of climate change on soil erosion and sediment yield**

- Climate change is projected to significantly increase soil erosion and sediment yield in the Beressa watershed, with average soil erosion increasing by 21.2–50.2% and sediment yield by 19.2–45.4% relative to the baseline under the SSP2-4.5 and SSP5-8.5 climate scenarios.
- The baseline average sediment yield in the Beressa watershed already exceeds the tolerable soil loss threshold (<11 Mg/ha/year) for the Ethiopian Highlands, and projected climate change is expected to further accelerate land degradation unless effective soil and water conservation measures are implemented.
- Sediment yield is governed by extreme rainfall events, with 29.5% of total sediment yield originating from the 20% of years characterized by the highest frequency of P99 rainfall events, indicating the dominant control of extreme precipitation on erosion processes.

ii. **Spatial and temporal dynamics of erosion and sediment hotspots under climate change**

- Under SSP2-4.5 and SSP5-8.5 scenarios, several sub-watersheds transition from low severity classes to high severity classes, with the most extensive hotspot expansion occurring under SSP5-8.5 climate scenarios.
- Smaller and steeper sub-watersheds are more sensitive to climate change due to rapid runoff generation and high sediment connectivity, whereas larger sub-watersheds exhibit relatively lower sensitivity because of relatively flatter slopes and increased sediment deposition along longer flow paths.

iii. Effectiveness of selected best management practices (BMPs) in reducing sediment yield under projected climate conditions

- Terracing reduced sediment yield by 47.6–50.64%, conservation agriculture by 29.68–32.76%, contour farming by 19.65–20.40%, and the combined measures by 58.20–59.86% under the SSP2-4.5 and SSP5-8.5 climate scenarios.
- The combined measures achieved the greatest reduction in sediment yield hotspots by shifting most sub-watersheds from high to lower sediment severity classes, with its effectiveness influenced by watershed characteristics.
- Increasing rainfall extremes are expected to enforce greater stress on conservation measures, highlighting the need for climate-resilient design, periodic maintenance, and targeted implementation to sustain erosion control.

5.2 Recommendations

5.2.1 Recommendations for Short-Term Priority Actions

i. The combined measures should be prioritized in erosion hotspot sub watersheds because this approach consistently achieved the greatest sediment reduction under changing future climate conditions.

ii. Contour farming and conservation agriculture should be promoted on agricultural lands with slopes less than 10%, because these practices are easy to implement and provide cost-effective erosion control.

iii. To improve the adoption of conservation agriculture and address issues related to crop residue retention, capacity-building initiatives should be strengthened through farmer training, extension services, and incentive mechanisms.

iv. In high-risk erosion hotspot areas where Combined BMPs alone are insufficient, site-specific structural measures, and strategic land-use conversion to perennial vegetation should be implemented to achieve sustainable soil and water conservation under future climate change.

5.2.2 Recommendations for Long-Term Watershed Management

i. Watershed management agencies should establish routine monitoring and maintenance programs for terraces and other physical conservation structures to sustain their effectiveness under increasing rainfall intensity.
ii. Climate change projections should be incorporated into national and regional watershed management planning and the design standards of soil and water conservation structures to improve resilience against future extreme rainfall events.

5.2.3 Recommendations for Future Research

i. Integrate multiple land use change scenarios with ensembles of climate models to better quantify uncertainty in future erosion and sediment yield projections.
ii. Conduct field experiments to validate the effectiveness of BMPs under different land uses, slope classes, and rainfall conditions.
iii. Integrate the SWAT model with economic models to evaluate economic feasibility and adoption potential of alternative BMP combinations, thereby supporting evidence-based investment and policy decisions for sustainable watershed management.

REFERENCES

Abbaspour, K. C. (2015). SWAT-CUP: SWAT calibration and uncertainty programs—a user manual. *Eawag: Dübendorf, Switzerland*, 100.

Abbaspour, K. C., Yang, J., Maximov, I., Siber, R., Bogner, K., Mieleitner, J., … Srinivasan, R. (2007). Modelling hydrology and water quality in the pre-alpine/alpine Thur watershed using SWAT. *Journal of Hydrology*, *333*(2–4), 413–430.

Abebe, B. K., Zimale, F., Gelaye, K., Gashaw, T., Dagnaw, E., & Adem, A. (2022). Application of Hydrological and Sediment Modeling with Limited Data in the Abbay (Upper Blue Nile) Basin, Ethiopia. *Hydrology*, *9*(10), 167.

Abebe, T. G., Lemma, T. M., & Meshesha, T. W. (2025). Exploring best soil conservation practices using the tolerable soil loss limit in central highland of Ethiopia: A case study of Andit Tid watershed. *International Soil and Water Conservation Research*, *13*(2), 348–361.

Abebe, T. G., & Woldemariam, A. (2024). Spatial distribution mapping of erosion and sediment yield estimation using RUSLE and Arc GIS of Ayigebire watershed , North Shewa zone of Amhara region , Ethiopia. *Water-Energy Nexus*, *7*, 124–134.

Addis, H. K., Strohmeier, S., Ziadat, F., Melaku, N. D., & Klik, A. (2016). Modeling streamflow and sediment using SWAT in Ethiopian Highlands. *Int J Agric & Biol Eng*, *9*(5), 51–66.

Adem, A. A., Tilahun, S. A., Ayana, E. K., Worqlul, A. W., Assefa, T. T., Dessu, S. B., & Melesse, A. M. (2016). Climate Change Impact on Sediment Yield in the Upper Gilgel Abay Catchment , Blue Nile Basin , Ethiopia. *Landscape Dynamics, Soils and Hydrological Processes in Varied Climates, Springer Geography*, 615–644.

Adeyeri, O. E., Folorunsho, A. H., Adeliyi, T. E., Ayegbusi, K. I., Akinsanola, A. A., Ndehedehe, C. E., … Babalola, T. E. (2024). Climate change is intensifying rainfall erosivity and soil erosion in West Africa. *Science of the Total Environment*, *955*, 177174.

Admas, M., Melesse, A. M., Abate, B., & Tegegne, G. (2022). Soil Erosion , Sediment Yield , and Runoff Modeling of the Megech Watershed Using the GeoWEPP Model. *Hydrology*, *9*, 208.

Admas, M., Melesse, A. M., & Tegegne, G. (2024). Predicting the impacts of land use/cover and climate changes on water and sediment flows in the megech watershed, upper blue nile basin. *Remote Sensing*, *16*(13), 2385.

Aghsaei, H., Dinan, N. M., Moridi, A., Asadolahi, Z., Delavar, M., Fohrer, N., & Wagner, P. (2020). Effects of dynamic land use/land cover change on water resources and sediment yield in the Anzali wetland catchment, Gilan, Iran. *The Science of the Total Environment*, *712*, 136449.

Akoko, G., Le, T. H., Gomi, T., & Kato, T. (2021). A review of SWAT model application in Africa. *Water*, *13*(9), 1313.

Alaminie, A. A., Tilahun, S. A., Legesse, S. A., Zimale, F. A., Tarkegn, G. B., & Jury, M. R. (2021). Evaluation of Past and Future Climate Trends under CMIP6 Scenarios for the UBNB (Abay), Ethiopia. *Water*, *13*, 2110.

Alavinia, M., Saleh, F. N., & Asadi, H. (2019). Effects of rainfall patterns on runoff and rainfall-induced erosion. *International Journal of Sediment Research*, *34*(3), 270–278.

Alegre, P., Clara, A., & Franco, L. (2017). Multi-variable SWAT model calibration with remotely sensed evapotranspiration and observed flow. *Rbrh*, *22*, e35.

Amare, A., & Simane, B. (2017). Determinants of smallholder farmers ' decision to adopt adaptation options to climate change and variability in the Muger Sub basin of the Upper Blue Nile basin of Ethiopia. *Agriculture & Food Security*, *6*(1), 64.

Amsalu, A., & Graaff, de J. (2006). Farmers' Views of Soil Erosion Problems and their Conservation Knowledge at Beressa Watershed, Central Highlands of Ethiopia. *Agriculture and Human Values*, *23*(1), 99–108.

Amsalu, A., Stroosnijder, L., & Graaff, J. De. (2007). Long-term dynamics in land resource use and the driving forces in the Beressa watershed , highlands of Ethiopia. *Journal of Environmental Management*, *83*(4), 448–459.

An, Y., Zhao, W., Li, C., & Ferreira, C. S. S. (2022). Temporal changes on soil conservation services in large basins across the world. *CATENA*, *209*, 105793.

Anandhi, A., Frei, A., Pierson, D. C., Schneiderman, E. M., Zion, M. S., Lounsbury, D., & Matonse, A. H. (2011). Examination of change factor methodologies for climate change impact assessment. *Water Resources Research*, *47*(3), 1–10. https://doi.org/10.1029/2010WR009104

Aouissi, J., Benabdallah, S., Lili Chabaâne, Z., & Cudennec, C. (2016). Evaluation of potential evapotranspiration assessment methods for hydrological modelling with SWAT—Application in data-scarce rural Tunisia. *Agricultural Water Management*, *174*, 39–51.

Arabkhedri, M., Heidary, K., & Parsamehr, M. (2021). Relationship of sediment yield to connectivity index in small watersheds with similar erosion potentials. *Journal of Soils and Sediments*, *21*(7), 2699–2708.

Araya, T., Cornelis, W. M., Nyssen, J., Govaerts, B., Bauer, H., Gebreegziabher, T., … Deckers, J. (2011). Effects of conservation agriculture on runoff, soil loss and crop yield under rainfed conditions in Tigray, Northern Ethiopia. *Soil Use and Management*, *27*(3), 404–414.

Arekhi, S., Shabani, A., & Rostamizad, G. (2012). Application of the modified universal soil loss equation (MUSLE) in prediction of sediment yield (Case study : Kengir Watershed , Iran). *Arabian Journal of Geosciences*, *5*(6), 1259–1267.

Argüeso, D., Evans, J. P., & Fita, L. (2013). Precipitation bias correction of very high resolution regional climate models. *Hydrology and Earth System Sciences, 17*(11), 4379–4388.

Arnáez, J., Lana-Renault, N., Lasanta, T., Ruiz-Flaño, P., & Castroviejo, J. (2015). Effects of farming terraces on hydrological and geomorphological processes. A review. *CATENA*, *128*, 122–134.

Arnold, J. G., Moriasi, D. N., Gassman, P. W., Abbaspour, K. C., White, M. J., Srinivasan, R., … Van Liew, M. W. (2012). SWAT: Model use, calibration, and validation. *Transactions of the ASABE*, *55*(4), 1491–1508.

Asfaw, A., Simane, B., Hassen, A., & Bantider, A. (2018). Variability and time series trend analysis of rainfall and temperature in northcentral Ethiopia: A case study in Woleka sub-basin. *Weather and Climate Extremes*, *19*, 29–41.

Asselman, N. E. M. (2000). Fitting and interpretation of sediment rating curves. *Journal of Hydrology*, *234*(3–4), 228–248.

Bambury, M. A. R. K., Elgy, J. O. H. N., Bogen, J. F., & Walling, D. (2003). Development of a sediment yield model for Ghana using sediment transport data. *Lhas Publication*, 96–102.

Basile, P. A., Riccardi, G. A., Zimmermann, E. D., & Stenta, H. R. (2010). Simulation of erosion-deposition processes at basin scale by a physically-based mathematical model. *International Journal of Sediment Research*, *25*(2), 91–109.

Bayar, A. S., Yılmaz, M. T., Yücel, İ., & Dirmeyer, P. (2023). CMIP6 Earth System Models Project Greater Acceleration of Climate Zone Change Due To Stronger Warming Rates Earth ' s Future. *Earth's Future*, *11*(4), e2022EF002972.

Belay, T., & Mengistu, D. A. (2021). Impacts of land use / land cover and climate changes on soil erosion in Muga watershed , Upper Blue Nile basin (Abay), Ethiopia. *Ecological Processes*, *10*(1), 68.

Betela, B., & Wolka, K. (2021). Evaluating soil erosion and factors determining farmers ' adoption and management of physical soil and water conservation measures in Bachire watershed , southwest Ethiopia. *Environmental Challenges, 5*, 100348.

Bewket, W., & Teferi, E. (2009). Assessment of soil erosion hazard and prioritization for treatment at the watershed level: case study in the Chemoga watershed, Blue Nile basin, Ethiopia. *Land Degradation & Development*, *20*(6), 609–622.

Beyer, R., Krapp, M., & Manica, A. (2020). An empirical evaluation of bias correction methods for palaeoclimate simulations. *Climate of The Past*, *16*(4), 1493–1508.

Bezak, N., Mikoš, M., Borrelli, P., Liakos, L., & Panagos, P. (2021). An in-depth statistical analysis of the rainstorms erosivity in Europe. *Catena*, *206*, 105577.

Bhattacharya, R. K., Chatterjee, N. Das, & Das, K. (2020). Estimation of erosion susceptibility and sediment yield in ephemeral channel using RUSLE and SDR model: Tropical Plateau Fringe Region, India. *Gully Erosion Studies from India and Surrounding Regions*, 163–185.

Blanco, H., & Lal, R. (2023). Mechanical Structures and Engineering Techniques. In *Soil Conservation and Management* (pp. 299–329). Cham: Springer Nature Switzerland.

Boutaleb, F. Z. E. S., Ouchchen, S. T. M., Belqas, M. I., & Abioui, R. B. K. M. (2022). Assessment of soil erosion risk in a semi - arid climate watershed using SWAT model : case of Tata basin , South - East of Morocco. *Applied Water Science, 12*(6), 1–15. https://doi.org/10.1007/s13201-022-01664-w

Bracken, L. J., Turnbull, L., Wainwright, J., & Bogaart, P. (2015). Sediment connectivity: a framework for understanding sediment transfer at multiple scales. *Earth Surface Processes and Landforms, 40*(2), 177–188.

Brazier, R. E., Beven, K. J., Freer, J., & Rowan, J. S. (2000). Equifinality and uncertainty in physically based soil erosion models: Application of the glue methodology to wepp-the water erosion prediction project-for sites in the UK and USA. *Earth Surface Processes and Landforms*, *25*(8), 825–845.

Cárceles Rodríguez, B., Durán-Zuazo, V. H., Soriano Rodríguez, M., García-Tejero, I. F., Gálvez Ruiz, B., & Cuadros Tavira, S. (2022). Conservation Agriculture as a Sustainable System for Soil Health: A Review. *Soil Systems*, *6*(4), 1–37.

Carvalho, D., Rafael, S., Monteiro, A., Rodrigues, V., Lopes, M., & Rocha, A. (2022). How well have CMIP3 , CMIP5 and CMIP6 future climate projections portrayed the recently observed warming. *Scientific Reports*, *12*(1), 11983.

Chen, D., Wei, W., & Chen, L. (2017). Effects of terracing practices on water erosion control in China: A meta-analysis. *Earth-Science Reviews*, *173*, 109–121.

Chen, L., Xiao, Y., Yin, S., Wang, W., Strohmeier, S., Vásquez, C., … Strauss, P. (2025). Disproportionate contributions and spatiotemporal patterns of extreme rainfall and erosivity events across mainland China. *International Soil and Water Conservation Research*.

Chen, Y., Wang, N., Jiao, J., Li, J., Bai, L., Liang, Y., … Wang, J. (2024). Predicting soil loss in small watersheds under different emission scenarios from CMIP6 using random forests. *Earth Surface Processes and Landforms*, *49*(13), 4469–4484.

Chervenkov, H., & Slavov, K. (2019). ETCCDI climate indices for assessment of the recent climate over Southeast Europe. *International Conference on Variability of the Sun and Sun-like Stars: From Asteroseismology to Space Weather*, 398–412. Springer.

Chimdessa, K., Quarashi, S., Kebede, A., & Alamirew, T. (2019). Effect of Land Use Land Cover and Climate Change on River Flow and Soil Loss in Didessa River Basin ,. *Hydrology*, *6*(1), 2.

Cho, S. J., Karwan, D. L., Skalak, K., Pizzuto, J., & Huffman, M. E. (2023). Sediment sources and connectivity linked to hydrologic pathways and geomorphic processes: a conceptual model to specify sediment sources and pathways through space and time. *Frontiers in Water*, *5*, 1241622.

Christensen, J., Boberg, F., Christensen, O., & Lucaspicher, P. (2008). On the need for bias correction of regional climate change projections of temperature and precipitation. *Geophysical Research Letters*, *35*(20).

Cibin, R., Sudheer, K., & Chaubey, I. (2010). Sensitivity and identifiability of stream flow generation parameters of the SWAT model. *Hydrological Processes*, *24*(9), 1133–1148.

Crowder, D. W., Demissie, M., & Markus, M. (2007). The accuracy of sediment loads when log-transformation produces nonlinear sediment load–discharge relationships. *Journal of Hydrology*, *336*(3), 250–268.

Dakhlalla, A. O., & Parajuli, P. B. (2019). Assessing model parameters sensitivity and uncertainty of streamflow, sediment, and nutrient transport using SWAT. *Information Processing in Agriculture*, *6*(1), 61–72.

Das, J., Mandal, T., Rahman, A. T. M. S., & Saha, P. (2021). Spatio-temporal characterization of rainfall in Bangladesh: an innovative trend and discrete wavelet transformation approaches. *Theoretical and Applied Climatology*, *143*(3–4), 1557–1579.

Das, S., Jain, M. K., & Gupta, V. (2024). An assessment of anticipated future changes in water erosion dynamics under climate and land use change scenarios in South Asia. *Journal of Hydrology*, *637*, 131341.

Debie, E., Singhb, K. N., & Belay, M. (2018). Effect of Terracing on Combating Soil Erosion by Water: Case Study In The Beribere Catchment, Northwest Ethiopia. *Ethiopian Journal of Social Sciences*, *4*(2).

den Biggelaar, C., Lal, R., Wiebe, K., & Breneman, V. (2003). The Global Impact Of Soil Erosion On Productivity. I: Absolute and Relative Erosion-induced Yield Losses. *Advances in Agronomy*, *81*(03), 1–48.

Di, Bai, Z., Xu, Y., Gu, H., & Gao, C. (2024). Assessing streamflow and sediment responses to future climate change over the Upper Mekong River Basin: A comparison between CMIP5 and CMIP6 models. *Journal of Hydrology: Regional Studies*, *52*, 101685.

Dibaba, W. T., Demissie, T. A., & Miegel, K. (2021). Evaluation of best management practices in highland Ethiopia, Finchaa Catchment. *Land*, *10*, 650.

Dogiso, D., Muluneh, A., & Ketema, A. (2025). Soil Erosion Responses to CMIP6 Climate Scenarios and Land Cover Changes in the Gidabo Watershed, Ethiopia: Implications for Sustainable Watershed Management. *Land Degradation and Development*, *36*(9), 2981–3002.

Doi, M., & Kim, J. (2022). Future Projections and Uncertainties of CMIP6 for Hydrological Indicators and Their Discrepancies from CMIP5 over South Korea. *Water*, *14*(18), 2926.

Dollinger, J., Dagès, C., Bailly, J. S., Lagacherie, P., & Voltz, M. (2015). Managing ditches for agroecological engineering of landscape. A review. *Agronomy for Sustainable Development*, *35*(3), 999–1020.

Dowdeswell-Downey, E., Grabowski, R. C., & Rickson, R. J. (2023). Do temperature and moisture conditions impact soil microbiology and aggregate stability? *Journal of Soils and Sediments*, *23*(10), 3706–3719.

Dutta, S., & Sen, D. (2018). Application of SWAT model for predicting soil erosion and sediment yield. *Sustainable Water Resources Management*, *4*(3), 447–468.

Eekhout, J. P. C., & Vente, J. De. (2022). Global impact of climate change on soil erosion and potential for adaptation through soil conservation. *Earth-Science Reviews*, *226*, 103921.

Enyew, F. B., Sahlu, D., Tarekegn, G. B., Hama, S., & Debele, S. E. (2024). Performance Evaluation of CMIP6 Climate Model Projections for Precipitation and Temperature in the Upper Blue Nile Basin, Ethiopia. *Climate*, *12*(11), 1–22.

FAO. (2020). *FAO calls for actions to reduce global soil erosion*. 789–790.

Felix, M. L., & Jung, K. (2022). Impacts of Spatial Interpolation Methods on Daily Streamflow Predictions with SWAT. *Water (Switzerland)*, *14*(20), 3340.

Fentaw, A. E., & Abegaz, A. (2024). Soil erosion assessment and identification of erosion hotspot areas in the upper Tekeze Basin, Northern Ethiopia. *Heliyon*, *10*(12), e32880.

Fernández, C., & Vega, J. A. (2018). Evaluation of the rusle and disturbed wepp erosion models for predicting soil loss in the first year after wildfire in NW Spain. *Environmental Research*, *165*, 279–285.

Ferro, V., & Porto, P. (2000). Sediment delivery distributed (SEDD) model. *Journal of Hydrologic Engineering*, *5*(4), 411–422.

Friedman, J. S., Blake, W. H., Rabinovich, A., Wynants, M., Kelly, C., & Nasseri, M. (2018). Soil erosion in East Africa : an interdisciplinary approach to realising pastoral land management change. *Environ.Res.Lett*, *13*, 124014.

Gashaw, T., Bantider, A., Zeleke, G., Alamirew, T., Jemberu, W., Worqlul, A. W., … Addisu, S. (2021). Evaluating InVEST model for estimating soil loss and sediment export in data scarce regions of the Abbay (Upper Blue Nile) Basin: Implications for land managers. *Environmental Challenges*, *5*, 100381.

Gashaw, T., Dile, Y. T., Worqlul, A. W., Bantider, A., Zeleke, G., Bewket, W., & Alamirew, T. (2021). Evaluating the effectiveness of best management practices on soil erosion reduction using the SWAT Model: for the case of Gumara watershed, Abbay (Upper Blue Nile) Basin. *Environmental Management*, *68*(2), 240–261.

Gassman, P. W., Reyes, M. R., Green, C. H., & & Arnold, J. G. (2007). The soil and water assessment tool: historical development, applications, and future research directions. *Transactions of the ASABE*, *50*(4), 1211–1250.

Gathagu, J., Mourad, K., & Sang, J. (2018). Effectiveness of Contour Farming and Filter Strips on Ecosystem Services. *Water*, *10*(10), 1312.

Gebre, A. M., Belete, M. D., & Belayneh, M. Z. (2024). Soil Loss and Sediment Yield Prediction in Lake Hawassa Sub-Basin, Central Rift Valley Basin, Ethiopia. *Air, Soil and Water Research*, *17*, 11786221241261824.

Gelagay, H. S. (2016). RUSLE and SDR model based sediment yield assessment in a GIS and remote sensing environment; a case study of Koga watershed, Upper Blue Nile Basin, Ethiopia. *Hydrology Current Research*, *7*(2), 239.

Geleta, C. D., & Ameja, L. G. (2022). Climate Change Induced Temperature Prediction and Bias Correction in Finchaa Watershed. *Agric. Environ. Sci*, *18*, 324–337.

Girmay, G., Moges, A., & Muluneh, A. (2021). Assessment of Current and Future Climate Change Impact on Soil Loss Rate of Agewmariam Watershed , Northern Ethiopia. *Air, Soil and Water Research*, *14*, 1178622121995847.

Gitima, G., Teshome, M., Kassie, M., & Jakubus, M. (2022). Spatiotemporal land use and cover changes across agroecologies and slope gradients using geospatial technologies in Zoa watershed , Southwest Ethiopia. *Heliyon*, *8*(9), e10696.

Gu, Z., Ji, K., Xu, G., Reheman, M., Feng, D., Shen, Y., … Pan, S. (2025). Runoff and Sediment Response to Rainfall Events in China's North-South Transitional Zone: Insights from Runoff Plot Observations. *Atmosphere*, *16*(10), 1207.

Güçlü, Y. S. (2020). Improved visualization for trend analysis by comparing with classical Mann-Kendall test and ITA. *Journal of Hydrology*, *584*, 124674.

Guo, L., Liu, R., Men, C., Wang, Q., Miao, Y., Shoaib, M., … Zhang, Y. (2021). Multiscale spatiotemporal characteristics of landscape patterns, hotspots, and influencing factors for soil erosion. *Science of the Total Environment*, *779*, 146474.

Guo, Y., Yu, X., Xu, Y., Wang, G., Xie, J., & Gu, H. (2022). A comparative assessment of CMIP5 and CMIP6 in hydrological responses of the Yellow River Basin , China. *Hydrology Research*, *53*(6), 867–891.

Gurmu, Z. A., Ritzema, H., Fraiture, C. De, Riksen, M., & Ayana, M. (2021). Sediment Influx and Its Drivers in Farmers ' Managed Irrigation Schemes in Ethiopia. *Water*, *13*, 1747.

Haddeland, I., Heinke, J., Voss, F., Eisner, S., Chen, C., Hagemann, S., & Ludwig, F. (2011). Effects of climate model radiation, humidity and wind estimates on hydrological simulations. *Hydrology and Earth System Sciences*, *16*(2), 305–318.

Hailu, M. B., Mishra, S. K., & Jain, S. K. (2023). Evaluation of Spatial-Temporal Variation of Soil Loss and Best Conservation Measures in an East Africa Catchment. *Sustainability*, *15*(10), 1–17.

Hajisheko, K. K., Venkata Suryabhagavan, K., & Soumya, K. (2025). WebGIS-based decision support system for soil erosion risk assessment for Guder River catchment, Ethiopia. *Geosystems and Geoenvironment*, *4*(2), 100387.

Halder, J. C. (2023). The integration of RUSLE-SDR lumped model with remote sensing and GIS for soil loss and sediment yield estimation. *Advances in Space Research*, *71*(11), 4636–4658.

Haregeweyn, N., Tsunekawa, A., Poesen, J., Tsubo, M., Meshesha, D. T., Fenta, A. A., … Adgo, E. (2017). Comprehensive assessment of soil erosion risk for better land use planning in river basins: Case study of the Upper Blue Nile River. *Science of the Total Environment*, *574*, 95–108.

Hassan, A. (2012). Eastern Nile Planning Model (ENPM) Project. *Unpublished*.

He, R., Bao, Z., Tang, X., Zhang, J., Wang, G., Jin, J., … Bao, Z. (2021). Uncertainty analysis of SWAT modeling in the lancang river basin using four different algorithms. *Water*, *13*(3), 341.

Hong, Y. I. N., & Ying, S. U. N. (2019). Characteristics of extreme temperature and precipitation in China in 2017 based on ETCCDI indices. *Advances in Climate Change Research*, *9*(4), 218–226. https://doi.org/10.1016/j.accre.2019.01.001

Hu, Y. (2022). *Effect of Conservation Tillage on Soil and Water Quality*. *3*(3), 3–5.

Hurni, H. (1983). Soil erosion and soil formation in agricultural ecosystems: Ethiopia and Northern Thailand. *Mountain Research and Development*, *4*, 131–142.

Hurni, K., Zeleke, G., Kassie, M., Tegegne, B., Kassawmar, T., Teferi, E., … Hurni, H. (2015). Soil Degradation and Sustainable Land Management in the Rainfed Agricultural Areas of Ethiopia: An Assessment of the Economic Implications. *Report for the Economcs of Land Degradation*, 94 PP.

Ipcc. (2023). *Summary for Policymakers of the Intergovernmental Panel on Climate Change*.

IPCC. (2021). *Climate Change 2021 The Physical Science Basis Working Group I Contribution to the Sixth Assessment Report of the Intergovernmental Panel on Climate Change*. *2*(1).

Islami FA, SDTarigan, ED Wahjunie, B. D. (2022). Accuracy Assessment of Land Use Change Analysis Using Google Earth in Sadar Watershed Mojokerto Regency. *Earth and Environmental Science*, *950*(1), 012091.

Jain, H. (2025). Engineering Approaches for Soil Erosion Control and Restoration: Advancements in Sustainable Practices and Technologies. In *Soil Degradation, Desertification and Restoration: Application of Geospatial Technology and Modeling* (pp. 467–490). Springer.

Jenny, J., Koirala, S., Gregory-eaves, I., Francus, P., Niemann, C., & Ahrens, B. (2019). Human and climate global-scale imprint on sediment transfer during the Holocene. *Proceedings of the National Academy of Sciences*, *116*(46), 22972–22976.

Jiang, F., Xue, X., Zhang, L., Zuo, Y., Zhang, H., Zheng, W., Bian, L., Hu, L., Hao, C., Du, J., Ci, Y., Cheng, R., Dawa, C., & Biswas, M., Islam, M. U., Meng, F., & Peng, X. (2024). (2024). Soil wind erosion, nutrients, and crop yield response to conservation tillage in North China: A field study in a semi-arid and wind erosion region after 9 years. Field Crops Research. In *Field Crops Research* (Vol. 316). pringer Netherlands.

Jilo, N., Gebremariam, B., Harka, A., Woldemariam, G., & Behulu, F. (2019). Evaluation of the Impacts of Climate Change on Sediment Yield from the Logiya Watershed , Lower. *Hydrology*, *6*(3), 81.

Jung, C.-G., Lee, D.-R., & Moon, J.-W. (2016). Comparison of the Penman-Monteith method and regional calibration of the Hargreaves equation for actual evapotranspiration using SWAT-simulated results in the Seolma-cheon basin, South Korea. *Hydrological Sciences Journal*, *61*(4), 793–800.

Khalaf, R. M., Hussein, H. H., Hassan, W. H., Mohammed, Z. M., & Nile, B. K. (2022). Projections of precipitation and temperature in Southern Iraq using a LARS-WG Stochastic weather generator. *Physics and Chemistry of the Earth*, *128*, 103224.

Kroese, J. S., Batista, P. V. G., Jacobs, S. R., Breuer, L., Quinton, J. N., & Rufino, M. C. (2020). Agricultural land is the main source of stream sediments after conversion of an African montane forest. *Scientific Reports*, *10*(1), 14827.

Kumar, N., Singh, S. K., Srivastava, P. K., & Narsimlu, B. (2017). SWAT Model calibration and uncertainty analysis for streamflow prediction of the Tons River Basin, India, using Sequential Uncertainty Fitting (SUFI-2) algorithm. *Modeling Earth Systems and Environment*, *3*(1), 30.

Lamba, J., Thompson, A. M., Karthikeyan, K. G., Panuska, J. C., & Good, L. W. (2016). Effect of best management practice implementation on sediment and phosphorus load reductions at subwatershed and watershed scale using SWAT model. *International Journal of Sediment Research*, *31*(4), 386–394.

Lan, M., Junyou, L., & Jingjing, L. (2020). Effects of antecedent soil water content on in fi ltration and erosion processes on loessial slopes under simulated rainfall Lan Ma , Junyou Li and Jingjing Liu. *Hydrology Research*, *51*(5), 882–893.

Leander, R., Buishand, T. A., van den Hurk, B. J. J. M., & de Wit, M. J. M. (2008). Estimated changes in flood quantiles of the river Meuse from resampling of regional climate model output. *Journal of Hydrology*, *351*(3–4), 331–343. https://doi.org/10.1016/j.jhydrol.2007.12.020

Lee, J., Lee, S., Park, W. J., Shin, M., & Lim, K. (2025). Assessment of Integrated BMPs for Subbasin-Scale Soil Erosion Reduction Considering Spatially Distributed Farmland Characteristics. *Agriculture*, *15*(8), 893.

Lemann, T., Zeleke, G., Amsler, C., Giovanoli, L., Suter, H., & Roth, V. (2016). Modelling the effect of soil and water conservation on discharge and sediment yield in the upper Blue Nile basin, Ethiopia. *Applied Geography*, *73*, 89–101.

Lepcha, P. T., Pandey, P. K., & Pandey, V. (2026). Evaluating the Effects of Climate Change on Hydro-Sedimentology Processes in the Upstream Teesta River Basin: A SWAT Simulation Using CMIP6 Multi-Model Ensemble Approach. *Hydrological Processes*, *40*(3), e70464.

Leta, M. K., Waseem, M., Rehman, K., & Tränckner, J. (2023). Sediment yield estimation and evaluating the best management practices in Nashe watershed, Blue Nile Basin, Ethiopia. *Environmental Monitoring and Assessment*, *195*(6), 716.

Li, C., Li, Z., Yang, M., Ma, B., & Wang, B. (2021). Article grid-scale impact of climate change and human influence on soil erosion within east african highlands (Kagera basin). *International Journal of Environmental Research and Public Health*, *18*(5), 1–17.

Liou, Y., Nguyen, Q.-V., Hoang, D., & Tran, D.-P. (2022). Prediction of soil erosion and sediment transport in a mountainous basin of Taiwan. *Progress in Earth and Planetary Science*, *9*(1), 52.

Londhe, D., Katpatal, Y., & Bokde, N. (2023). Performance Assessment of Bias Correction Methods for Precipitation and Temperature from CMIP5 Model Simulation. *Applied Sciences*, *13*(16), 9142.

Lyu, X., Du, J., Qiu, Y., Jia, Y., Hao, C., & Dong, H. (2025). Spatiotemporal characteristics of future precipitation variability in the Tianshan Mountain region of China. *Journal of Hydrology: Regional Studies*, *57*, 102124.

Majewski, M., & Szpikowski, J. (2024). Effect of rainfall parameters on soil erosion in Chwalimski Brook catchment, NW Poland. *Geomorphology*, *454*, 109167.

Makumbura, R. K., Gunathilake, M. B., Samarasinghe, J. T., Confesor, R., Muttil, N., & Rathnayake, U. (2022). Comparison of Calibration Approaches of the Soil and Water Assessment Tool (SWAT) Model in a Tropical Watershed. *Hydrology*, *9*, 183.

Marcinkowski, P., & Szporak-Wasilewska, S. (2024). Assessing monthly dynamics of agricultural soil erosion risk in Poland. *Geoderma Regional*, *39*, e00864.

Martel, J., Brissette, F., Troin, M., Arsenault, R., Chen, J., & Su, T. (2022). CMIP5 and CMIP6 Model Projection Comparison for Hydrological Impacts Over North America. *Geophysical Research Letters*, *49*(15), e2022GL098364.

Martínez-Mena, M., Carrillo-López, E., Boix-Fayos, C., Almagro, M., García Franco, N., Díaz-Pereira, E., … de Vente, J. (2020). Long-term effectiveness of sustainable land management practices to control runoff, soil erosion, and nutrient loss and the role of rainfall intensity in Mediterranean rainfed agroecosystems. *Catena*, *187*, 104352.

Mekuria, E. T., Derib, S., & Melesse, E. A. (2024). Sediment yield assessment and suggesting mitigation measures—A case study of Deme watershed, Omo-Gibe Basin, Ethiopia. *World Water Policy*, *10*(1), 172–212.

Mequanient, M. B., & Kebede, H. H. (2023). Simulation of sediment yield and evaluation of best management practices in Azuari watershed, Upper Blue Nile

Basin. *H2Open Journal*, *6*(3), 493–506.

Meshesha, T. W., & Tripathi, S. K. (2017). Farmer ' s Perception on Soil Erosion and Land Degradation Problems and Management Practices in the Beressa Watershed of Ethiopia. *Journal of Water Resources and Ocean Science*, *5*(5), 64–72.

Mihret, T., Zemale, F., Worqlul, A., Ayalew, A., & Fohrer, N. (2025). Unlocking watershed mysteries: Innovative regionalization of hydrological model parameters in data-scarce regions. *Journal of Hydrology: Regional Studies*, *57*, 102163.

Mitiku, G. K., Woldemariam, A. D., Abebe, T. G., Bekele, K., Yilma, T., & Getaneh, L. (2024). Comparative Evaluation of the Effects of Conservation Agriculture Integrated with Various Land Management Practices on Vertisol Productivity in Highlands of Ethiopia. *International Journal on Food, Agriculture and Natural Resources*, *05*(04), 67–73.

Moges, D. M., Kmoch, A., Bhat, H. G., & Uuemaa, E. (2020). Future soil loss in highland Ethiopia under changing climate and land use. *Regional Envirinmental Change*, *20*(1), 1–14.

Mohammed, M. (2020). Hydrological Impacts of Climate Change in Tikur Wuha Watershed , Ethiopian Rift Valley Basin. *Journal of Environmental and Earth Science*, *10*(2), 28–49.

Moriasi, D. N., Arnold, J. G., Liew, M. W. Van, Bingner, R. L., Harmel, R. D., Veith, T. L., … Veith, T. L. (2007). Model evaluation guidelines for systematic quantification of accuracy in watershed simulations. *Transactions of the ASABE*, *50*(3), 885–900.

Mukheef, R. A. H., Hassan, W. H., & Alquzweeni, S. (2024). Projections of temperature and precipitation trends using CMhyd under CMIP6 scenarios: A case study of Iraq's Middle and West. *Atmospheric Research*, *306*, 107470.

Mukundan, R., Pradhanang, S. M., Schneiderman, E. M., Pierson, D. C., Anandhi, A., Zion, M. S., … Steenhuis, T. S. (2013). Suspended sediment source areas and future climate impact on soil erosion and sediment yield in a New York City water supply watershed, USA. *Geomorphology*, *183*, 110–119.

Munoth, P., & Goyal, R. (2020). Impacts of land use land cover change on runoff and sediment yield of Upper Tapi River Sub-Basin, India. *International Journal of River Basin Management*, *18*(1), 177–189.

Munye, K., Sintayehu, G., Belayneh, A., & Mulat, C. (2022). Identifying Soil Erosion Hotspot Area Using GIS and MCDA Techniques , Case Study of Dengora and Meno Watersheds in Belesa Woredas , Amhara Region. *Cham: Springer Nature Switzerland.*, 111–137.

N'dri, W. K. C., Pistre, S., Kouamé, K. J., & Jourda, J. P. (2021). Potential Impact of Climate Change on the Sediment Fluxes of a Watershed in West Africa: Cas of the Aghien Lagoon, Côte d'Ivoire. *Atmospheric and Climate Sciences*, *12*(1), 18–30.

Nearing, M. A., Pruski, F. F., & Neal, M. R. O. (2004). Expected climate change impacts on soil erosion rates : A review. *Journal of Soil and Water Conservation*, *59*(1), 43–50.

Negewo, T. F., & Sarma, A. K. (2021). Evaluation of climate change-induced impact on streamflow and sediment yield of Genale watershed, Ethiopia. In *The Nature, Causes, Effects and Mitigation of Climate Change on the Environment.IntechOpen.* IntechOpen.

Neitsch, S. L., Arnold, J. G., Kiniry, J. R., & Williams, J. R. (2009). 1.1 Overview of soil and water assessment tool (SWAT) model. *Tier B*, *8*, 3–23.

Nguyen, H. H., Recknagel, F., Meyer, W., Frizenschaf, J., Ying, H., & Gibbs, M. S. (2019). Comparison of the alternative models SOURCE and SWAT for predicting catchment streamflow, sediment and nutrient loads under the effect of land use changes. *Science of the Total Environment*, *662*, 254–265.

Panagos, P., Borrelli, P., & Meusburger, K. (2015). A new European slope length and steepness factor (LS-Factor) for modeling soil erosion by water. *Geosciences, 5*(2), 117–126.

Pandey, A., Bishal, K. C., Kalura, P., Chowdary, V. M., Jha, C. S., & Cerdà, A. (2021). A soil water assessment tool (SWAT) modeling approach to prioritize soil conservation management in river basin critical areas coupled with future climate scenario analysis. *Air, Soil and Water Research*, *14*, 11786221211021396.

Pelletier, J. D. (2012). A spatially distributed model for the long-term suspended sediment discharge and delivery ratio of drainage basins. *Journal of Geophysical Research*, *117*, 1–15.

Pimentel, D., Harvey, C., Resosudarmo, P., Sinclair, K., Kurz, D., Mcnair, M., … Blair, R. (1995). Environmental and Economic Costs of Soil Erosion and Conservation Benefits. *Science*, *267*(5201), 1117–1123.

Pimentel, D., & Kounang, N. (1998). Ecology of Soil Erosion in Ecosystems OF. *Ecosystems*, *1*, 416–426.

Quamar, S., Kumar, P., & Singh, H. P. (2025). Streamflow and sediment simulation in the Song River basin using the SWAT model. *Frontiers in Water*, *7*, 1500086.

Rajbanshi, J., & Bhattacharya, S. (2020). Assessment of soil erosion, sediment yield and basin specific controlling factors using RUSLE-SDR and PLSR approach in Konar river basin, India. *Journal of Hydrology, 587*, 124935.

Rao, K. K., Samal, S. K., Poonia, S. P., Kumar, R., Mishra, J. S., Bhatt, B. P., … Dalal, R. C. (2022). Conservation agriculture improves soil physical properties and crop productivity: A long-term study in middle Indo-Gangetic Plains of India. *Soil Research*, *60*(6), 442–454.

Regasa, M. S., & Nones, M. (2024). Modeling best management practices to reduce future sediment yield in the Fincha watershed, Ethiopia. *International Journal of Sediment Research*, *39*(5), 737–749.

Reinsch, S., Robinson, D. A., van Soest, M. A. J., Keith, A. M., Parry, S., & Tye, A. M. (2024). Temperate soils exposed to drought—Key processes, impacts, indicators, and unknowns. *Land*, *13*(11), 1759.

Renfro, R., & Waldo, P. (1983). Validations of sediment delivery ratio Prediction techniques. *Research Paper*, *95*.

Rhodes, C. J. (2014). Soil erosion, climate change and global food security: Challenges and strategies. *Science Progress*, *97*(2), 97–153.

Riahi, K., Vuuren, D. P. Van, Kriegler, E., Edmonds, J., Neill, B. C. O., Fujimori, S., … Tavoni, M. (2017). The Shared Socioeconomic Pathways and their energy , land use , and greenhouse gas emissions implications : An overview. *Global Environmental Change*, *42*, 153–168.

Ricard, S., & Anctil, F. (2019). Forcing the Penman-Montheith Formulation with Humidity, Radiation, and Wind Speed Taken from Reanalyses, for Hydrologic Modeling. *Water*, *11*(6), 1214.

Roba, Z. R., Moisa, M. B., Purohit, S., Deribew, K. T., & Gemeda, D. O. (2025). Assessment of soil erosion and sediment yield in response to land use and land cover changes using geospatial techniques in Dumuga Watershed, Ethiopia. *All Earth*, *37*(1), 1–18. https://doi.org/10.1080/27669645.2025.2460917

Saggau, P., Kuhwald, M., & Duttmann, R. (2023). Effects of contour farming and tillage practices on soil erosion processes in a hummocky watershed. A model-based case study highlighting the role of tramline tracks. *CATENA*, *228*, 107126.

Saygın, S. D., Ozcan, A. U., Basaran, M., Timur, O. B., Dolarslan, M., Yılman, F. E., & Erpul, G. (2014). The combined RUSLE/SDR approach integrated with GIS and geostatistics to estimate annual sediment flux rates in the semi-arid catchment, Turkey. *Environmental Earth Sciences*, *71*(4), 1605–1618.

Schuol, J., & Abbaspour, K. C. (2007). Using monthly weather statistics to generate daily data in a SWAT model application to West Africa. *Ecological Modelling*, *201*(3), 301–311.

Sedighi, F., Khaledi Darvishan, A., & Zare, M. R. (2021). Effect of watershed geomorphological characteristics on sediment redistribution. *Geomorphology*, *375*, 107559.

Seitz, S., Goebes, P., Puerta, V. L., Isadora, E., Pereira, P., Wittwer, R., … Scholten, T. (2019). Conservation tillage and organic farming reduce soil erosion. *Agronomy for Sustainable Development*, *39*, 1–10.

Şen, Z. (2012). Innovative trend analysis methodology. *Journal of Hydrologic Engineering*, *17*(9), 1042–1046.

Senent-Aparicio, J., Jimeno-Sáez, P., López-Ballesteros, A., Giménez, J. G., Pérez-Sánchez, J., Cecilia, J. M., & Srinivasan, R. (2021). Impacts of swat weather generator statistics from high-resolution datasets on monthly streamflow simulation over Peninsular Spain. *Journal of Hydrology: Regional Studies*, *35*, 100826.

Setyawan, C., Lee, C.-Y., & Prawitasari, M. (2019). Investigating spatial contribution of land use types and land slope classes on soil erosion distribution under tropical environment. *Natural Hazards*, *98*(2), 697–718.

Shelar, R., Nandgude, S., Tiwari, M., Gorantiwar, S., & Atre, A. (2023). Impact Assessment of Soil and Water Conservation Measures on Carbon Sequestration : A Case Study for the Tropical Watershed Using Advanced Geospatial Techniques. *Sustainability*, *15*(1), 531.

Shi, Z. H., Fang, N. F., Wu, F. Z., Wang, L., Yue, B. J., & Wu, G. L. (2012). Soil erosion processes and sediment sorting associated with transport mechanisms on steep slopes. *Journal of Hydrology*, *454*, 123–130.

Shrestha, B., Cochrane, T. A., Caruso, B. S., Arias, M. E., & Wild, T. B. (2021). Sediment Management for Reservoir Sustainability and Cost Implications Under Land Use/Land Cover Change Uncertainty. *Water Resources Research*, *57*(4), 1–

20.

Siabi, E. K., Awafo, E. A., Kabo-bah, A. T., Derkyi, N. S. A., Akpoti, K., Mortey, E. M., & Yazdanie, M. (2023). Assessment of Shared Socioeconomic Pathway (SSP) climate scenarios and its impacts on the Greater Accra region. *Urban Climate*, *49*, 101432.

Sinshaw, B. G., Belete, A. M., Mekonen, B. M., Wubetu, T. G., Anley, T. L., Alamneh, W. D., … Mossie Birhanu, M. (2021). Watershed-based soil erosion and sediment yield modeling in the Rib watershed of the Upper Blue Nile Basin, Ethiopia. *Energy Nexus*, *3*, 100023.

Sirikaew, U., Seeboonruang, U., Tanachaichoksirikun, P., & Wattanasetpong, J. (2020). Impact of Climate Change on Soil Erosion in the Lam. *Water*, *12*(12), 3527.

Sivakumar, M. V. K. (2011). Climate and Land Degradation. In *Sustaining soil productivity in response to global climate change: Science, policy, and ethics* (pp. 141–154). John Wiley & Sons, Ltd.

Stouffer, R. J., Eyring, V., Meehl, G. A., Bony, S., Senior, C., Stevens, B., & Taylor, K. E. (2017). CMIP5 scientific gaps and recommendations for CMIP6. *Bulletin of the American Meteorological Society*, *98*(1), 95–105.

Sun, M., Wang, Z., Li, Z., Xu, X., Qin, L., & Song, T. (2023). Temporal variations in rainfall, runoff and sediment yield in small karst watersheds. *CATENA*, *231*, 107292.

Tadese, S., Soromessa, T., & Bekele, T. (2021). Analysis of the current and future prediction of land use/land cover change using remote sensing and the CA-Markov model in Majang forest biosphere reserves of Gambella, Southwestern Ethiopia. *The Scientific World Journal*, *2021*(1), 6685045.

Taharin, M. R., Taha, N. A., Amaludin, A., Shaifuddin, M., Razak, A., Zulkifli, M. F., & Ming, C. W. (2026). High-Resolution Silt Distribution Mapping Using

Ordinary Kriging From Borehole Data in a Geohazard-Prone Area. *Civil Engineering Journal*, *12*(01), 292–306.

Tamene, L, Abera, W., Demissie, B., Desta, G., Woldearegay, K., & Mekonnen, K. (2022). Soil erosion assessment in Ethiopia : A review. *Journal of Soil and Water Conservation*, *77*(2), 144–157.

Tamene, Lulseged, Adimassu, Z., Aynekulu, E., & Yaekob, T. (2017). Estimating landscape susceptibility to soil erosion using a GIS-based approach in Northern Ethiopia. *International Soil and Water Conservation Research*, *5*(3), 221–230.

Tamene, Lulseged, & Bao, Q. (2015). Estimating soil erosion in sub-Saharan Africa based on landscape similarity mapping and using the revised universal soil loss equation (RUSLE). *Nutrient Cycling in Agroecosystems*, *102*, 17–31.

Tenaw, W. G., Tadesse, K. B., & Kerebih, M. S. (2024). Estimation of Sediment Yield and Evaluation of Management Options in the Watershed Using SWAT Model. *Air, Soil and Water Research*, *17*, 11786221241284460. https://doi.org/10.1177/11786221241284461

Teutschbein, C., & Seibert, J. (2012). Bias correction of regional climate model simulations for hydrological climate-change impact studies : Review and evaluation of different methods. *Journal of Hydrology*, *456–457*, 12–29.

Theron, S. N. (2021). Modelling potential climate change impacts on sediment yield in the Tsitsa River catchment , South Africa. *Water SA*, *47*(1), 67–75.

Thomas, R. (1985). Estimating Total Suspended Sediment Yield With Probability Sampling. *Water Resources Research*, *21*(9), 1381–1388.

Tilahun, K., Desta, G., & Science, W. (2021). Impact of Physical Soil and Water Conservation Measures on Soil Erosion Reduction and Associated Constraints in the Highland of Ethiopia. *Journal of Soil and Water Science, 5*(1), 171–183.

Trenberth, K. E. (2011). Changes in precipitation with climate change. *Climate*

Research, *47*(1–2), 123–138.

Tsegaye B. (2019). Effect of Land Use and Land Cover Changes on Soil Erosion in Ethiopia. *International Journal of Agricultural Science and Food Technology*, *5*(1), 26–34.

Tullu, K. T., & Tumsa, B. C. (2024). Evaluating the impacts of climate change on soil loss using the CMIP6 model and RUSLE in the Muger watershed, Ethiopia. *Earth Science Informatics*, *18*(1), 99.

Tuppad, P., Kannan, N., Srinivasan, R., Rossi, C. G., & Arnold, J. G. (2010). Simulation of Agricultural Management Alternatives for Watershed Protection. *Water Resources Management*, *24*(12), 3115–3144.

Uber, M., Rössler, O., Astor, B., Hoffmann, T., & Oost, K. Van. (2022). Climate Change Impacts on Soil Erosion and Sediment Delivery to German Federal Waterways : A Case Study of the Elbe Basin. *Atmosphere*, *13*(11), 1–21.

Uddin, S. Z. (2021). Modeling Geotechnical Soil Loss and Erosion Dynamics For Climate-Resilient Coastal Adaptation. *American Journal of Interdisciplinary Studies*, *2*(04), 1–38.

Uniyal, B., Jha, M. K., Verma, A. K., & Anebagilu, P. K. (2020). Identification of critical areas and evaluation of best management practices using SWAT for sustainable watershed management. *Science of the Total Environment*, *744*, 140737.

Usman, M., Gul, A. A., Abbas, S., Rabbani, U., & Irteza, S. M. (2023). Identifying morphological hotspots in large rivers by optimizing image enhancement. *Remote Sensing Letters*, *14*(11), 1173–1185.

Van Griensven, A., Ndomba, P., Yalew, S., & Kilonzo, F. (2012). Critical review of SWAT applications in the upper Nile basin countries. *Hydrology and Earth System Sciences*, *16*(9), 3371–3381.

Waheed, A., Jamal, M. H., Javed, M. F., & Muhammad, K. I. (2024). A CMIP6 multi-model based analysis of potential climate change effects on watershed runoff using SWAT model: A case study of kunhar river basin, Pakistan. *Heliyon*, *10*(8).

Wang.Z and J.Cao. (2021). Spatial-temporal pattern study on water conservation function using the SWAT model. *Water Supply*, *12*(7), 3629–3642.

Waseem, M., Mani, N., Andiego, G., & Usman, M. (2017). A review of criteria of fit for hydrological models. *International Research Journal of Engineering and Technology (IRJET)*, *4*(11), 1765–1772.

Watene, G., Yu, L., Nie, Y., Zhang, Z., Hategekimana, Y., Mutua, F., … Ayugi, B. (2021). Spatial-temporal variability of future rainfall erosivity and its impact on soil loss risk in Kenya. *Applied Sciences*, *11*(21), 9903.

Welch, I. (2024). The IPCC Shared Socioeconomic Pathways (SSPs): Explained, Evaluated, Replaced. *National Bureau of Economic Research*, *15*(1), 37–48.

Wen, X., & Zhen, L. (2020). Soil erosion control practices in the Chinese Loess Plateau : A systematic review. *Environmental Development*, *34*, 100493.

Wen, X., Zhen, L., Jiang, Q., & Xiao, Y. (2023). A global review of the development and application of soil erosion control techniques. *Environmental Research Letters*, *18*(3), 033003.

Williams, J. R., & Berndt, H. D. (1977). Sediment yield prediction based on watershed hydrology. *Transactions of the ASAE, 20*(6), 1100–1104.

Williams, Jimmy R, & Berndt, H. D. (1972). Sediment yield computed with universal equation. *Journal of the Hydraulics Division*, *98*(12), 2087–2098.

Woldemariam, A. D., Ddumba, S. D., & Addis, H. K. (2024). Modeling Sediment Yield with Current and Projected Climatic Scenarios in Andit Tid Watershed, Central Highland of Ethiopia. *Journal of Agriculture and Environment for International Development*, *118*(2), 83–118.

Woldemariam, A. D., Ddumba, S. D., Addis, H. K., & Ayele, B. G. (2024). Spatiotemporal variability of streamflow under current and projected climate scenarios of Andit Tid watershed, central highland of Ethiopia. *Discover Sustainability*, *5*(1), 227.

Worku, T., Khare, D., & Tripathi, S. K. (2017). Modeling runoff–sediment response to land use/land cover changes using integrated GIS and SWAT model in the Beressa watershed. *Environmental Earth Sciences*, *76*(16), 1–14.

Worku, T., Tripathi, M. S. K., & Khare, D. (2016). Analyses of land use and land cover change dynamics using GIS and remote sensing during 1984 and 2015 in the Beressa Watershed Northern Central Highland of Ethiopia. *Modeling Earth Systems and Environment*, *2*(4), 1–12.

Worku, T., Tripathi, S. K., & Khare, D. (2018). Household level tree planting and its implication for environmental conservation in the Beressa Watershed of Ethiopia. *Environmental Systems Research*, *6*(1), 10.

Woznicki, S. A., & Nejadhashemi, A. P. (2013). Spatial and Temporal Variabilities of Sediment Delivery Ratio. *Water Resources Management*, *27*(7), 2483–2499. https://doi.org/10.1007/s11269-013-0298-z

Xiao, L., Yu, B., Li, R., Wu, P., & Cai, F. (2024). Defining watershed-scale sediment delivery ratio using functional connectivity: Exploring the relationship between monthly-scale sediment delivery ratio and soil erosion — A case study from a karst watershed. *CATENA*, *246*, 108443.

Xu, L., Zhang, D., Proshad, R., Chen, Y., Huang, T., & Ugurlu, A. (2023). Effects of soil conservation practices on soil erosion and the size selectivity of eroded sediment on cultivated slopes. *Journal of Mountain Science*, *18*(5), 1222–1234.

Yadeta, L. T., Switoniak, M., Tessema, Y. M., & Gebregeorgis, E. G. (2020). Soil Loss Estimation for Conservation Planning in the Welmel Watershed of the Genale Dawa. *Agronomy*, *10*(6), 777.

Yesuf, H. M., Assen, M., Alamirew, T., & Melesse, A. M. (2015). Modeling of sediment yield in Maybar gauged watershed using SWAT, northeast Ethiopia. *Catena*, *127*, 191–205.

Yigez, B., Xiong, D., Zhang, B., Belete, M., Chalise, D., Chidi, C. L., … Rai, D. K. (2023). Dynamics of soil loss and sediment export as affected by land use/cover change in Koshi River Basin, Nepal. *Journal of Geographical Sciences*, *33*(6), 1287–1312.

Yohannes, H., Soromessa, T., Argaw, M., & Dewan, A. (2020). Changes in landscape composition and con fi guration in the Beressa watershed , Blue Nile basin of Ethiopian Highlands : historical and future exploration. *Heliyon*, *6*(9), e04859.

Yohannes, H., Soromessa, T., Argaw, M., & Dewan, A. (2021). Impact of landscape pattern changes on hydrological ecosystem services in the Beressa watershed of the Blue Nile Basin in Ethiopia. *Science of the Total Environment*, *793*, 148559.

Yohannes, H., Soromessa, T., Argaw, M., & Warkineh, B. (2021). Spatio-temporal changes in ecosystem service bundles and hotspots in Beressa watershed of the Ethiopian highlands : Implications for landscape management. *Environmental Challenges*, *5*, 100324.

Yu, Y.-S. S., Zou, S., & Whittemore, D. (1993). Non-parametric trend analysis of water quality data of rivers in Kansas. *Journal of Hydrology*, *150*(1), 61–80.

Zahedipour, H., & Gallus, W. A. (2026). Impacts of climate change on Alaska's coastal villages: Bias-corrected NEX-GDDP-CMIP6 downscaling for anticipating local climate impacts. *Theoretical and Applied Climatology*, *157*(7), 404.

Zantet oybitet, M., Sambeto Bibi, T., & Abdulkerim Adem, E. (2023). Evaluation of best management practices to reduce sediment yield in the upper Gilo watershed, Baro akobo basin, Ethiopia using SWAT. *Heliyon*, *9*(10), e20326.

Zhang, G., Deng, A., Chen, J., Wang, D., Yin, Y., & Wang, H. (2024). Impacts of climate change and human activities on sediment load in Longchuan River Basin, China. *Journal of Hydrology: Regional Studies*, *51*, 101613.

Zone, E. W., Megersa, T., Nedaw, D., & Argaw, M. (2019). Combined effect of land use / cover types and slope gradient in sediment and nutrient losses in Chancho and Sorga sub watersheds ,. *Environmental Systems Research*, *8*(1), 24.

APPENDICES

Appendix I: Location of Meteorological Stations

Table 1: List of Meteorological Stations Within and Around the Beressa watershed

Station Name	Longitude	Latitude	Altitude (m)
Debre Birhan	39.51	9.66	2762
Debele	36.7	9.65	3204
Faji	39.5	9.6	2817
Ankober	39.73	9.59	2983
Gudoberet	39.68	9.8	3075
Mendida	39.31	9.66	2791
River gauge station (outlet)	39.5	9.67	2745

Appendix II: Streamflow–Sediment Rating Curves for the Beressa Watershed

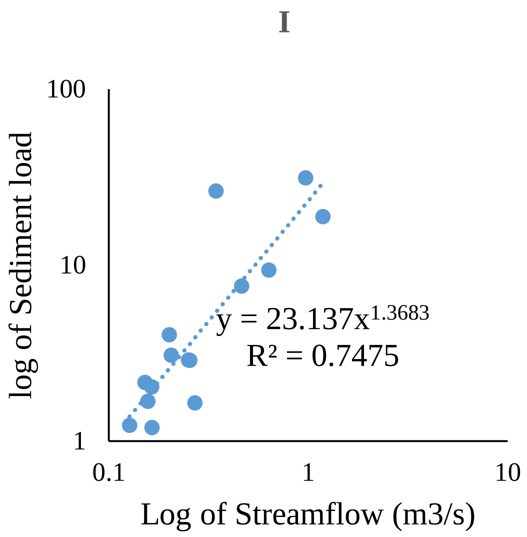

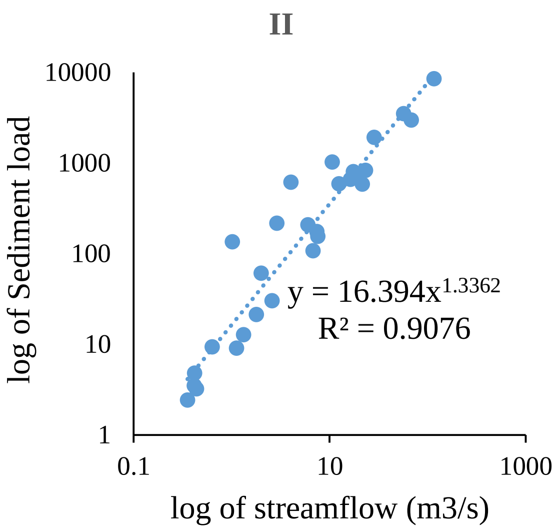

Figure 1: The stream flow-sediment-rating curve of the Beressa watershed for dry season (I) and wet season (II)

Appendix III: Steps of Bias Correction and Data Extraction using the CMhyd Tool

1. Preparing observed data in ASCII format, select climate variables, and add the observed gauge location file.
2. Select a bias correction method for precipitation and Temperature
3. Add simulated climate data (netCDF format), extracting historical and future climatic model data
4. process the bias correction(check files, overlapping period and perform Bias correction)
5. Comparing bias-corrected, before-corrected, and observed climate data

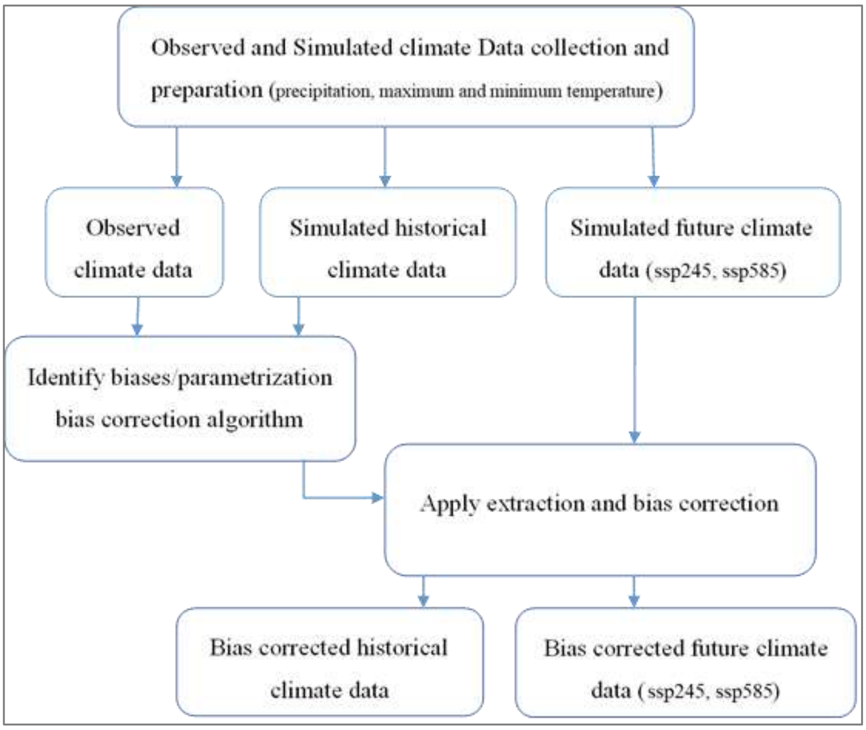

Figure 2: Workflow for Climate Data Bias Correction and Extraction Using the CMhyd Tool

Appendix IV: Streamflow and Sediment Parameters used for Sensitivity Analysis

Table 2: List of SWAT Model Parameters Related to Streamflow and Sediment Considered for Sensitivity Analysis

Variable	Parameter Name	Description
Stream flow	V__SOL_BD(..).sol	Moist bulk density
	V__RCHRG_DP.gw	Deep aquifer percolation fraction
	V__GWQMN.gw	Threshold depth of water in the shallow aquifer required for return flow to occur (mm)
	V__ESCO.hru	Soil evaporation compensation factor
	R__SOL_AWC(..).sol	Available water capacity of the soil layer
	V__SURLAG.bsn	Surface runoff lag time
	V__CANMX.hru	Maximum canopy storage
	V__GW_DELAY.gw	Groundwater delay (days)
	V__EPCO.hru	Plant uptake compensation factor
	V__GW_REVAP.gw	Groundwater “revap” coefficient
	R__CN2.mgt	SCS runoff curve number
	V__CH_K2.rte	Effective hydraulic conductivity in main channel alluvium
	V__ALPHA_BF.gw	Base flow alpha factor (days)
Sediment	V__SOL_K(..).sol	Saturated hydraulic conductivity.
	V__CH_N2.rte	Manning's "n" value for the main channel.
	V__HRU_SLP.hru	Average slope steepness
	V__CH_COV2.rte	Channel cover factor
	V__USLE_K(..).sol	USLE equation soil erodibility (K) factor
	V__SLSUBBSN.hru	Average slope length.
	V__USLE_C{AGRL}.plant.dat	Min value of USLE C factor for cultivated land cover
	V__SPCON.bsn	Linear parameter for calculating the maximum amount of sediment that can be

	re-entrained during channel sediment routing
V__USLE_P.mgt	USLE equation support practice
V__CH_S2.rte	Average slope of main channel.
V__USLE_C{FRST}.plant.dat	Minimum value of USLE C factor for forest land cover
V__USLE_C{GRAS}.plant.dat	Minimum value of USLE C factor for grassland cover
V__CH_COV1.rte	Channel Erodibility Factor
V__C_FACTOR.bsn	Scaling parameter for Cover and management factor in ANSWERS erosion model
V__ADJ_PKR.bsn	Peak rate adjustment factor for sediment routing in the sub-basin (tributary channels)
V__LAT_SED.hru	Sediment concentration in lateral flow and groundwater flow
V__SPEXP.bsn	Exponent parameter for calculating sediment re-entrained in channel sediment routing.

Appendix V: Projected Sediment Severity at Sub-Watershed Level under Future Climate Scenarios (SSP2-4.5 and SSP5-8.5)

Table 3: Sediment severity at the sub-watershed level for near- and far-term of SSP2-4.5 and SSP5-8.5 scenarios (before BMP implementation), with management practice requirements indicated by severity class

Sediment severity class(Mg/ha/year)	SSP245-near			SSP585-Near			BMP implementation
	no. of sub-watersheds	Area (km2)	%age	no. of Sub-Watersheds	Area (km2)	%age	

very low (0-5)	1	48.54	22.93	1	48.54	22.93	no
Low (5-11)	2	33.11	15.64	2	33.11	15.64	no
Moderate (11-18)	11	93.05	43.97	12	98.40	46.5	yes
High (18-25)	1	5.35	2.53	1	3.89	1.84	yes
Very high (>25)	8	31.59	14.93	7	27.70	13.09	yes
	SSP245-Far			SSP585-Far			
Very low(0-5)	1	48.54	22.93	1	48.54	22.93	no
Low(5-11)	1	9.19	4.34	0	0	0	no
Moderate(11-18)	9	103.14	48.73	8	85.98	40.62	yes
High(18-25)	4	21.65	10.23	6	45.54	21.52	yes
Very high(>25)	8	31.59	14.93	8	31.59	14.93	yes

Appendix VI: Mitigation Scenarios Implemented under SSP2-4.5 and SSP5-8.5 Climate Conditions

Table 4: Description of best management practices (BMPs), terracing, contour farming (CF), conservation agriculture (CA), combined measures, and baseline, under near- and far-term periods of SSP2-4.5 and SSP5-8.5 climate conditions.

Scenarios	Mitigation measures	Climate scenario	time frame	Description

S0	no mitigation measures	SSP2-4.5	2050	Baseline data on sediment yield before implementing any mitigation measures
		SSP2-4.5	2080	
		SSP5-8.5	2050	
		SSP5-8.5	2080	
S1	Terracing	SSP2-4.5	2050	Evaluation of terracing practices to mitigate sediment yield across varying climatic scenarios
		SSP2-4.5	2080	
		SSP5-8.5	2050	
		SSP5-8.5	2080	
S2	contour farming	SSP2-4.5	2050	Evaluation of CF to mitigate sediment yield across varying climate scenarios
		SSP2-4.5	2080	
		SSP5-8.5	2050	
		SSP5-8.5	2080	
S3	Conservation agriculture	SSP2-4.5	2050	Evaluation of CA to reduce sediment yield across varying climate scenarios
		SSP2-4.5	2080	
		SSP5-8.5	2050	
		SSP5-8.5	2080	
S4	Combined measures	SSP2-4.5	2050	Evaluation of the combined measures to reduce sediment yield under different scenarios and time frames
		SSP2-4.5	2080	
		SSP5-8.5	2050	
		SSP5-8.5	2080	

Appendix VII: Accuracy Assessment of Land Use and Land Cover Classification

Table 5: Confusion matrix for land use and land cover classification showing user's accuracy, producer's accuracy, overall accuracy, and the Kappa coefficient.

	WATR	AGRL	GRAS	BARR	FRST	URBN	Row Total	User Accuracy
WATR	8	0	0	0	0	0	8	100
AGRL	0	36	1	0	0	0	37	97.3
GRAS	0	1	29	0	1	0	31	93.5
BARR	0	0	1	12	0	0	13	92.3
FRST	0	0	1	0	29	0	30	96.67
URBN	0	0	0	1	1	25	27	92.6
Column Total	8	37	32	13	31	25	146	
producer accuracy	100	97.3	90.6	92.31	93.55	100		
Overall accuracy = 95.21%		kappa coefficient=89.41%						

Appendix VIII: Sediment Yield and Soil Erosion at the Sub-Watershed Level under Climate Change

Table 6: Sediment yield (Mg/ha/year) at the sub-watershed level within Beressa Watershed under baseline and future climate (SSP2-4.5 & SSP5-8.5).

Sub-basin	Area (km2)	Baseline (1995-2023)	SSP245 near (2030-59)	SSP245 far (2060-89)	SSP585 near (2030-59)	SSP585 far (2060-89)
1	7.38	9.36	12.42	13.26	12.65	17.67
2	0.37	68.51	73.07	70.30	69.43	74.17
3	6.72	7.30	10.42	9.19	10.65	14.94
4	5.05	16.04	16.73	18.17	15.04	19.93
5	5.43	11.93	12.93	14.01	11.56	15.32

6	5.97	8.81	12.79	14.62	13.37	18.81
7	5.25	8.55	13.65	14.64	13.94	19.53
8	0.29	23.89	40.14	33.40	29.82	41.81
9	0.14	49.10	56.90	45.88	55.84	58.52
10	48.54	0.67	1.78	1.92	1.82	2.57
11	11.54	14.25	15.00	13.11	13.69	17.71
12	5.46	42.99	48.41	43.12	44.04	54.34
13	5.50	8.34	17.83	20.50	13.88	18.74
14	3.89	10.12	25.00	27.56	19.45	26.22
15	5.35	9.08	20.09	21.80	15.63	21.14
16	2.33	47.56	54.84	47.84	54.38	55.90
17	18.42	16.44	16.27	16.63	14.82	18.19
18	5.75	7.30	16.58	16.05	12.90	17.39
19	26.39	2.13	10.15	11.65	7.89	11.62
20	5.36	7.53	16.89	19.41	13.15	17.71
21	8.07	39.65	42.43	43.24	39.94	47.69
22	11.05	37.71	45.21	42.68	41.36	49.98
23	17.40	3.34	14.60	16.74	11.34	15.32
mean		19.59	25.83	25.03	23.33	28.45

Table 7: Soil Erosion Rate (Mg/ha/year) at the Sub-Watershed Level of the Beressa Watershed under Baseline and Future Climate (SSP2-4.5 & SSP5-8.5)

Sub Basin	Area (km2)	Baseline (1995-2023)	Ssp245 near (2030-59)	SSP245 far (2060-89)	SSP585 near (2030-59)	SSP585 far (2060-89)
1	7.38	41.04	54.45	58.18	55.49	77.50
2	0.37	158.94	169.54	163.10	161.10	172.10
3	6.72	31.33	44.73	39.44	45.73	64.11
4	5.05	64.94	67.72	73.58	60.91	80.67
5	5.43	48.89	52.98	57.44	47.39	62.80

6	5.97	36.85	53.53	61.15	55.95	78.69
7	5.25	34.89	55.71	59.74	56.91	79.73
8	0.29	52.73	88.61	73.73	65.83	92.30
9	0.14	93.51	108.38	97.39	106.36	111.47
10	48.54	4.37	11.60	12.58	11.91	16.83
11	11.54	68.49	72.12	63.02	65.80	85.16
12	5.46	176.89	199.23	177.46	181.23	223.61
13	5.50	34.33	73.39	84.36	57.13	77.13
14	3.89	38.79	95.79	105.59	74.52	100.46
15	5.35	37.20	82.33	89.34	64.06	86.64
16	2.33	163.43	188.45	164.41	186.86	192.10
17	18.42	87.46	86.54	88.48	78.84	96.76
18	5.75	30.28	68.80	66.60	53.52	72.15
19	26.39	12.24	58.36	60.93	45.35	61.03
20	5.36	30.86	69.22	69.53	53.88	72.59
21	8.07	177.00	189.43	193.03	178.31	212.92
22	11.05	179.59	215.28	203.23	196.93	238.02
23	17.40	17.48	76.44	87.67	59.36	80.22
Mean		70.50	94.90	93.48	85.36	105.87

Appendix IX: Photographic Evidence of Conservation Activities, Erosion Severity in the Beressa Watershed

Figure 3: Stone-Faced Soil Bund Constructed by the Community Mobilization

Figure 4. Erosion Severity in the Beressa Watershed